GEORGIA DOT RESEARCH PROJECT 13-21

DRAFT FINAL REPORT

EVALUATING THE PERFORMANCE OF GUARDRAIL POSTS INSTALLED BY DRIVING THROUGH ASPHALT LAYERS

Georgia Department of Transportation

OFFICE OF RESEARCH
15 Kennedy Drive
Forest Park, GA 30297-2534

TECHNICAL REPORT DOCUMENTATION PAGE

1.Report No.: FHWA-GA-15-1321	2. Government Accession No.:	3. Recipient's Catalog No.:

4. Title and Subtitle: **Evaluating the Performance of Guardrail Systems for Installation in Georgia by Driving Through Asphalt Layers**	5. Report Date: December 4, 2015 6. Performing Organization Code:
7. Author(s): D.W. Scott, D.W. White, L.K. Stewart, C. Arson, E. Bakhtiary, and S.-H. Lee	8. Performing Organ. Report No.: 13-21
9. Performing Organization Name and Address: Georgia Institute of Technology School of Civil and Environmental Engineering 790 Atlantic Drive NW Atlanta, GA 30332	10. Work Unit No.: 11. Contract or Grant No.:
12. Sponsoring Agency Name and Address: Georgia Department of Transportation Office of Research 15 Kennedy Drive Forest Park, GA 30297-2534	13. Type of Report and Period Covered: Final; July 2013 – December 2015 14. Sponsoring Agency Code:

15. Supplementary Notes:
Prepared in cooperation with the U.S. Department of Transportation, Federal Highway Administration.

16. Abstract:

The preferred procedure for guardrail installation in the State of Georgia includes a layer of asphalt (usually referred to as a "mow strip") placed to retard vegetation growth around the guardrail. The objective of this multi-phase research program is to develop effective alternatives to post installation methods that incorporate a leave-out around the post. The work described in this report represents Phase I of the overall research effort. The research team evaluated the structural performance of guardrail posts installed in accordance with current GDOT (Georgia Department of Transportation) procedures that include an asphalt mow strip, as well as alternative installation options developed in conjunction with GDOT personnel. The current state of practice related to the use of asphalt vegetation barriers in the United States was identified through on a nationwide survey. An experimental program was carried out in accordance with applicable AASHTO guidelines. In parallel with the experimental program, a three dimensional finite element model was developed for a guardrail post installed through an asphalt layer. Results from the experimental program and finite element analyses were used to develop a series of quantitative criteria to evaluate the performance of the various post/mow strip configurations. Parametric studies were conducted on pertinent geometric variables in terms of the quantitative performance criteria. The results of this Phase I research program demonstrate that (1) there are potential combinations of mow strip thickness and rear distance that are likely to result in satisfactory dynamic performance, and (2) two techniques appear effective in reducing the ground-level restraint imparted by a mow strip on a guardrail system: decreasing the mow strip rear distance behind the post, and pre-cutting the mow strip in the region behind the post.

17. Key Words: Guardrails, Mow Strip, Experimental Program, Finite Element Analysis	18. Distribution Statement:

19. Security Class (this report): Unclassified	20. Security Class (this page): Unclassified	21. Number of Pages: 155	22. Price:

Form DOT 1700.7 (8-69)

GDOT Research Project No. 13-21

Evaluating the Performance of Guardrail Systems for Installation in Georgia by Driving Through Asphalt Layers

Final Report

EVALUATING THE PERFORMANCE OF GUARDRAIL POSTS INSTALLED BY DRIVING THROUGH ASPHALT LAYERS

By
David Scott, Donald White, Lauren Stewart, Chloe Arson
Esmaeel Bakhtiary, Seo-Hun Lee

Georgia Tech Research Corporation
Atlanta, Georgia 30332

Contract with

Georgia Department of Transportation

December 4, 2015

The contents of this report reflect the views of the author(s) who is (are) responsible for the facts and the accuracy of the data presented herein. The contents do not necessarily reflect the official views or policies of the Georgia Department of Transportation or the Federal Highway Administration. This report does not constitute a standard, specification, or regulation

TABLE OF CONTENTS

Page

LIST OF TABLES v

LIST OF FIGURES vi

EXECUTIVE SUMMARY ix

ACKNOWLEDGMENTS xii

CHAPTER 1 - INTRODUCTION AND BACKGROUND 1

CHAPTER 2 - DEVELOPMENT OF ALTERNATIVES BASED ON CURRENT PRACTICE 11

CHAPTER 3 – STATIC TEST PROGRAM 17

CHAPTER 4 – FINITE ELEMENT SIMULATIONS 35

CHAPTER 5 – CORRELATION OF RESULTS AND DISCUSSION 49

CHAPTER 6 – CONCLUSIONS FROM PHASE I PROJECT AND RECOMMENDATIONS FOR PHASE II 62

CHAPTER 7 - REFERENCES 74

APPENDICES

Appendix A—SURVEY OF OTHER STATE DOT PRACTICES…….....80

Appendix B—STATIC TEST DETAILS…….....91

Appendix C—DETAILED DESCRIPTION OF THE FINITE ELEMENT MODEL AND MATERIAL TESTING …….....….125

LIST OF TABLES

Table Page

1. Bogie vehicle tests on steel guardrail posts with asphalt mow strips……... 7
2. Static test matrix…… 25
3. Summary of test results for experimental program…… 29
4. Steel mechanical properties used in the FE model…… 39
5. Soil mechanical properties used in the FE model…….. 41
6. Comparison of deflection of the post between FEA and experimental results….. 41
7. Asphalt concrete mechanical properties used in the numerical model for asphalt 44
8. The peak force for different pre-cutting designs…… 46
9. Maximum strain and normalized strain with yield strain (static test)…… 59
10. Proposed dynamic test matrix for evaluation of installation alternatives…….. 71

LIST OF FIGURES

Figure Page

1. (a) Typical guardrail installation in Georgia; (b) Guardrail installation incorporating grout leave-outs as recommended in the Roadside Design Guide… 1
2. Standard GDOT Mow strip Detail…….. 11
3. Asphalt mow strip configuration by state based on electronic/phone survey…… 13
4. Asphalt mow strip geometric parameters found in various State DOT drawings: (a) maximum thickness, and (b) maximum rear distance…….. 13
5. Guardrail post setups with (a) different asphalt thicknesses and (b) various rear distances……15
6. Schematic Illustration of a guardrail post setup with a pre-cut asphalt layer…… 16
7. Hot mixed asphalt (HMA) mow strip installation……. 19
8. Guardrail post installation…….. 20
9. Static test setup with instrumentation…… 21
10. Loading fixture and instrumentation details……. 22
11. Strain gage installation details……... 22
12. Baseline setup with no mow strip (0-0 configuration)…….. 25
13. GDOT preferred mow strip setup (2-24 configuration)…… 26
14. Mow strip with grout-filled leave-out…… 27
15. Pre-cut mow strip patterns tested: (a) parallel, (b) diagonal……. 27
16. Typical Pre-cut configuration (parallel)…… 28
17. Representative load-displacement curves (baseline and GDOT preferred setups) 30
18. Representative load-displacement curve (alternative mow strip setups)……... 31

19. GDOT standard configuration (3.5-24), Post 3-3: (a) before test; (b) post-test… 32

20. Reduced rear distance (2-12), Post 4-1: (a) before test; (b) post-test…… 32

21. Pre-cut mow strip (2-24-C1), Post 4-2: (a) before test; (b) post-test……. 33

22. Comparison of load-displacement curves between FEA and experimental results…… 42

23. Comparison between FEA result and the experimental result for 2" asphalt and 3.5" asphalt…… 45

24. Comparison of asphalt rupture in (a) static tests and (b) FEA simulation……. 45

25. Different pre-cutting designs for the asphalt mow strip…… 47

26. FEA results for different pre-cutting designs…… 48

27. Behavior of guardrail post in different embedment conditions……. 51

28. Relationship between ground level displacement and dissipated energy…….. 52

29. MASH test 3-10 crash condition……... 53

30. Representative load-displacement curves from experimental program…… 55

31. FEA Contour plot of peak force (kips) in a guardrail post demonstrating the influence of mow strip geometric parameters……56

32. Relative performance of various mow strip configurations in terms of ground-level displacement for a specified value of work done……. 57

33. FEA Contour plot of ground-level displacement (inch) at a specified energy level in a guardrail post demonstrating the influence of mow strip geometric parameters……. 58

34. FEA Contour plot of normalized maximum strain in a guardrail post demonstrating the influence of mow strip geometric parameters……. 60

35. CEE Velocity Generator…… 68

36. Basic concept for moveable test bed……. 69

37. Schematic of hydraulic system including parameters for calibration…… 70

EXECUTIVE SUMMARY

The preferred procedure for steel guardrail installation in the state of Georgia employs a post-installation machine to drive the posts through a layer of asphalt (usually referred to as a "mow strip") placed to retard vegetation growth around the system. However, in order to avoid undesirable restraint at the ground line, the Fourth Edition of the *AASHTO Roadside Design Guide* recommends the use of a mow strip incorporating leave-outs. The installation method preferred by the Georgia Department of Transportation (GDOT) is considered to be more economical and allows better quality control during the construction process. Using a leave-out for posts in vegetation barriers is seen as less desirable because of issues including significantly higher expected costs for new construction and repairs, variability in the placement and spacing of posts, and the need for additional construction scheduling.

The objective of this multi-phase research program is to develop alternatives to the guardrail post installation methodology outlined in the *AASHTO Roadside Design Guide*. The work described in this report represents Phase I of the overall research effort. The research team evaluated the structural performance of guardrail posts installed in accordance with current GDOT procedures that include a mow strip, as well as alternative installation options developed in conjunction with GDOT personnel and transportation contractors in the State of Georgia.

To identify potential alternatives to the *Roadside Design Guide's* leave-out method, a survey was undertaken to evaluate the current state of practice related to the use of asphalt vegetation barriers in the United States. Publically accessible websites were investigated and phone solicitations were performed for all 50 state Departments of

Transportation. Based on the obtained information, it was determined that 11 states currently do not use mow strips, 18 states use mow strips without incorporating a leave-out, and 15 states use mow strips including a leave-out. No information was found for four states, and two states stated that their practice is to pave up to the face of the post.

A workshop with selected GDOT personnel was held on 05/22/14 to present the results from the state DOT surveys and to discuss alternative design and installation strategies. Bases on these discussions, alternate mow strip design strategies were identified and prioritized. GDOT officials strongly recommended that alternative mow strip designs identified for further evaluation should attempt to incorporate as many elements of the current GDOT preferred method as possible, and avoid unnecessary deviations.

An experimental testing program was carried out on an outdoor test site constructed on the Georgia Institute of Technology Campus in accordance with applicable AASHTO guidelines. A total of 19 posts installed with mow strips were subjected to static loading to provide a better understanding of the behavior of a post restrained with an asphalt layer at the ground line. Results from the tests demonstrated that the performance of the post was directly affected by the mow strip geometry as well as service conditions.

In parallel with the experimental program, a three dimensional finite element model was developed for a guardrail post installed through an asphalt layer. The Mohr-Coulomb material model was used to model the behavior of the asphalt. The model was refined using the experimental results from the static test program as well as material testing.

Results from the experimental program and finite element analyses were used in the development of quantitative criteria to evaluate the performance of the various post/mow strip configurations tested in this program in comparison to the performance of posts installed in mow strips including a leave-out. Parametric studies were performed on pertinent geometric variables in terms of the quantitative performance criteria. The results indicate that there are combinations of mow strip thickness and rear distance that are more likely to result in satisfactory dynamic performance.

The results of Phase I of this research program resulted in the identification of two techniques that appear effective in reducing the restraint imparted by a mow strip on a guardrail system; decreasing the mow strip rear distance behind the post, and pre-cutting the mow strip in the region behind the post. The following alternative mow strip configurations are recommended for further evaluation under dynamic loading in Phase II of the research program:

- Mow strips of 2 inch thickness with a maximum 12 inch rear distance behind the post;
- Mow strips of 3.5 inch thickness with a maximum 12 inch rear distance behind the post;
- Mow strips of 2 inch thickness with a maximum 24 inch rear distance behind the post with the asphalt pre-cut prior to testing;
- Mow strips of 3.5 inch thickness with a maximum 24 inch rear distance behind the post with the asphalt pre-cut prior to testing;

ACKNOWLEDGEMENTS

The research reported herein was sponsored by the Georgia Department of Transportation through Research Project Number 13-21. Mr. Brent Story, State Design Policy Engineer, Mr. Daniel Pass, Assistant State Design Policy Engineer, Mr. Beau Quarles, Civil Engineering Group Leader, Mr. Walter Taylor, Senior Design Engineer, Mr. David Jared, Assistant State Research Engineer, and Ms. Gretel Sims, Research Engineer at GDOT provided many valuable suggestions throughout this study. Special thanks go to Mr. Josh Watson, Division 3 Maintenance Manager for GDOT, who provided the means of driving the guardrail posts in the experimental study. The opinions and conclusions expressed herein are those of the authors and do not represent the opinions, conclusions, policies, standards or specifications of the Georgia Department of Transportation or of other cooperating organizations.

At the Georgia Institute of Technology, Ms. Lakshmi Subramanian assisted the research team with the electronic and phone survey of State Departments of Transportation. Mr. Jeremy Mitchell provided help and expertise with equipment and research tasks at the Georgia Tech SEMM Laboratory. Messrs. Javaid Anwar, Clifford Tribble, and John Young assisted with the construction of the experimental test site as well and the setup and completion of the static load experiments.

The authors express their profound gratitude to all of these individuals for their assistance and support during the completion of this research project.

CHAPTER 1
INTRODUCTION AND BACKGROUND

1.1 Problem Statement

The preferred procedure for steel guardrail installation in the state of Georgia [1] employs a post-installation machine (typically hydraulic) to drive the posts through a layer of asphalt (usually referred to as a "mow strip") placed to retard vegetation growth around the system (Figure 1(a)). However, in order to avoid undesirable restraint at the ground line, the Fourth Edition of the *AASHTO Roadside Design Guide* [2] recommends a post installed incorporating grout leave-outs (Figure 1(b)). This recommendation is based on research performed by the Texas Transportation Institute [3,4]. While these investigations did involve posts embedded in asphalt, the specific configuration preferred by GDOT was not included in the study.

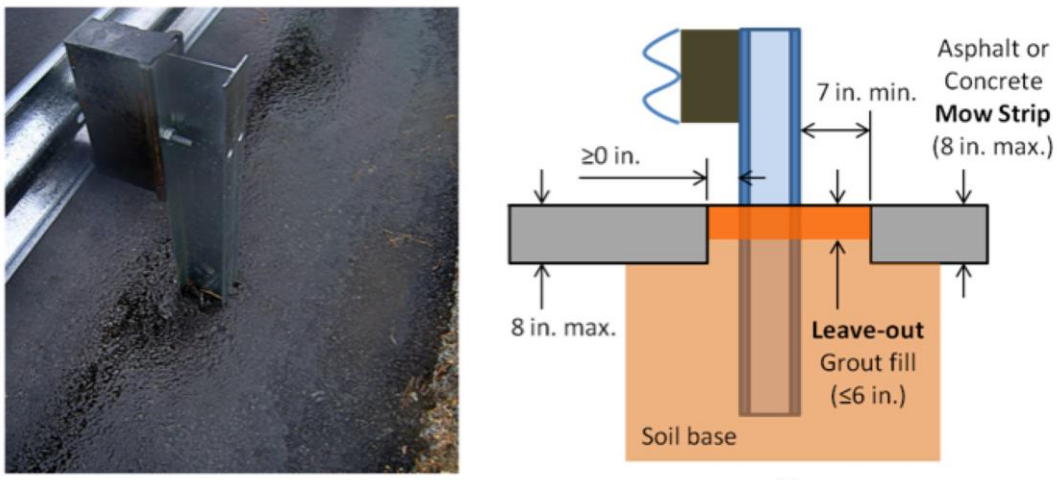

(a) (b)

FIGURE 1

(a) Typical guardrail installation in Georgia; (b) Guardrail installation incorporating grout leave-outs as recommended in the Roadside Design Guide.

1.2 Project Objectives

The objective of this research program is to develop alternatives to the guardrail post installation methodology outlined in the *AASHTO Roadside Design Guide*. The work described in this report represents Phase I of the overall research effort. The researchers evaluated the structural performance of guardrail posts installed in accordance with current GDOT procedures that include a mow strip, as well as alternative installation options developed in conjunction with GDOT personnel and transportation contractors in the State of Georgia. A subset of the most promising alternative installation methods will be selected for further evaluation under subcomponent dynamic loading in Phase II of the research effort. The dynamic tests results will be used to refine and expand results of finite element analysis (FEA) simulations already underway. Following the Phase II project, multiple installation procedures will be selected for full-scale crash testing in Phase III of the research program. The final objective is to provide support for a submittal to FHWA for approval of a more constructible and cost-effective detail than that recommended in the current *Roadside Design Guide*.

The major deliverable of this research project will be the identification of cost-effective installation methodologies for steel guardrail systems with asphalt mow strips that meet FHWA safety and performance criteria. Steel guardrail is the most common roadside barrier installed along Georgia's 20,000 miles of interstates and state routes [5]. The overall research program addresses a specific concern raised by GDOT personnel relating to the compliance of current state guardrail installation procedures in comparison to guidelines found in the *Roadside Design Guide*. The installation method preferred by

GDOT is considered to be more economical and allows better quality control during the construction process. Using a leave-out for posts in vegetation barriers is seen as less desirable because of issues including significantly higher expected costs for new construction and repairs, variability in the placement and spacing of posts, and the need for multi-phase construction scheduling. However, the safety and effectiveness of the guardrail systems installed using these procedures must be rigorously evaluated to ensure compliance with FHWA guidelines.

1.3 Background

General

A large volume of work exists in the literature regarding the testing of guardrail posts and systems. Summaries of representative work are presented below.

A synthesis report by Ray and McGinnis [6] provides a broad summary of crash testing for various barrier types. Articles by Reid [7] and Atahan [8] provide detailed reviews of finite element simulations of vehicle barrier impacts. Atahan [9] conducted an explicit nonlinear finite element simulation of a strong-post W-beam guardrail system. The results of a previously conducted full-scale crash test of a failed guardrail system were used in the study. Before the next full-scale crash test, numerical simulations of the failed system were used to identify the cause of the failure, and to propose possible improvements to the system. Borovinšek et al. [10] and Ren et al. [11] used computational crash simulations for the early evaluation of different guardrail setups and determination of the best barrier design for high and low containment levels. In the study done by Hampton et al. [12], the effect of missing posts on the guardrail crash performance was quantitatively evaluated. Mohan et al. [13] developed a detailed finite

element model of a three-strand cable barrier and validated this model against a previously conducted full-scale crash test. Sicking et al. [14] used numerical and experimental full-scale crash testing for the development of the Midwest guardrail system. Mak et al. [15] reported the results of eight full-scale crash tests on typical guardrail systems including W-beam, cable, box-beam and Thrie-beam configurations. All crash tests were performed in accordance with *NCHRP Report 350* [16]; three of the test configurations did not satisfy the *NCHRP* criteria. Plaxico et al. [17] performed a full-scale crash test on a W-beam guardrail system and also performed a nonlinear finite element analysis using LS-DYNA [18]. The guardrails were found to satisfy the requirements of *NCHRP 350*. Gabauer et al. [19] investigated the crash performance of longitudinal barriers with minor damage using pendulum tests. The authors tested systems with five different types of typical damage seen in existing guardrail systems. They found that vertical tears in the guardrail provided a significant threat to the structural performance of the system. Bligh et al. [20] performed a full-scale crash test on a 31-inch W-beam guardrail with standard offset blocks. The *AASHTO Manual for Assessing Safety Hardware* (*MASH*) criteria [21] was used to perform the crash test; the elevated post design met all safety criteria. Abu-Odeh et al. [22] reviewed full-scale crash test reports performed at a number of accredited testing facilities. Fifty-three different guardrail configurations and corresponding test results were examined and tabulated. Schrum et al. [23] performed two full-scale crash tests on the non-blocked Midwest Guardrail System (MGS) in accordance with *MASH* criteria; the system was shown to meet *MASH* requirements.

A number of studies have focused more on the soil behavior and its interaction with the guardrail post. Dewey et al. [24] studied the soil-structure interaction behavior of highway guardrail posts. Although the models used in this study were simpler than the sophisticated continuum models utilized in Phase-I of the current project, this work did emphasize the importance of soil modeling for the guardrail system. Ferdous et al. [25] identified performance limits of commonly used barriers in terms of acceptable vehicle impact using non-linear finite element methodology. In this study, the soil was modeled with a Joint-Rock material model. This model cannot capture the soil physical behavior because it was built to be used for rocks with joints. The *LS-DYNA user's manual* [26] recommends using the Mohr-Coulomb material model instead. Rohde et al. [27] discussed the instrumentation required for determination of guardrail-soil interaction in bogie vehicle testing. Plaxico et al. [28] performed finite element modeling of guardrail timber posts and the post soil interaction. In this study, the post soil interaction was modeled using the subgrade reaction approach, which involves an array of nonlinear springs attached along the length of the post below grade. Wu et al. [29] studied the interaction between a guardrail post and soil during quasi-static and dynamic bogie vehicle testing. This study employed the methodology of using static testing to inform dynamic testing. According to the measurement data, the dynamic resistance of the soil in the bogie vehicle testing was approximately twice the quasi-static resistance. Tabiei and Wu [30,31] performed finite element simulation of a strong W-beam guardrail post to be used in full-scale crash test simulations using an Eulerian formulation to model the soil media as part of the overall system [32].

Guardrail Posts with Mow strips

Research performed by the Texas Transportation Institute to investigate the impact of mow strips on the performance of guardrail systems [3] formed the basis for the adoption of the guardrail post installation detail incorporating grout leave-outs into the *Roadside Design Guide*. The researchers examined the performance of guardrail/mow strip systems using experimental testing and numerical simulation. Mow strip dimensions, materials, and depths were considered in addition to the presence of "leave-out" sections around posts. Seventeen configurations of wood and steel guardrail posts embedded in various mow strip systems and confinement conditions were subjected to dynamic impact testing with a bogie vehicle. The dynamic impact tests were numerically simulated, and full-scale mow strip system models were assembled using the subcomponent models. Based on predictive numerical simulations, a concrete mow strip with grout-filled leave-outs was selected for full-scale crash testing in accordance with *NCHRP 350* criteria [16]. Crash tests of a steel post guardrail system and wood post guardrail system encased in the selected mow strip configuration were deemed successful.

Of primary interest to the current project was the subcomponent dynamic testing involving post installation configurations including an asphalt mow strip. A summary of the tests performed and the outcomes from the tests are given in Table 1.

Further research on the performance of guardrail systems with concrete mow strips was presented in 2009 [4]. This work focused primarily on alternative materials used in the post leave-outs: two-part urethane foam, two types of molded rubber mat, and a precast concrete wedge. The alternative configurations were evaluated using the bogie vehicle

employed in the previous study. The authors asserted that three of the four alternative leave-out materials demonstrated satisfactory performance in comparison with a post with no mow strip installed.

TABLE 1
Bogie vehicle tests on steel guardrail posts with asphalt mow strips [3]

Test Configuration			Test Results				
Mow Strip	**Leave-out Material**	**Leave-out Size**	**Peak Accel (g)**	**Post Deflection**	**Vehicle Position**	**Test result**	**Notes**
None	None	N/A	9	Rotational Translation	Stopped on post	Satisfactory	Baseline test
Asphalt	Asphalt	12 inch	12.5	Yielded at ground level	Slid over the post	Unsatisfactory	8 inch thickness
Asphalt	Asphalt	18 inch	11	Deflected before yield	Slid over post	Unsatisfactory	8 inch thickness
Asphalt	Asphalt	18 inch	12	Yielded at ground level	Slid over the post	Unsatisfactory	4 inch thickness
Asphalt	Grout	18 inch	10	Rotational Translation	Stopped on post	Satisfactory	
Asphalt	Asphalt	Rubber Mat	9	Rotational Translation	Stopped on post	Satisfactory	

In the studies cited above, assessment of the guardrail post performance was based on the following qualitative observations:

- Post rotation and translation versus deformation were observed, but quantitative values were not reported. Further, some installation methods were deemed unsatisfactory because "…the steel post yielded at the ground line without significant translation…" and did not prevent the bogie vehicle from "…sliding up and over the posts…" [3]. No specific criteria were identified to determine what constituted a post failure in this manner.

- In both studies, peak accelerations were recorded and presented for each test, but no threshold value was offered except for the baseline response without mow strips.

- Tests performed relating to direct encasement of the posts used asphalt thicknesses of four and eight inches, the latter of which is significantly higher than that typically used in Georgia.

In addition, it was noted that, in finite element models developed in these former studies:

- The extent of the domain meshed was close to that of the zone of influence of the loaded posts, which implies that boundary effects can affect the results.
- The external boundaries of the domain were fixed, which can result in oscillations in dynamic solvers.
- The mesh was coarse, and the independence of the numerical results to mesh refinement was not checked.
- The asphalt mow strip was modeled as a rigid layer.
- Soil plowing was not modeled, which precludes the prediction of post large deformation regimes, after the peak of the load-displacement curve.

Two recent research studies including the performance of guardrail posts encased in asphalt mow strips were performed by Midwest Roadside Safety Facility (MwRSF).

In 2012, Jowza et al. [33] conducted research sponsored by the Wisconsin Department of Transportation investigating the performance of wood guardrail posts encased in asphalt mow strips and placed on slopes. Dynamic bogie vehicle tests were performed on wood posts encased in a 2 inch asphalt mow strip. In the majority of the tests, the wood posts could rotate backward and break the asphalt layer but with an increase in post-soil resistance as compared to tests conducted without the asphalt confinement. Thus, the authors recommended that wood posts on 2H:1V or 4H:1V slopes

should not be surrounded completely by asphalt and should be treated in the same way as posts installed on sloped terrain.

In 2015, Rosenbaugh et al. [34] performed a series of dynamic impact tests on weak steel posts (S3x5.7) embedded in three different surrounding soil conditions: weak soil, strong soil, and strong soil covered by asphalt mow strip. A total of ten bogie vehicle tests were run, and one of the tests included the asphalt mow strip of 4" thickness and 24" rear distance.

1.4 Report Organization

Chapter 2 of this report summarizes the results of an electronic and phone survey of State Departments of Transportation to determine the current state of practice in the use of asphalt mow strips around guardrail systems. The results of the survey along with a Workshop held in conjunction with GDOT formed the basis for the preliminary selection of potential alternative design and installation procedures for guardrail posts in asphalt mow strips.

Chapter 3 summarizes the results of the static test program carried out on the alternative design and installation procedures. These results were analyzed to provide a better understanding of the behavior of a post restrained with an asphalt layer at the ground line.

Chapter 4 summarizes the results of the development of advanced finite element models to analyze the performance of the posts installed with mow strips. The development of this model allowed a broader and more rigorous parametric study to be undertaken on critical design variables.

Chapter 5 correlates the experimental data with the finite element analysis results to develop a set of rational criteria to evaluate the potential efficacy of the proposed alternative design and installation procedures for guardrail posts installed in mow strips.

Chapter 6 contains the Conclusions for the Phase I research program and recommendations for the Phase II effort.

Chapter 7 contains the references cited in this report.

The Appendices contain detailed descriptions of the survey process, testing procedures and results, and computational methods and procedures utilized in Phase I of the research program.

CHAPTER 2
DEVELOPMENT OF ALTERNATIVES BASED ON CURRENT PRACTICE

2.1 GDOT Standard Practice

The most widely used guardrail post in the state of Georgia is the "Type D" wide-flange steel post. According to GDOT Construction Specification 641.3.05 [1], asphalt mow strip installation around the post as shown in Figure 2 is optional but recommended for roadside vegetation control. In Georgia, the mow strip typically consists of two layers of asphalt: a top layer of 1.5 inch thickness and a 2 inch thick bottom layer [35]. However, in some cases the top layer is not extended beyond the guardrail post due to constructability considerations.

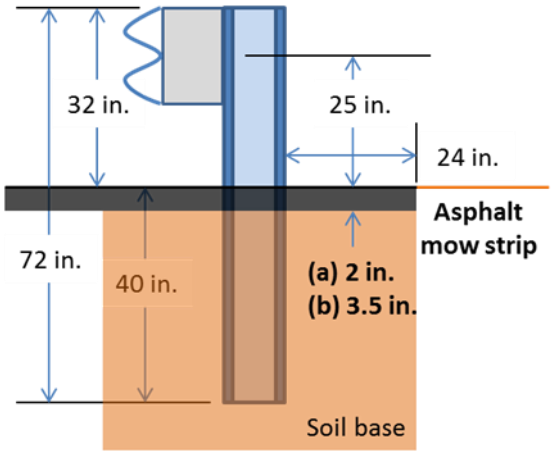

FIGURE 2

Standard GDOT Mow strip Detail [35]

The GDOT Construction Specification allows multiple methods for guardrail post installation in areas with asphalt mow strips. The preferred method employs a post-installation machine (typically hydraulic) to drive the posts through the asphalt mow strip and into the soil base. This installation method is considered by GDOT to be the most

economical and allows better quality control during the construction process [36]. Using a leave-out for posts in vegetation barriers is seen as less desirable because of issues including significantly higher expected costs for new construction and repairs, variability in the placement and spacing of posts, and the need for multi-phase construction scheduling.

2.2 Survey of Other State DOT's Practices

To identify potential alternatives to the *Roadside Design Guide's* leave-out method, a survey was undertaken to evaluate the current state of practice related to the use of asphalt vegetation barriers in the United States. Publically accessible websites were investigated and phone solicitations were performed for all 50 state Departments of Transportation. Based on the obtained information, it was determined that 11 states currently do not use mow strips, 18 states use mow strips without incorporating a leave-out, and 15 states use mow strips including a leave-out. No information was found for four states, and two states stated that their practice is to pave up to the face of the post. Based on the information gathered, there does not appear to be a significant correlation between geographic location and the current state of practice for mow strip usage as shown in Figure 3. Details of the survey results for each state DOT is provided in Appendix A.

The range of asphalt mow strip geometric parameters was also investigated. Figure 4 shows the summary of mow strip maximum thickness and rear distance obtained from the survey. From 25 states where the maximum thickness of mow strip is specified, the thickness ranges from 1.5 inch to 8 inch, with a nationwide average of 3.2 inch, median of 3 inch, and mode of 2 inch. Similarly, from the 17 states where the maximum

rear distance of mow strip is specified, the rear distance ranges from 6 inch to 48 inch, with a nationwide average of 21.4 inch, median of 24 inch, and mode of 24 inch. These ranges were used in the development of the research program.

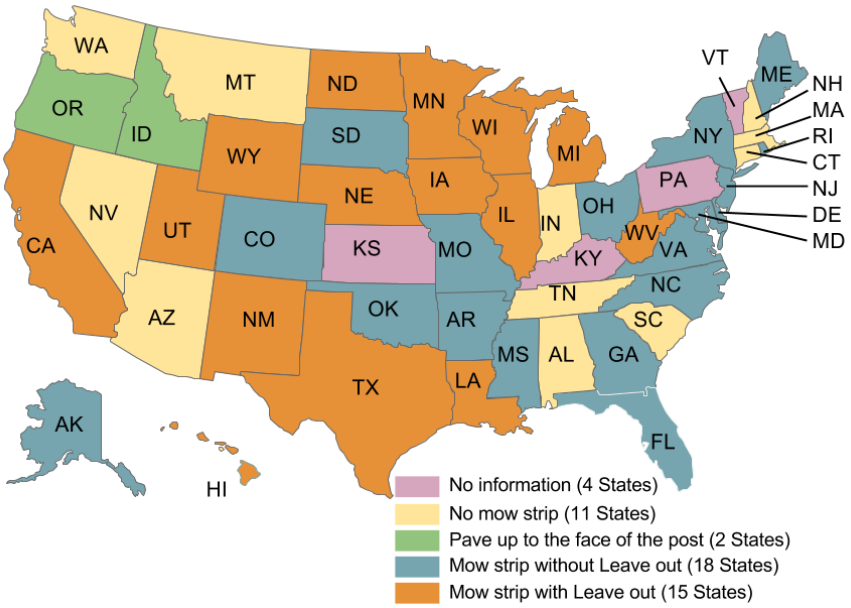

FIGURE 3

Asphalt mow strip configuration by state based on electronic/phone survey

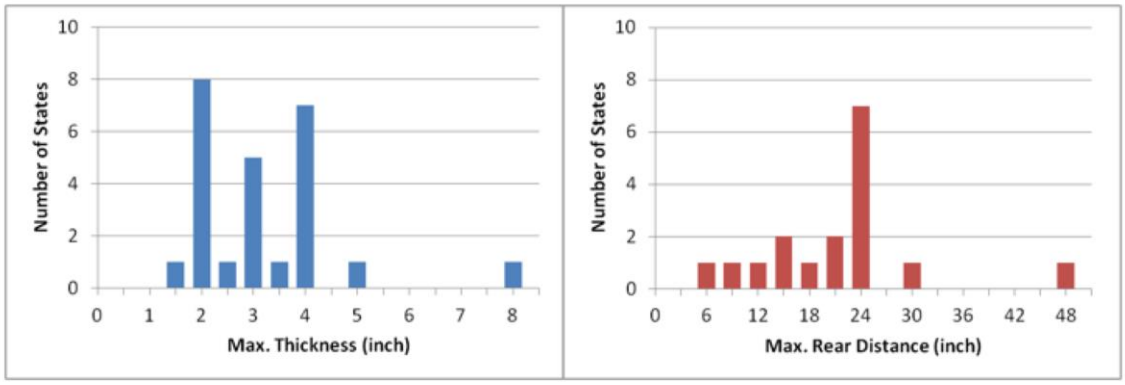

(a) (b)

FIGURE 4

Asphalt mow strip geometric parameters found in various State DOT drawings: (a) maximum thickness, and (b) maximum rear distance

2.3 Proposed Alternative Mow Strip Designs Based on the GDOT Workshop

A workshop with selected GDOT personnel was held on 05/22/14 to present the results from the state DOT surveys and to discuss alternative design and installation strategies. Five alternative design strategies were identified and prioritized:

1) Limiting the maximum rear distance and thickness of the asphalt layer;
2) Pre-cutting the asphalt mow strip behind the post;
3) Using a tapered mow strip;
4) Removing a portion in the mow strip behind the post; and
5) Replacing the asphalt with gravel to prevent vegetation growth.

After much discussion among the Workshop attendees taking into consideration constructability and potential maintenance issues, options (1) and (2) were selected by consensus for further investigation.

The guardrail post system performance changes as the geometry of the asphalt mow strip and its material properties change. The main variable geometric parameters of the mow strip which influence guardrail performance are the thickness of the asphalt layer and the rear distance behind the post. As the thickness and the rear distance increase, the effect of the asphalt layer on the system performance becomes more pronounced. The common asphalt thickness used in the state of Georgia for mow strips is 3.5 inches and the minimum feasible asphalt thickness considering constructability is 2 inches (Figure 5(a)). This minimum thickness is based on the aggregate size, construction equipment, and effectiveness at retarding vegetation growth (a very thin asphalt layer does not typically work well in this regard). The proposed rear distance values are 6, 12 and 24 inches (Figure 5(b)). This range was identified as having the

potential to provide a desirable restriction in vegetation growth without significant increases in construction cost. A combination of different thicknesses and rear distances were evaluated to gauge the effect of each of these parameters on the system performance. A detailed discussion of the experimental static test results for these cases is provided in Chapter 3. A larger combination of different thicknesses and rear distances have been studied using advanced finite element analysis (FEA) techniques; these results are presented in Chapter 5.

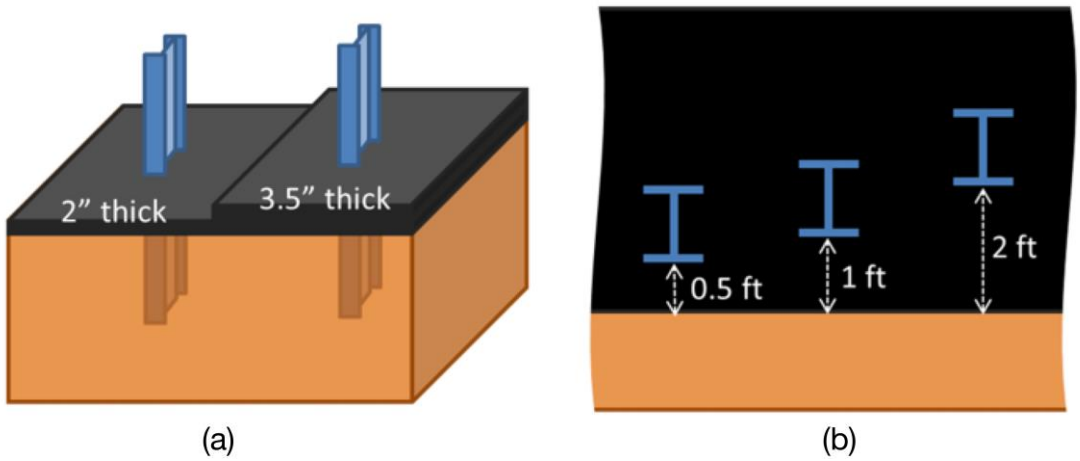

FIGURE 5

Guardrail post setups with
(a) different asphalt thicknesses and (b) various rear distances

Based on the experimental results, rupture appears to be the primary mechanism of the asphalt failure under static loading. As the rupture extends in the asphalt, the strength of the asphalt layer decreases up to the point that one section of the asphalt detaches from the rest of the mow strip. After this occurs the asphalt has a negligible impact on the system and the soil is the only source of ground restraint. Therefore, one potentially effective way to decrease mow strip restraint would be to introduce predetermined fracture planes (referred to as "cuts") in the asphalt layer. A controlled

rupture along a predetermined fracture plane in the asphalt avoids uncontrolled crack propagation in a large area and potentially reduces expected maintenance costs. The cuts would be designed based on the experimental and numerical investigation of rupture patterns of the asphalt layer. An example of a pre-cut mow strip is shown in Figure 6. This cut pattern was tested experimentally, and more design patterns were investigated using finite element simulations to find the most effective fracture pattern. Analysis of the results of these tests is provided in Chapters 3 and 4.

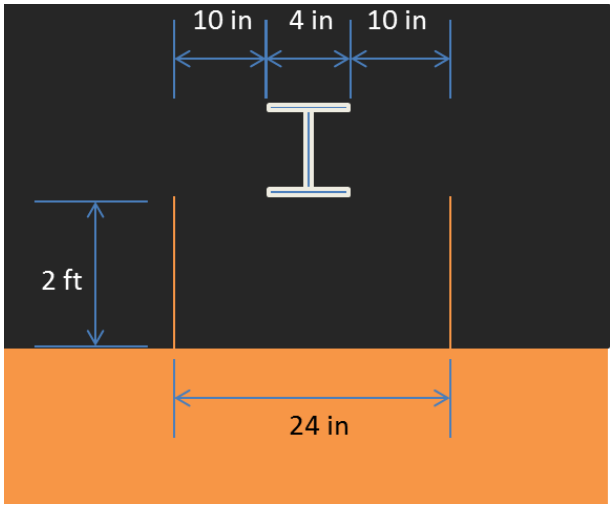

FIGURE 6

Schematic illustration of a guardrail post setup with a pre-cut asphalt layer

CHAPTER 3
STATIC TEST PROGRAM

3.1 Use of Static Tests to Evaluate Alternatives

The main objective of the static test program of Phase I of the overall research effort was to evaluate the structural performance of the guardrail post systems with different asphalt mow strip design and installation techniques. By applying a static lateral load to a single guardrail post, the amount of external work done by lateral loading can be estimated from the load-displacement response. The external work is the sum of the strain energy due to bending of the guardrail post and the dissipated energy of the surrounding soil and mow strip. In principle, the external work can thus be related to potential and/or kinetic energy (e.g., vehicle impact load) in a closed system.

It is well-known that static tests are not sufficient to fully evaluate the expected performance of a structural system under dynamic loading [37]. Nonetheless, it is reasonable to expect a correlation between the static load-displacement response of a given alternative post installation method (mow strip design) and the expected response under dynamic loads. As such, a targeted series of static tests paired with rational finite element analysis can provide a reasonable first-stage evaluation of the relative importance of a variety of geometric and material parameters on the structural performance of a guardrail post encased in a mow strip.

Additionally, a number of previous studies have reported that asphalt strength and other material properties are sensitive to ambient temperature and age of the asphalt [36-40]. Considering this sensitivity of the asphalt behavior to service conditions, a single static test cannot be considered a complete indicator of a post's structural behavior when

encased in a mow strip. As such, static tests in a variety of service conditions were conducted as part of this research program. Some of the tests performed were used to calibrate a refined finite element model (described in Chapter 4) which was then used to evaluate a number of different design and installation alternatives in a range of service conditions.

3.2 Test Setup

The outdoor test site used in this program is located adjacent to the Structural Engineering, Mechanics, and Materials Laboratory at the Georgia Institute of Technology's Atlanta, GA campus. Since the condition of the native silty soil at the test site was unknown, it was deemed essential to standardize the soil conditions to provide consistency for each test configuration. As such, the static test bed was constructed in accordance with guidelines found in the *AASHTO Manual for Assessing Safety Hardware* (*MASH*) [21]. As directed by the *MASH* guidelines, the base material was selected to meet *AASHTO M147* grading A/B requirements [43] and placed in an excavated trench 6 feet wide, 30 feet long and 5 feet deep. The soil was compacted to exceed 95% of the maximum dry density of soil as determined by the Modified Proctor test described in *AASHTO T180* [44].

Figure 7 shows a typical asphalt mow strip installation. In each test which included a mow strip, a hot mixed asphalt (HMA) layer was installed by a local contractor with GDOT paving experience. The asphalt mix type used in this project was classified as PG 76-22 binder and ¾ inch aggregate size, which is a typical asphalt mix type in Georgia roadway construction. Figure 8 shows a typical post installation procedure. About a week after the asphalt installation, steel guardrail posts were driven

through the asphalt layer (if present) and into the ground to reach the standard embedment depth 40 inches. The posts were driven by blows from a hydraulic post driver, owned by Georgia Department of Transportation. The time duration of a single post installation was typically less than 2 minutes.

FIGURE 7

Hot mixed asphalt (HMA) mow strip installation

FIGURE 8

Guardrail post installation

A schematic illustration of the static test setup including the loading fixture and instrumentation is given in Figure 9. A static load on the guardrail post is produced by the retraction of the hydraulic actuator. The self-weight of a reaction block prevents its lateral movement, forcing the post to displace toward the wall as the actuator retracts. Each component of the loading fixture was designed to carry at least twice the maximum expected lateral load for a post embedded in a mow strip. A more detailed description of the static test site and loading fixture setup is provided in Appendix B.

A computer-controlled data acquisition system was used to measure and record the following test data:

- Lateral load on the post
- Displacements of the post
- Longitudinal strains along the steel post flange

An S-type load cell connected the hydraulic cylinder to the post via a loading bracket. Threaded bearing rod ends were attached on both sides of the load cell to prevent bending and torsion along the load axis as shown in Figure 10. Two string potentiometers were mounted on a reference pole to measure lateral displacement at the load point (25 inches above ground level) and at the ground level. Nine gauges were attached on the tension side flange of each guardrail post to measure the longitudinal strain at locations ranging from 30 inches below ground level to 10 inches above ground level. A typical layout of the instrumentation is shown in Figure 11. A more detailed description of the instrumentation setup is provided in Appendix B.

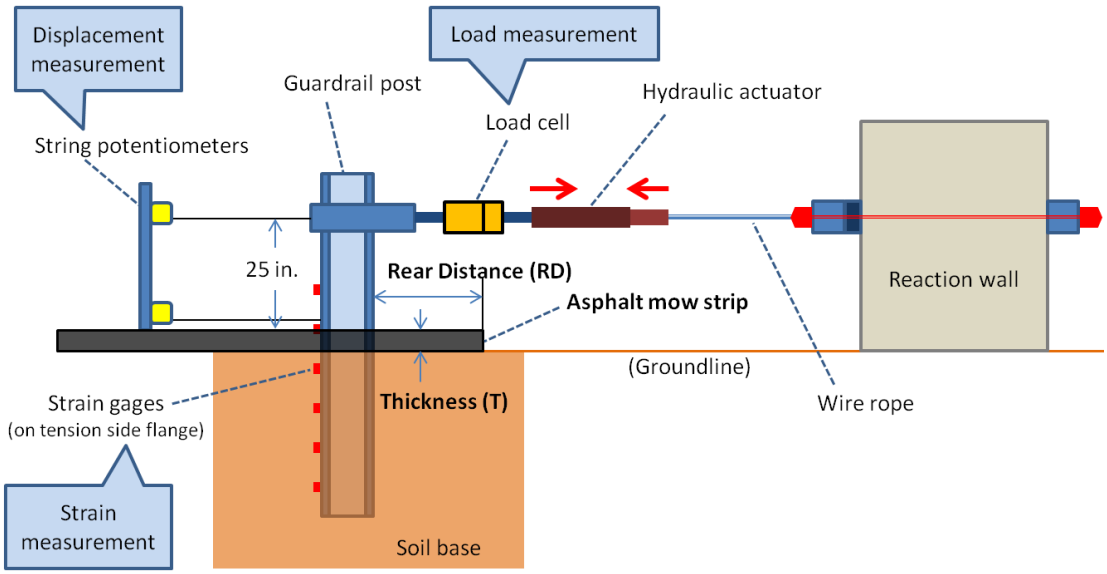

FIGURE 9

Static test setup with instrumentation

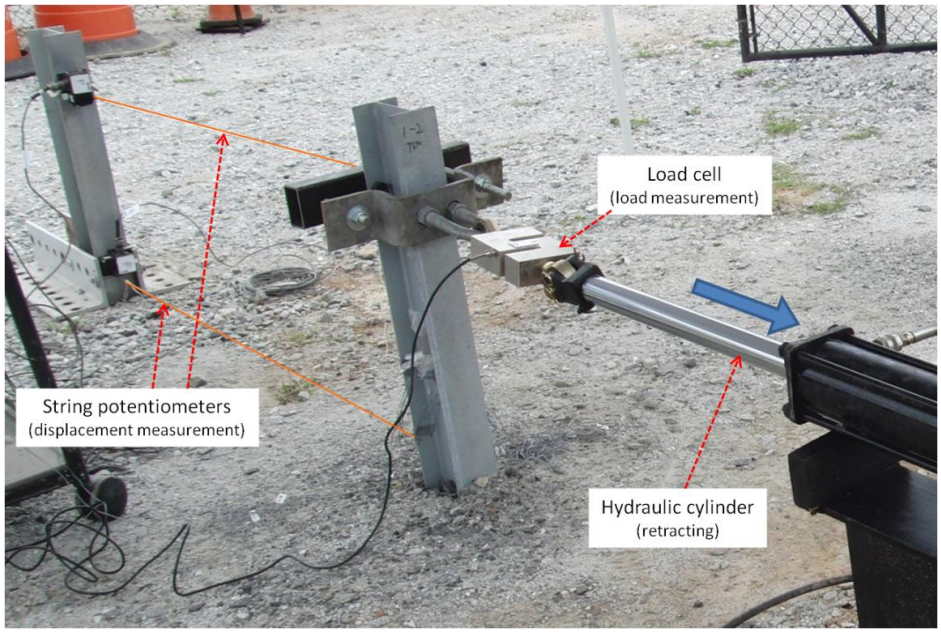

FIGURE 10

Loading fixture and instrumentation details

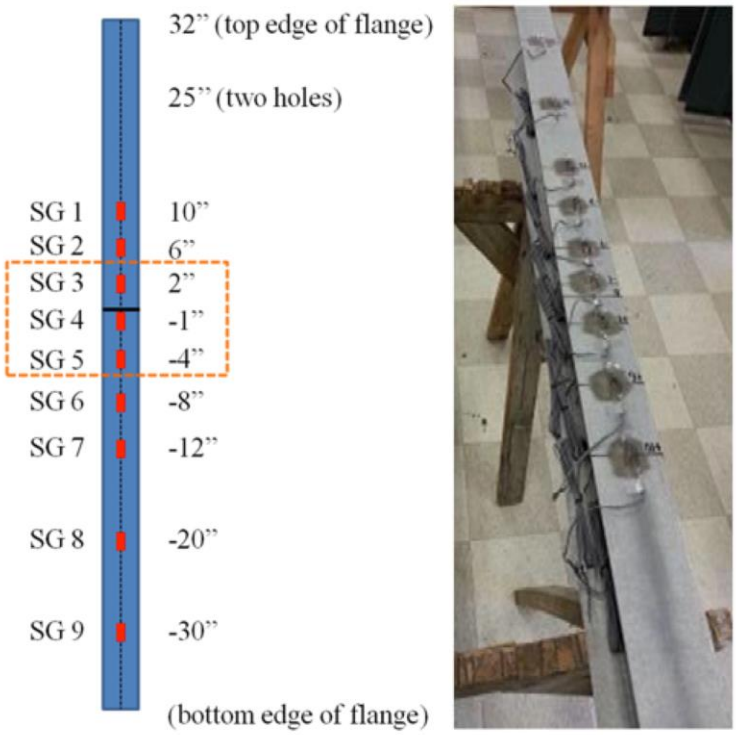

FIGURE 11

Strain gage installation details

As discussed in Chapter 2, the influence of two major design parameters- mow strip thickness (shown as *T* in Figure 9) and rear distance (*RD* in Figure 9) – were evaluated in the static test program. To aid in the test identification, a designation was adopted as follows: mow strip thickness followed by rear distance followed if necessary by a code which indicates additional modification in the mow strip (e.g., L when a leave-out was installed around the post). For example, a test designation of "2-24" indicates a typical mow strip configuration with 2 inch thickness and 24 inch rear distance, whereas "0-0" refers to a test setup with no mow strip.

3.3 Test Schedule for Experimental Program

Based on the results of the electronic survey and subsequent GDOT Workshop discussed in Chapter 2, a baseline setup with no mow strip along with the typical GDOT mow strip installation were identified for testing. In addition, a number of alternative test setups were identified for evaluation in the experimental program. These alternates included modified asphalt thickness and rear distance in the mow strip, installation of a leave-out in accordance with recommendations in the *Roadside Design Guide*, and pre-fracturing the mow strip prior to performing the test. Table 2 outlines the test matrix for the experimental program. A total of nineteen guardrail posts were tested in groups of 3 or 4. Pertinent test information including the age of the asphalt and the ambient temperature on the day of testing was also recorded. A more detailed description of all the static tests carried out in this project is given in Appendix B.

Initially, three different test configurations were identified to provide a useful frame of reference to compare to the alternative post installation methods evaluated in the project. The first configuration consisted of posts driven directly into the soil as shown in

Figure 12; this test setup was designated as “0-0” and referred to as the baseline configuration. To simulate the current GDOT preferred post installation method, two configurations involved posts driven through a mow strip, with an asphalt layer thickness of 2 inches for one setup and 3.5 inches for the other. Both configurations had the same rear distance of 24 inches as specified in the GDOT standard detail [35]; a typical setup for this configuration is shown in Figure 13. To attempt to provide some indication of the potential impact of ambient temperature and asphalt, tests using posts installed using GDOT’s preferred method were performed under two different service conditions. These service conditions are noted in Table 2 as Sets 2 and 3. The tests in Set 2 were performed in summer conditions with relatively young asphalt, which the research team felt would result in the most flexible asphalt layer and hence the least restraint. The tests in Set 3 were performed in winter conditions with older asphalt. These service conditions for Set 3 were expected to provide a less rigid asphalt layer and greater restraint than that seen in tests conducted in Set 2.

Based on the preliminary selection of post installation alternatives discussed in Chapter 2, three different alternative mow strip designs were identified for experimental evaluation under static loading:

- Inclusion of a leave-out in the mow strip
- Mow strip rear distance reduction
- Pre-cutting the mow strip behind the post prior to testing

TABLE 2
Static test matrix

Test set Test date	Test temp.	Asphalt age	Post No.	Test configuration	Description
1 of 5 6/3/2014	80ºF	-	1-1	0-0	Baseline: no mow strip
			1-2	0-0	
			1-3	0-0	
2 of 5 7/8/2014	90ºF	18 day	2-1	2-24	2” thick GDOT mow strip (summer)
			2-2	2-24	
			2-3	3.5-24	3.5” thick GDOT mow strip (summer)
			2-4	3.5-24	
3 of 5 2/12/2015	50ºF	118 day	3-1	3.5-24-L	Leave-out application
			3-2	3.5-24-L	
			3-3	3.5-24	3.5” thick GDOT mow strip (winter)
			3-4	2-24	2” thick GDOT mow strip (winter)
4 of 5 5/5/2015	75ºF	40 day	4-1	2-12	Reduced rear distance to 1/2
			4-2	2-24-C1	Parallel pre-cutting application
			4-3	2-24	Reference rear distance (24”)
			4-4	2-6	Reduced rear distance to 1/4
5 of 5 7/14/2015	70ºF	32 day	5-1	3.5-24-C2	Diagonal pre-cutting application
			5-2	3.5-12	Reduced rear distance by 1/2
			5-3	3.5-24-L	Leave-out application
			5-4	3.5-24-C2a	Diagonal pre-cutting application with asphalt sealer

FIGURE 12

Baseline setup with no mow strip (0-0 configuration)

FIGURE 13

GDOT preferred mow strip setup (2-24 configuration)

A total of three tests on the posts installed with leave-outs in accordance with the *Roadside Design Guide* were performed under a range of service conditions; a typical setup with leave-out is shown in Figure 14. Post installations with varying thickness (*T* in Figure 9) and mow strip rear distance (*RD* in Figure 9) were tested to better understand the influence of these parameters on the level of restraint provided by the asphalt layer. Additionally, three tests on posts with pre-cut mow strips setups were tested in Sets 4 and 5 of the experimental program. The orientation of the cuts placed in the asphalt layer were selected based on observations of the asphalt failure mechanism in tests performed in Sets 2 and 3 as well as finite element analysis results that will be discussed in Chapter 4. A schematic illustration of the pre-cut patterns employed in the experimental program is shown in Figure 15; a typical pre-cut post installation is shown in Figure 16 .

FIGURE 14

Mow strip with grout-filled leave-out

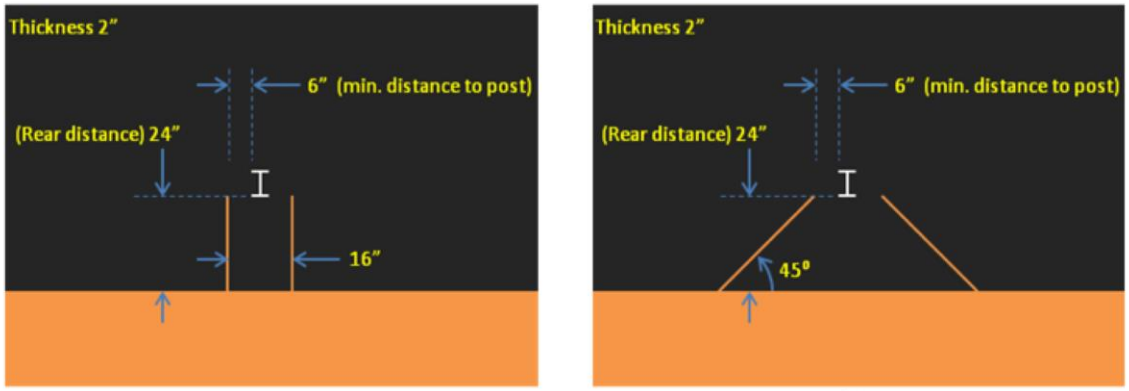

(a) (b)

FIGURE 15

Pre-cut mow strip patterns tested: (a) parallel, (b) diagonal

FIGURE 16

Typical Pre-cut configuration (parallel)

3.4 Test Results

Table 3 gives a summary of the results from the tests performed, including

- The peak force applied on the post
- The maximum recorded strain at the peak force
- The maximum strain at peak force normalized to the typical yield strain expected for steel, to provide an indication of whether post yielding occurred.

The load-displacement curves for selected tests are given in Figures 17 and 18; the test results shown in these Figures are considered representative of the various test configurations evaluated in the experimental program and are indicated using bold font in Table 3. Load displacement curves for all the tests are given in Appendix B.

TABLE 3
Summary of test results for experimental program

Post number	Test configuration	Peak force applied on the post (lb)	Maximum strain at peak force	Maximum strain at peak force divided by yield strain (0.00168)	Relevant figures for details
1-1	0-0	4673	0.000565	0.336	-
1-2	0-0	4247	-	-	-
1-3	**0-0**	**4743**	**0.000786**	**0.468**	**Figure 17**
2-1	2-24	4827	0.001177	0.701	-
2-2	**2-24**	**5491**	**0.001274**	**0.758**	**Figure 17**
2-3	**3.5-24**	**6663**	**0.001415**	**0.842**	**Figure 17**
2-4	3.5-24	5318	0.001062	0.632	-
3-1	3.5-24-L	6181	0.001579	0.940	-
3-2	**3.5-24-L**	**7262**	**0.001652**	**0.983**	**Figure 18**
3-3	**3.5-24**	**9553**	**0.002489**	**1.482**	**Figures 17,19**
3-4	**2-24**	**8672**	**0.002220**	**1.321**	**Figure 17**
4-1	**2-12**	**7429**	**0.001563**	**0.930**	**Figures 18,20**
4-2	**2-24-C1**	**6912**	**0.001662**	**0.989**	**Figures 18,21**
4-3	2-24	9598	0.002791	1.661	-
4-4	2-6	6492	0.001504	0.895	-
5-1	**3.5-24-C2**	**7577**	**0.001745**	**1.039**	**Figure 18**
5-2	3.5-12	9135	0.001729	1.029	-
5-3	**3.5-24-L**	**9096**	**0.001787**	**1.064**	**Figure 18**
5-4	**3.5-24-C2a**	**8689**	**0.001736**	**1.033**	**Figure 18**

Tests performed on posts installed using GDOT's preferred installation method demonstrate the impact of service conditions. The curves shown in Figure 17 indicate that tests performed in Set 2 under summer conditions resulted in less restraint provided by the asphalt layer than those tested in winter conditions (Set 3). As expected, for a given service condition mow strips of greater thickness provided a higher level of restraint on the post which is evidenced by the higher recorded peak force and strain in the post

recorded in Table 3. Test results using alternative installation procedures indicate that the selected alternatives did reduce post restraint at the ground line and resulted in static load-displacement behavior very similar to that exhibited by mow strips with leave-outs, as shown in Table 3 and Figure 18. The relative effectiveness of the alternative post installations compared to the GDOT preferred method will be discussed further in Chapter 5, where the results of the experimental program are correlated with results from finite element analysis.

The failure mechanisms in the asphalt layers observed in the experimental program varied depending on the specific test setup, and provided an indication of the relative amount of restraint imparted to the post by the mow strip. Figure 19 gives before and after conditions for a post tested using GDOT's preferred installation method and an asphalt thickness of 3.5 inches (designated as Post 3-3, 3.5-24 test configuration). This

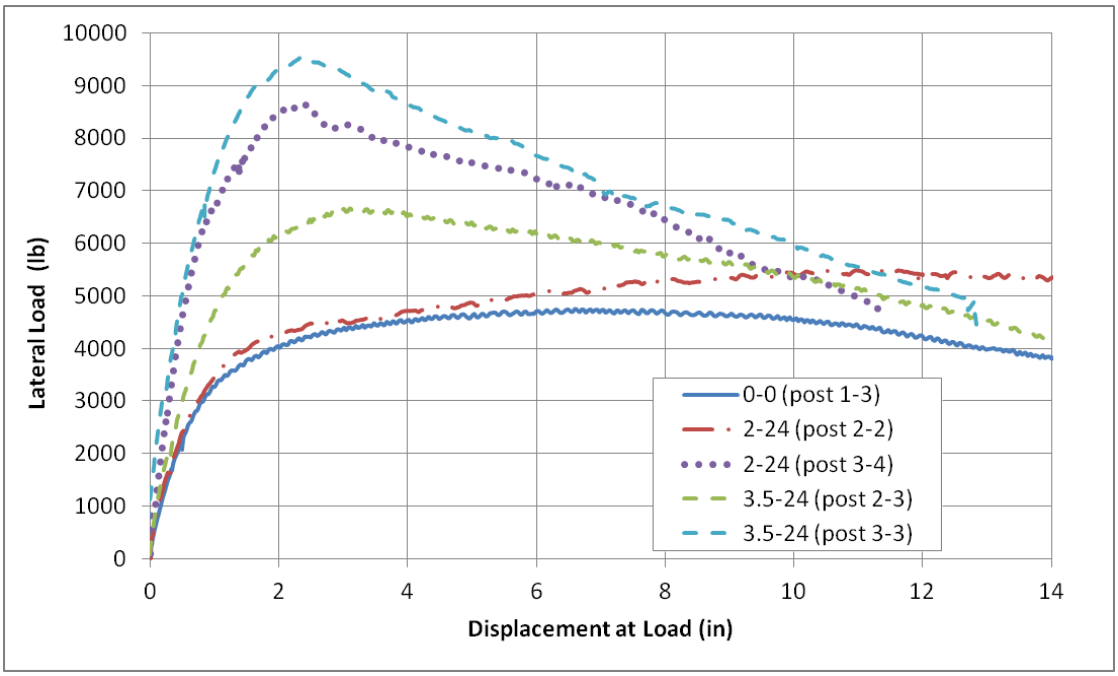

FIGURE 17

Representative load-displacement curves (baseline and GDOT preferred setups)

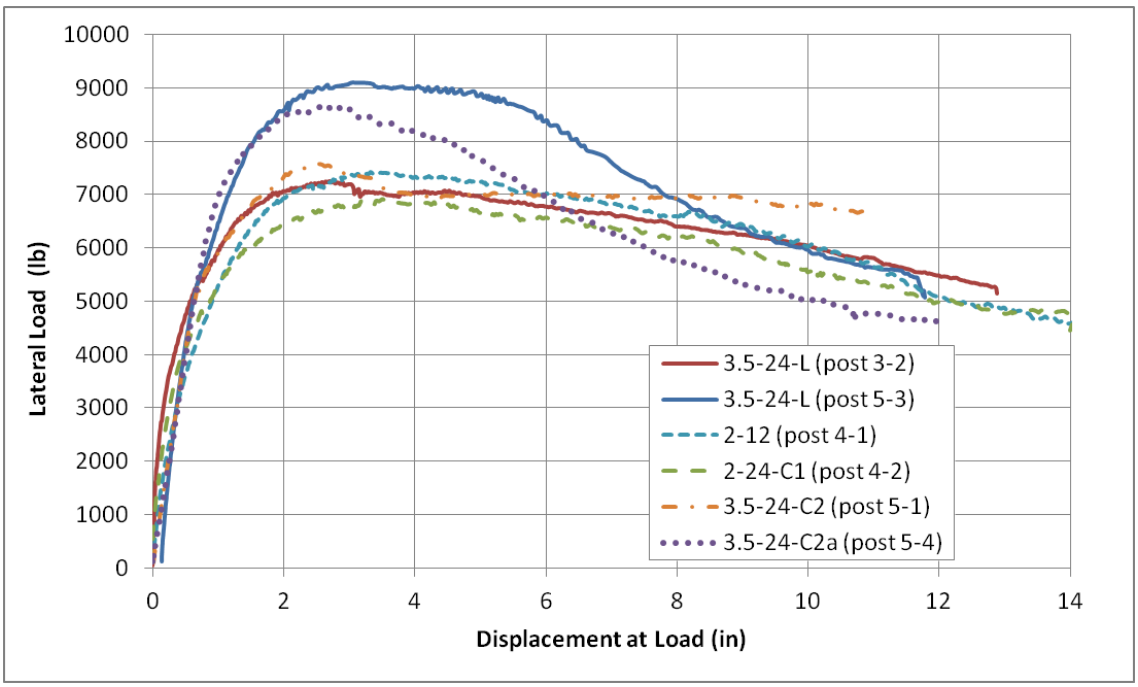

FIGURE 18

Representative load-displacement curve (alternative mow strip setups)

post installation resulted in higher relative restraint during the test, as shown by the test results given in Table 3 and the load displacement curve in Figure 17. During this test, two large cracks appeared at the leading edge of the post flange and propagated in a diagonal direction to the edge of mow strip. Another major crack initiated at the edge of the mow strip and propagated toward the post. Observations of the failure mechanisms in the asphalt layer in test Sets 2 and 3 were used in conjunction with finite element analysis results (discussed in Chapter 4) to select the orientation of cuts installed in the mow strips as an alternative during later testing.

Failure mechanisms in the asphalt layer for the tests with a reduced mow strip rear distance indicate a lower level of restraint on the post compared to the GDOT preferred design. This is also observed in tests on posts with pre-cut mow strip configurations. Figure 20 gives before and after conditions for a post tested with a reduced mow strip

rear distance (designated as Post 4-1, 2-12 test configuration in Table 3 and Figure 18). While the asphalt failure mechanism shown in Figure 20 is generally similar to that for the post installed using GDOT's preferred method, the measured values for the peak force and post strain are significantly lower than those from the previous tests.

(a) (b)

FIGURE 19

GDOT standard configuration (3.5-24), Post 3-3: (a) before test; (b) post-test

(a) (b)

FIGURE 20

Reduced rear distance (2-12), Post 4-1: (a) before test; (b) post-test.

Failure mechanisms in the asphalt layer for tests with a pre-cut mow strip are indicative of a potentially significantly lower level of restraint on the post compared to the GDOT preferred design. Figure 21 gives before and after conditions for a post tested with pre-installed cuts in the mow strip behind the post (designated as Post 4-2 and 2-24-C1 test configuration in Table 3 and Figure 18). The cuts introduced in the mow strip prior to testing resulted in a more controlled and easily predictable asphalt failure mechanism as shown. In addition, the measured values for the peak force and post strain for the tests performed with pre-cut mow strips were significantly lower than those from the previous tests using GDOT's preferred installation method. Figures showing the condition of the posts after loading are provided in Appendix B for all the tests conducted in this program.

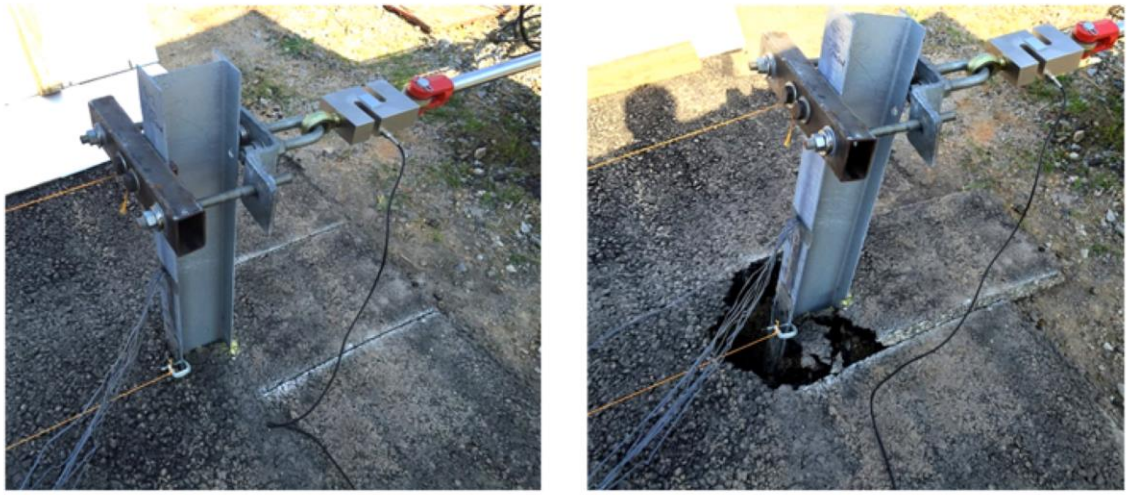

(a) (b)

FIGURE 21

Pre-cut mow strip (2-24-C1), Post 4-2: (a) before test; (b) post-test

3.5 Summary

The results of the experimental program indicate that the potential alternatives identified in Chapter 2 result in lower levels of post restraint compared to GDOT's preferred method under static loading. In addition, the static response of posts tested with the alternative configurations demonstrated very similar load-deformation behavior to posts installed with leave-outs as recommended in the *Roadside Design Guide*. As noted previously, behavior of a given structural system under static loading is not considered absolutely representative of the performance of that system under dynamic loading. However, results from the static experiments performed in this program were used to formulate criteria to provide a reasonable indication of expected dynamic performance, particularly in a relative sense. The development of these criteria is discussed in Chapter 5 of this report, where the static test results are correlated to results from parametric finite element analyses for guardrail posts embedded in asphalt mow strips.

CHAPTER 4
FINITE ELEMENT SIMULATIONS

4.1 Overview of Modeling of a Guardrail Post System

It is often not cost-effective to perform full-scale experimental tests on a fully inclusive set of parameters. Impact simulation of guardrail posts using nonlinear FE analysis is an effective way to design and assess these systems. Material properties can be obtained by experimental testing of material specimens and calibration of the model with a reference experimental test on the system. Once the model is calibrated with a reference experimental test, the material properties are kept constant. Then the performance and accuracy of the model is verified by comparing results from the model with further experimental tests. After this verification, the model can be used independently to conduct parametric studies.

In this research, soil type and density are determined from material tests on soil specimens. Then the other material properties of the soil are found by calibration of the model with a reference experimental test on a guardrail setup without mow strip. These parameters are subsequently maintained as constants in the model to predict further experimental results and conduct parametric studies.

Similarly, the asphalt density, cohesion, and shear modulus, are estimated from material tests on asphalt specimens. The other asphalt material parameters are found by calibration of the model with an experimental test on a guardrail post setup with a 3.5 inch thick asphalt mow strip. Then the asphalt parameters are held constant, and the results from the model are compared with experimental tests on guardrail posts with mow strips with various thicknesses and rear distances. The model proves to be able to

produce accurate results independently and is used to predict further experimental test results and conduct parametric studies.

The interactions between the soil, asphalt, and post play a vital role in the response of the post during an impact event. These interactions can be studied by considering the post to be a laterally loaded pile. There are various conventional techniques for solving laterally loaded pile problems; these methods are used for static conditions and infinite soil domain. In the analysis of these cases, two standard approaches are employed: (1) the finite element approach, in which the post is embedded in a soil continuum of solid finite elements, and (2) the subgrade reaction approach, in which the post is supported by a series of uncoupled springs. The subgrade reaction method has been used widely in the past because of the high computational cost associated with 3D FE modeling of the soil around the guardrail post. However, in recent years researchers have made efforts to model the post-soil interaction using the finite element approach. In this method, finite element models are constructed of the post embedded in a continuum of soil modeled using three-dimensional solid elements. Although, the subgrade reaction approach is still used as a practical method of analyzing the post-soil interaction, this method only provides an overall performance assessment of the soil-structure interaction and does not provide insights into the damage and soil deformation mechanisms.

At the present time, simulations of physical responses using 3D Finite Element Analysis (FEA) can be readily produced. The availability of FEA tools provides substantial promise for detailed numerical studies to address outstanding questions.

However, the quality of the results from 3D-FEA simulations depends on the accurate representation of the following:

- Geometry details
- Boundary conditions: loads and displacements, infinite boundaries.
- Assumed initial conditions such as gravity load applied to the components.
- The constitutive relationships for the various constituent materials such as loss of strength in the soil and asphalt at large deformations, asphalt material properties, and the rupture of asphalt.
- The assumed contact between various components such as the contact between the soil and the post as well as the asphalt layer and the soil.

These problems are addressed in detail in the following sections.

4.2 Description of Simulation Model without Mow Strip

In this research, 3D FEA is used accurately to calculate the guardrail post response subject to static loading. All of the 3-D FEA studies are conducted using the LS-DYNA® V971 R8.0 platform [18]. The soil domain considered in the model without mow strip is a rectangular prism, with a depth (z direction) of 5.6 feet, and planar dimensions of 32 feet in the x direction (perpendicular to the post lateral movement) and 16 feet in the y direction (parallel to the post lateral movement). The steel post is a W6x9 member with a total length of 72 inches and an embedded depth of 40 inches. The finite element model is comprised of 92200 solid elements for the soil and 1000 shell elements for the steel post. The bottom boundary of the soil is fixed for the pseudo-static loading, and the lateral soil boundaries are modeled using the nonreflecting boundary condition.

The nonreflecting (i.e., transmitting) boundary condition involves the application of viscous normal and shear stresses to the boundary segments:

$$\sigma_{normal} = -\rho c_d V_{normal} \tag{1}$$

$$\sigma_{normal} = -\rho c_d V_{normal} \tag{2}$$

Where ρ, c_d, and c_s are the material density, dilatational wave speed, and the shear wave speed of the transmitting media, respectively. The magnitudes of these stresses are proportional to the particle velocities in the normal (V_{normal}) and tangential ($V_{tangential}$) directions. This type of boundary condition only provides viscous stresses and cannot provide stiffness at the boundary of the model that would be present in the case of an infinite medium. Therefore, in the static problem, the lateral boundaries must be far enough away from the post such that the displacements at the boundaries are negligible and the response is insensitive to the lateral boundary assumption. In the case of dynamic loading, all the boundaries within the soil can be represented using nonreflecting boundary conditions. The static problem is solved with a dynamic explicit integration. Verifications have been made to check that the loading rate and the simulation time are long enough to avoid dynamic oscillations and mass inertia effects.

The constitutive model for the elements representing the post is piecewise linear metal plasticity, in which an experimental stress-strain curve, the yield strength of the steel, modulus of elasticity, and Poisson's ratio are given as inputs. This model enables simulating steel strain hardening and strain rate sensitivity. For the pseudo-static loading simulations, the strain rate sensitivity of the steel material is deactivated. However, this feature can be enabled during dynamic testing to account for strain rate effects in the steel material. The common steel parameters presented in Table 4 are employed. To account

for the strain hardening part an experimental stress-strain curve for a typical guardrail steel post material was utilized [3]. Shell element formulation number 16 (fully integrated shell element), which does not have hourglass modes, is used for the steel post.

TABLE 4
Steel mechanical properties used in the FE model

Constitutive Parameter	Value
Density, ρ	445 lb/ft^3
Young modulus, E	29000 ksi
Poisson's ratio, ν	0.3
Yield Strength, σ_y	50 ksi

4.3 Calibration of Simulation Model without Mow Strip

First, a model without an asphalt mow strip was created. The nodes in the post 25 inches above the ground level were moved perpendicular to the axis of the post (y direction). The displacement rate was changed from 5 ft/s to 0.16 ft/s, and it was observed that displacement rates slower than 0.8 ft/s show the same performance as 0.8 ft/s. Therefore, 0.8 ft/s (0.6 mph) displacement rate was chosen for the pseudo-static loading. The ratio of the kinetic energy to internal energy was also measured to ensure the displacement rate is a good representation of pseudo-static loading. The contact forces between the post and the soil in the y direction were determined to calculate the applied force-applied displacement curve. For the cases including a mow strip discussed below, evaluating the contact forces between the post and the soil and mow strip allows direct evaluation of the separate forces contributed from the soil and from the mow strip.

Based on the laboratory test on a soil sample, the density of the soil was 144 lb/ft^3. This value was used as the soil density in the numerical modeling. The soil friction angle, dilation angle, *C* parameter (known as cohesion), and elastic shear modulus were calibrated against experimental results obtained for the static tests. The model was calibrated to fit the force-displacement curve of the post before and after the peak force including the softening behavior. A standard value of 0.25 was used for the Poisson's ratio that is typical for the mixture of gravel, coarse sand, and silt [45]. The initial linear elastic portion of the force-displacement curve was used to calibrate the shear modulus equal to 7.3 ksi. The *C* parameter and peak friction angle were calibrated to capture the maximum force and the displacement at which the peak force happens: values of 1.3 psi and 45 degrees were found for the cohesion *C* and peak friction angle ϕ respectively, which are in the range of recommended values for the soil used in this experiment [46]. The small value of *C* was expected for a coarse grain soil since *C* represents soil cohesion that is typically associated with strength due to suction in fine grain soils. The value of the peak friction angle of 45 degrees falls within the range of recommended values for gravel with sand and silt. The dilation angle was set equal to zero to avoid the well-known issue of overestimation in the Mohr-Coulomb yield criterion for soils with dilation [47]. The critical friction angle was set equal to 15 degrees to capture the softening portion of the load-displacement response. A curve was specified to define the friction angle of the Mohr-Coulomb material model as a function of the effective plastic strain. The friction angle was assumed constant equal to 45 degrees up to the plastic strain of 0.4, and reduced linearly to 15 degrees between plastic strains of 0.4 to 0.5 and remained constant after that. The density of the soil obtained

using laboratory sieve test and other parameters obtained by calibration are shown in Table 5. The numerical force-displacement curve after calibration is compared to the experimental force-displacement curve in Figure 22. The FEA curve was filtered to remove high-frequency noise in the result. It can be observed that the FE simulation result shows good agreement with the experimental outcome. The ground level displacement for the post and the instantaneous center of rotation for the post are shown in Table 6 for the FEA simulation and the experimental test.

TABLE 5
Soil mechanical properties used in the FE model

Constitutive Parameter	Value
Density, ρ	144 lb/ft^3
Cohesion, C	1.3 psi
Peak friction angle, ϕ'	45°
Critical friction angle $\phi'_{critical}$	15°
Dilation angle, ψ	0°
Interface coefficient of friction, μ	0.6
Shear modulus, G	7.3 ksi
Poisson's ratio ν	0.25

TABLE 6
Comparison of deflection of the post between FEA and experimental results

Parameter	Test 1-3	FEM	% Difference
Ground level displacement	2.65”	2.56"	3.40%
Center of rotation	-28.0”	-29.0"	3.57%

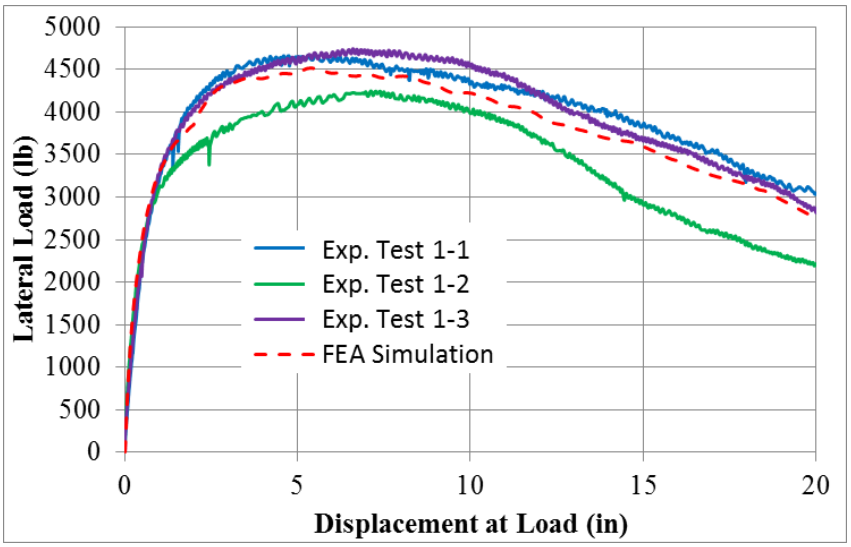

FIGURE 22

Comparison of load-displacement curves between FEA and experimental results

4.4 Modeling of the Asphalt Mow Strip

Asphalt is a viscous material. In this research, the ultimate goal is to perform dynamic testing of the guardrail system. The loading rate corresponding to a vehicle crash is relatively high, and the viscous effects of the asphalt have a slight effect on its performance. The problem was simplified by lowering the shear modulus of the material to account for the viscous deformation effects under the static loading. To model dynamic loading, the shear modulus will be scaled up to its actual value to remove the viscous deformation effects. The shear strength of the asphalt is known to be pressure dependent. Mohr-Coulomb and Drucker-Prager material models are widely used to model asphalt. Because the Mohr-Coulomb constitutive parameters - friction angle and cohesion - are directly obtainable from laboratory tests, this material model was chosen to effectively model the shear strength of the asphalt. The density of the asphalt was estimated to be equal 144 lb/ft^3 using laboratory tests. The Poisson's ratio and friction angle of the asphalt concrete were specified as 0.35 and 35 degrees, respectively, which

are typical values for asphalt concrete. The shear modulus of elasticity and cohesion of the 118 day old asphalt concrete at the temperature of 68 °F, using experimental unconfined compression tests on asphalt specimens, were estimated to be equal to 7 ksi and 69 psi. In addition, the *C* parameter for soil was increased to 1.9 to account for the increase of soil strength due to asphalt compaction and moisture being trapped in the soil because of the asphalt cover.

The tensile rupture in the asphalt observed in the experimental tests was modeled as follows. When an element fails by rupture, it loses stiffness and is removed from the computations. This is done in LS-DYNA software using an element erosion approach. Element erosion can be done through the material model by including erosion criteria in the material model's formulations. Another way to apply the element erosion is using general element erosion criteria for solid elements. Each criterion is applied independently, and satisfaction of one or more criteria causes deletion of an element for the calculation. The number of erosion criteria, which must be satisfied before an element is removed, can be specified by the user. The criteria for failure employed in this research were:

1) $\sigma_1 \geq \sigma_{max}$, where σ_{max} is the failure principle stress and σ_1 is the current maximum principal stress.
2) $\varepsilon_1 \geq \varepsilon_{max}$, where ε_{max} is the failure principal strain and ε_1 is the current maximum principal strain.

The maximum principal stress criterion was used to remove the elements when the tensile failure criterion is met. However, the rupture in the asphalt was abrupt when solely this criterion was used, and the strength decreased dramatically similar to what is commonly

observed in very brittle materials. To account for the fact that asphalt is not as brittle as rock (for example) and can accommodate larger strains before failing under tensile stress, an additional strain-based failure criterion was added to the material model - the maximum principle strain. Therefore, an element is removed when both the maximum principal stress criterion and the principle strain criterion are satisfied. By calibrating the post-peak response of the system, the maximum principle stress and maximum principle strain at failure were obtained as 87 psi and 0.09 respectively. A comparison between the results obtained from the FEA simulation and the experiment for 3.5" and 2" asphalt is presented in Figures 23 and 24. The model calibration was only conducted for 3.5" asphalt and the same parameters were used for the model for 2" asphalt. The asphalt's density, cohesion, and shear modulus, which were estimated using laboratory tests, and other parameters obtained from calibration are shown in Table 7. These parameters are kept constant for all parametric studies on mow strip geometry presented in the next section.

A detailed description of the FE model is presented in Appendix C.

TABLE 7
Asphalt concrete mechanical properties used in the numerical model for asphalt

Constitutive Parameter	Value
Density, ρ	144 lb/ft^3
Cohesion, C	69 psi
Friction angle, ϕ'	35°
Dilation angle, ψ	0°
Shear modulus, G	7.3 ksi
Poisson's ratio ν	0.35
Maximum principle stress, σ_{Max}	87 psi
Maximum principle strain, ε_{Max}	0.09

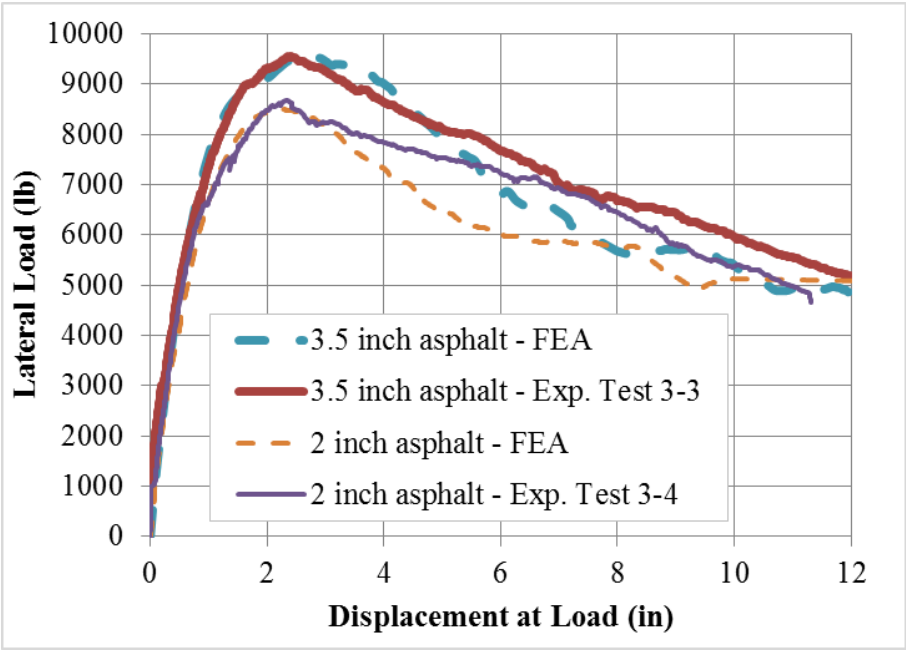

FIGURE 23

Comparison between FEA result and the experimental result for 2" asphalt and 3.5" asphalt

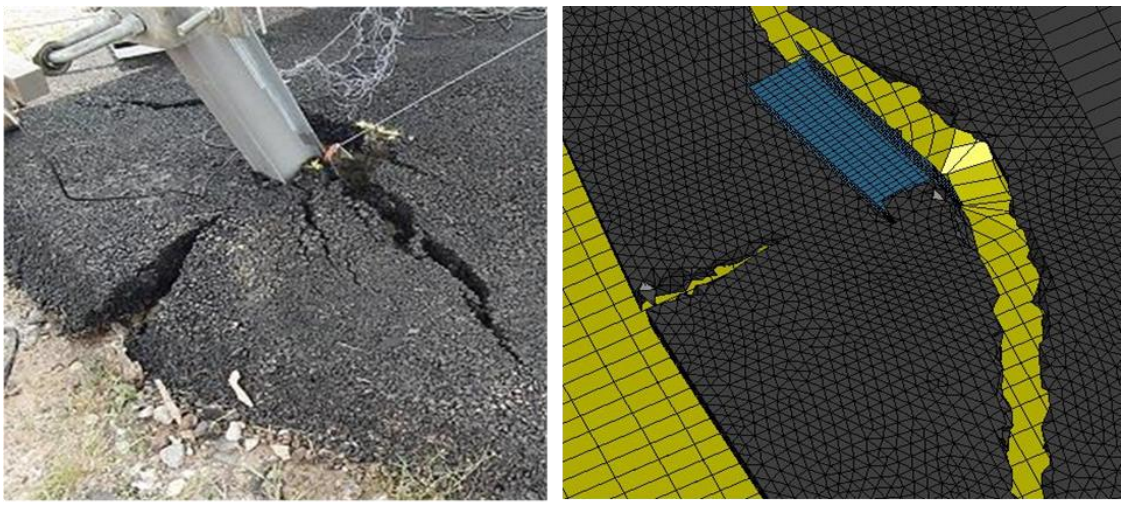

a. Experimental test b. FEA Simulation

FIGURE 24

Comparison of asphalt rupture in (a) static tests and (b) FEA simulation

4.5 Parametric Studies

Changing the asphalt mow strip geometry including the thickness of the asphalt layer and the rear distance influences the guardrail post system performance. Parametric studies on different thicknesses and rear distances are needed to study the impact of each of these parameters. Thicknesses equal to 1, 2, 3.5, 5, 7, and 10 inches were included in the simulations to show the system response for mow strips ranging from very thin to very thick. The rear distance values of 0, 0.5, 1, 2, and 4 feet were used. The results are presented in Chapter 5.

As mentioned in Chapter 2, one effective way to decrease the asphalt ground restraint is to pre-cut the asphalt. Different possible pre-cutting alternatives are presented in Figure 25. These alternatives were studied using FEA. The results of these FE simulations are shown in Figure 26. Based on the FEA results and analysis of peak forces and stresses in the post, designs 2 and 3 are determined as not being effective, since they do not significantly decrease the asphalt ground restraint. As shown in Table 8, Designs 1, 4, 5, and 6 are effective designs, since they decrease the peak load and ground restraint significantly.

TABLE 8
The peak force for different pre-cutting designs

Design Number	FEA Peak Force (kip)
1	6.65
2	8.01
3	8.23
4	6.34
5	6.20
6	6.30

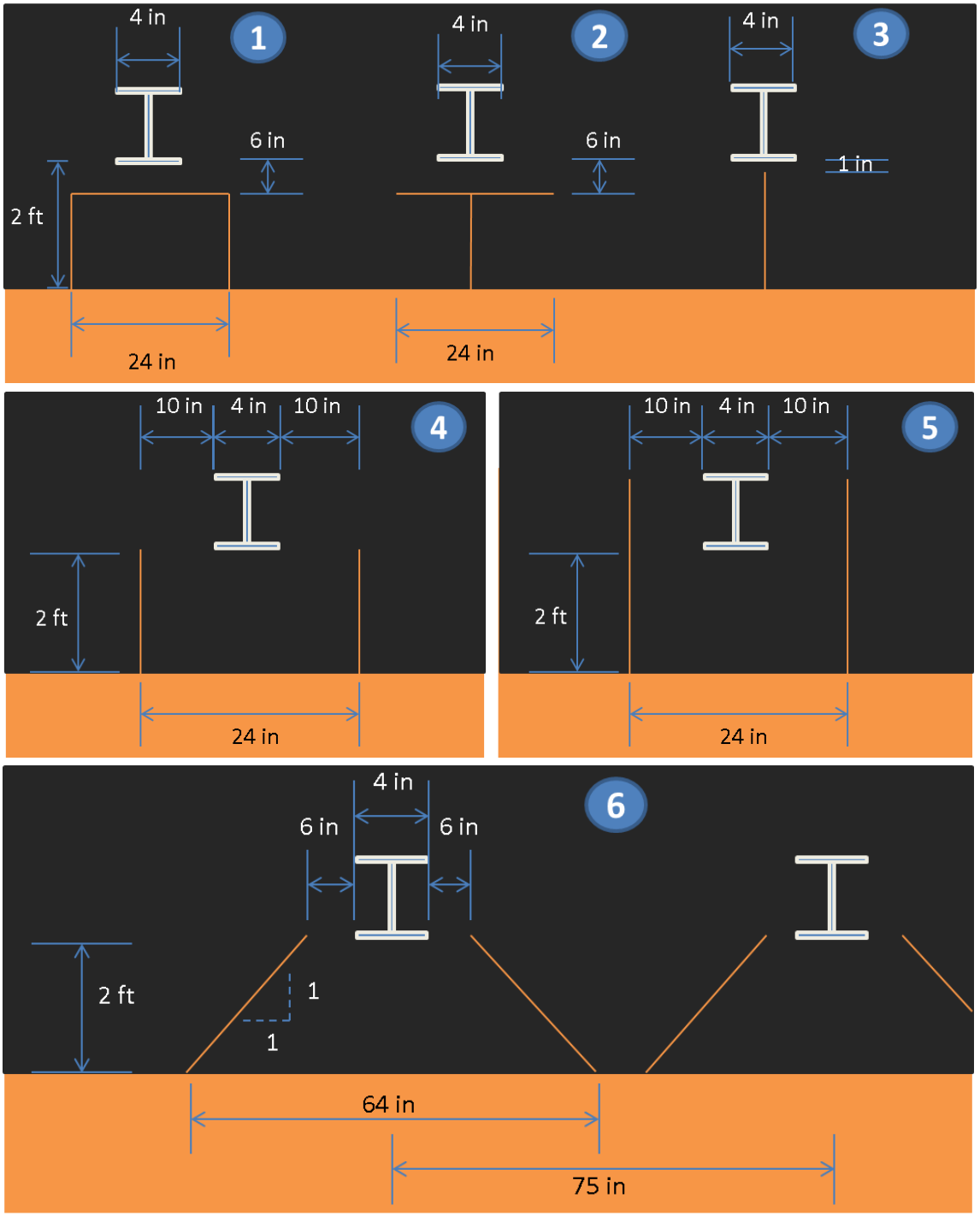

FIGURE 25

Different pre-cutting designs for the asphalt mow strip

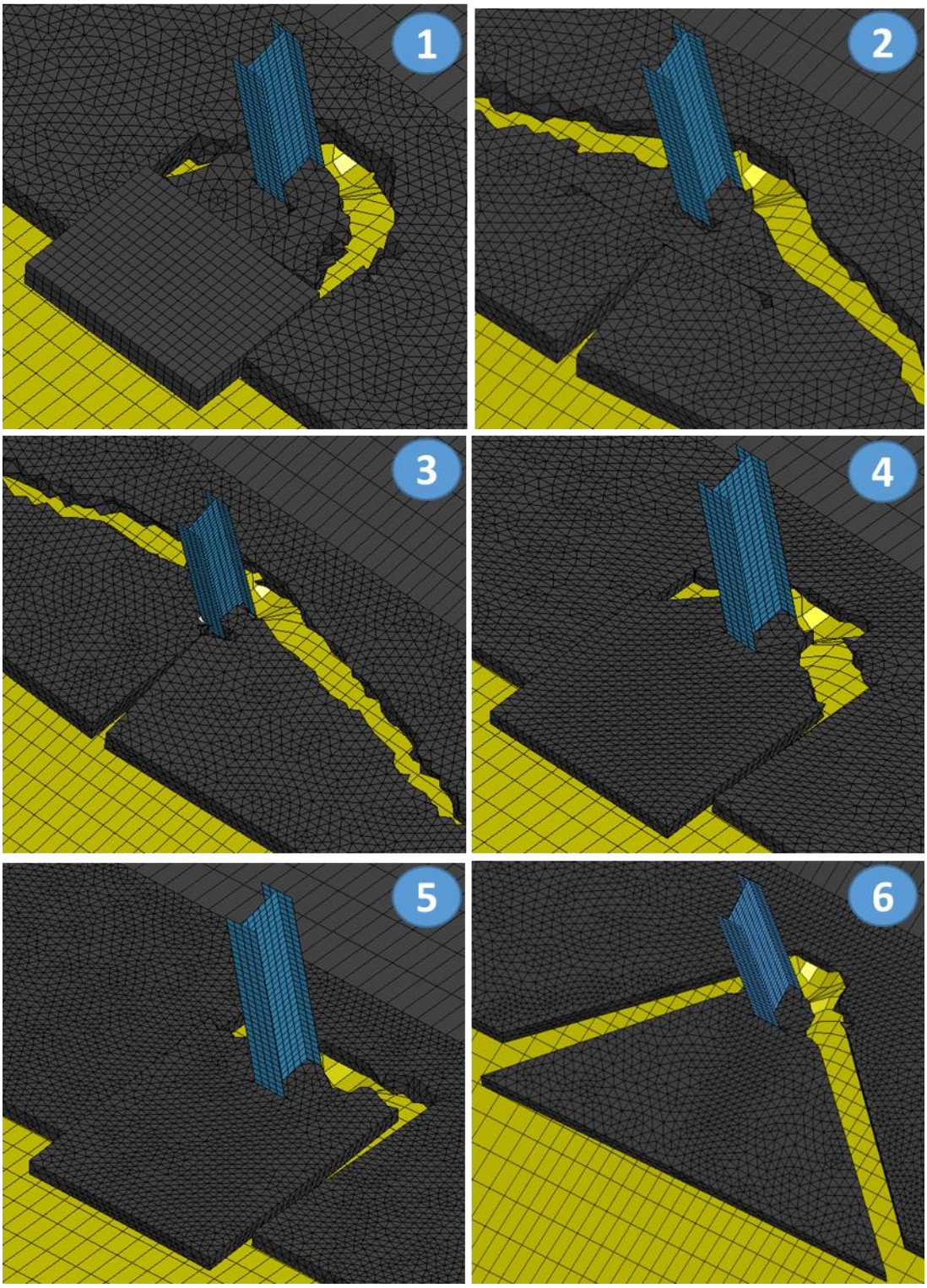

FIGURE 26

FEA results for different pre-cutting designs

CHAPTER 5
CORRELATION OF RESULTS AND DISCUSSION

5.1 Development of Quantitative Performance Criteria

The *AASHTO Roadside Design Guide* (the "*Guide*") uses qualitative observations to evaluate the performance of guardrail posts [2]. A guardrail system is considered to exhibit better performance if the post is allowed to rotate in the soil, since the post rotation absorbs some of the energy from an impact and reduces the chance for guardrail rupture. The *Guide* also asserts that premature breaking of the guardrail post can be avoided by allowing the post to rotate in the soil. The *Guide* recommends replacing a minimum of 7 inches on the rear side of the mow strip with a relatively weak material such as a low-strength cementitious grout. However, the *Guide* appears to classify the mow strip as a rigid foundation, which fundamentally precludes assessing the relative impact of mow strip configuration on the behavior of the guardrail system. The experimental and finite element analysis results presented in Chapters 3 and 4 of this report indicate that it is more appropriate to consider the asphalt layer as a deformable media, which can result in deformation and even failure in the mow strip itself. As such, quantitative assessment criteria should be developed to properly evaluate the relative performance of posts installed with mow strips that have varying geometric or material parameters. The use of quantitative assessment in lieu of a simple pass/fail criterion also enables a comparison between the structural performance of alternative mow strip designs and the mow strip leave-out recommended in the *Guide*. Ultimately, as stated previously in this report, dynamic testing will be necessary to ascertain if a given post/mow strip system will perform as expected. However, when properly applied, these

criteria can be used as a first-stage indication of the expected relative performance of guardrail posts in mow strips. Thus, post/mow strip combinations which have the best potential to give satisfactory performance (and those which are more likely not to perform satisfactorily) can be pre-identified using more cost effective evaluation techniques – such as tests under static rather than dynamic loading.

In the present work, three quantitative assessment criteria have been identified based on the description of desirable post behavior in the *Guide*. These criteria are identified as follows: Peak Applied Force, Ground Level Displacement, and Maximum Post Strain. These criteria can be explained by Figure 27, which gives an illustration of the behavior of two laterally loaded posts with significantly different embedment conditions. When a post embedded in a flexible material is subjected to lateral loading, bending of the post is negligible and ground-level displacement is proportional to the displacement at the top of the post. On the other hand, when a post is embedded in a rigid material, the post has no ground displacement and will exhibit plastic bending as the lateral load exceeds the yield load. The post embedded in a rigid material will therefore carry a higher lateral load and will have a higher longitudinal strain and reduced displacement at the ground level. One simple quantitative indication of relative post performance is to compare these values for different post/mow strip installations.

The peak force applied to the post is the simplest indicator of potentially excessive restraint in the post/mow strip system. From both the FEA and static tests, a mow strip setup with thicker or wider rear distance results in a higher peak force. Assuming static equilibrium at the peak load, this creates a higher flexural stress in the post at the ground level. If analysis and test results indicate that an alternative mow strip

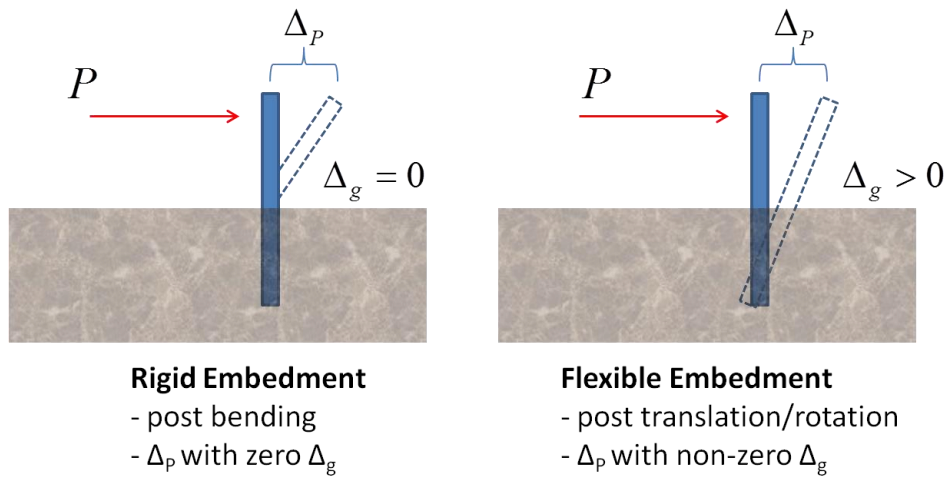

FIGURE 27

Behavior of guardrail post in different embedment conditions

setup gives a similar or lower peak force than a mow strip incorporating a leave-out, the alternative design may provide a similar level of restraint under dynamic loading.

The ground level displacement of the post can also be an indicator of lateral restraint of the system. When two identical posts with varying embedment conditions are subjected to an equal amount of external work in the lateral direction, a post embedded in a relatively rigid material will exhibit less ground level displacement. Since it is known in a closed system that dissipated energy is equivalent to the amount of work done by the external loading, the ground level displacement of the post can be plotted as shown in Figure 28. A slope that is less steep as shown by the dashed curve indicates the potential for a relatively desirable performance in the post/mow strip system.

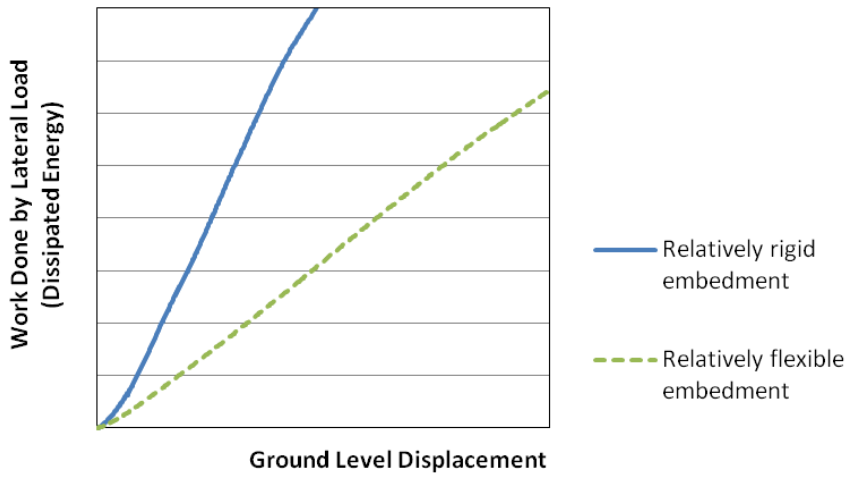

FIGURE 28

Relationship between ground level displacement and dissipated energy

A standard dissipated energy level based on the *MASH 3-10 test condition* was selected as a reference value to compare to computational and experimental results. This particular *MASH* test, shown in Figure 29, specifies a crash condition of a passenger car which weighs 2425 lbs (M=75.4 slug) and has an impact velocity of 62 mph (V=90.9 ft/s) with an impact angle of 25 degrees. The lateral kinetic energy (KE) is calculated as follows:

$$KE = \frac{1}{2}MV^2 = \frac{1}{2}(75.4\,\text{slug})(90.9\sin 25^\circ\,\text{ft/s})^2 = 55600\,\text{lb-in} = 667\,\text{kip-in} \tag{3}$$

Assuming the lateral kinetic energy is distributed over 10 guardrail posts (n=10) along the length of test section as shown in Figure 29, the average dissipated energy (ED_{avg}) on each post can be estimated as 66.7 kip-in.

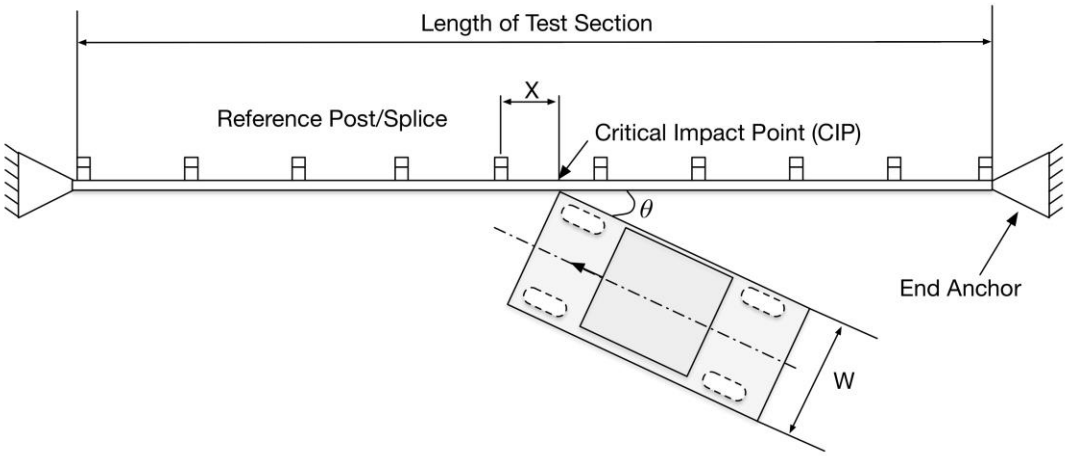

FIGURE 29

MASH test 3-10 crash condition (adapted from [21])

The maximum longitudinal strain in the post flanges is the third quantitative indicator of potential excessive restraint of a given post/mow strip system. As seen in Figure 27, a guardrail post embedded in a rigid material undergoes significant flexural bending when the lateral load increases beyond the yield load. For simplicity, a normalized maximum strain can be calculated from the maximum strain measured in the post divided by the yield strain. When yielding occurs during the lateral loading test or simulation, the normalized maximum strain will exceed 1.0. If computational analysis and experimental test results indicate that an alternative mow strip setup results in a similar or lower normalized strain than a mow strip incorporating a leave-out, the alternative design may provide a similar level of restraint under dynamic loading.

Based on this rationale, three quantitative criteria can be established to evaluate whether a given post/mow strip configuration, subjected to a controlled lateral loading, could potentially provide a similar or lower level of restraint compared to a post embedded in a mow strip incorporating a leave-out:

1) The post/mow strip system has a similar or higher ground level displacement at the reference value of dissipated energy (66.7 kip-in) compared to a mow strip incorporating a leave-out.
2) The post/mow strip system has a similar or lower peak force compared to a mow strip incorporating a leave-out.
3) The post/mow strip system has a similar or lower normalized strain compared to a mow strip incorporating a leave-out.

5.2 Performance Evaluation of Alternative Mow Strip Designs

Assuming there is relationship between the static and dynamic performance of a guardrail post installed in a mow strip, the quantitative criteria described in the previous section can be used to identify which alternative configurations have the greatest potential to perform under dynamic loading as well as or better than a post /mow strip system incorporating a leave-out as recommended in the *Guide*. If a given post/mow strip system does not satisfy any of the criteria, it is reasonable to assume that configuration would result in unacceptable performance in dynamic tests. For a conservative performance evaluation, alternative designs were evaluated in service conditions that would be expected to increase the level of restraint on the guardrail post by the mow strip. The lowest ambient temperature recorded during the static testing program (50°F) was selected as the reference temperature for this evaluation. Similarly, the most aged asphalt condition (~ 120 days) experienced in the static test program was selected as the reference age condition of asphalt. Appendix C contains additional details on asphalt testing performed in this project. These reference service conditions were used in the computational investigation to evaluate the influence of pertinent mow strip

parameters. Figure 30 shows representative lateral load versus displacement curves from static testing of a number of mow strip configurations as described in Chapter 3. Based on the peak force criterion described above, a given mow strip configuration could be expected to potentially perform well in dynamic testing if the peak force measured in static tests did not significantly exceed the reference value, which would be approximately 7.3 kips for the configuration including a leave-out. The two mow strip configurations preferred by GDOT (2-24 and 3.5-24), would appear less likely to perform satisfactorily when compared to the mow strip configuration incorporating a leave-out. However, alternative designs incorporating a reduced rear distance or pre-cutting the asphalt layer demonstrate a very similar performance to that of the reference value for the peak force criterion.

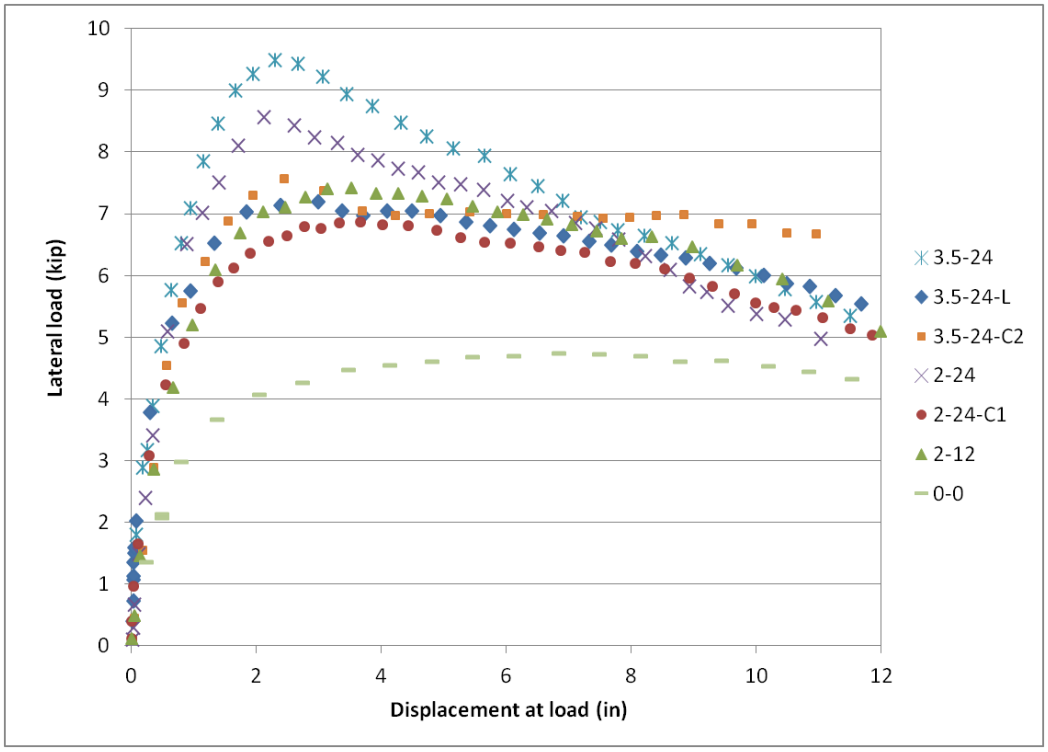

FIGURE 30

Representative load-displacement curves from experimental program

Figure 31 shows a contour plot of peak force applied to the post, which was created from the output of many FE analyses. Utilizing the FEA model, in conjunction with the experimental program, enables a consideration of a wide range of dimensional (thickness and rear-distance) combinations. The 7.3 kip target performance line of the typical leave-out design is indicated on the contour plot. Values below this reference line may be expected to have satisfactory performance relative to the mow strip configuration incorporating a leave-out. Experimental data from Figure 30 are indicated on the plot in parentheses, showing reasonable agreement with the computational results.

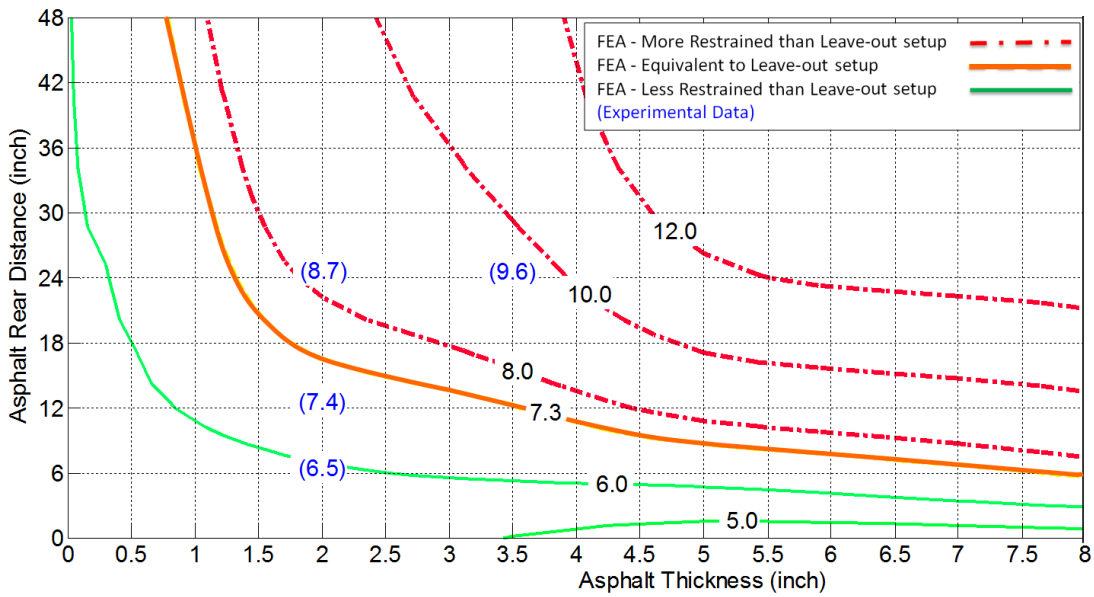

FIGURE 31

FEA Contour plot of peak force (kips) in a guardrail post demonstrating the influence of mow strip geometric parameters.

Figure 32 shows a plot of work done by lateral load versus ground level displacement based on the static tests described in Chapter 3. Assuming some equivalence between external work done and dissipated energy for a closed system, the reference energy value of 66.7 k-in determined in Section 5.1 can be used to evaluate the

relative performance of the various mow strip configurations. Post /mow strip systems that exhibited higher ground-level displacements at the reference energy level than that demonstrated by the post/mow strip incorporating a leave-out may reasonably be expected to demonstrate similar or better performance under dynamic loading. As with the peak force criterion, alternative designs incorporating a reduced rear distance or pre-cutting the asphalt layer demonstrate a very similar or in some cases better performance than that of the mow strip incorporating a leave-out.

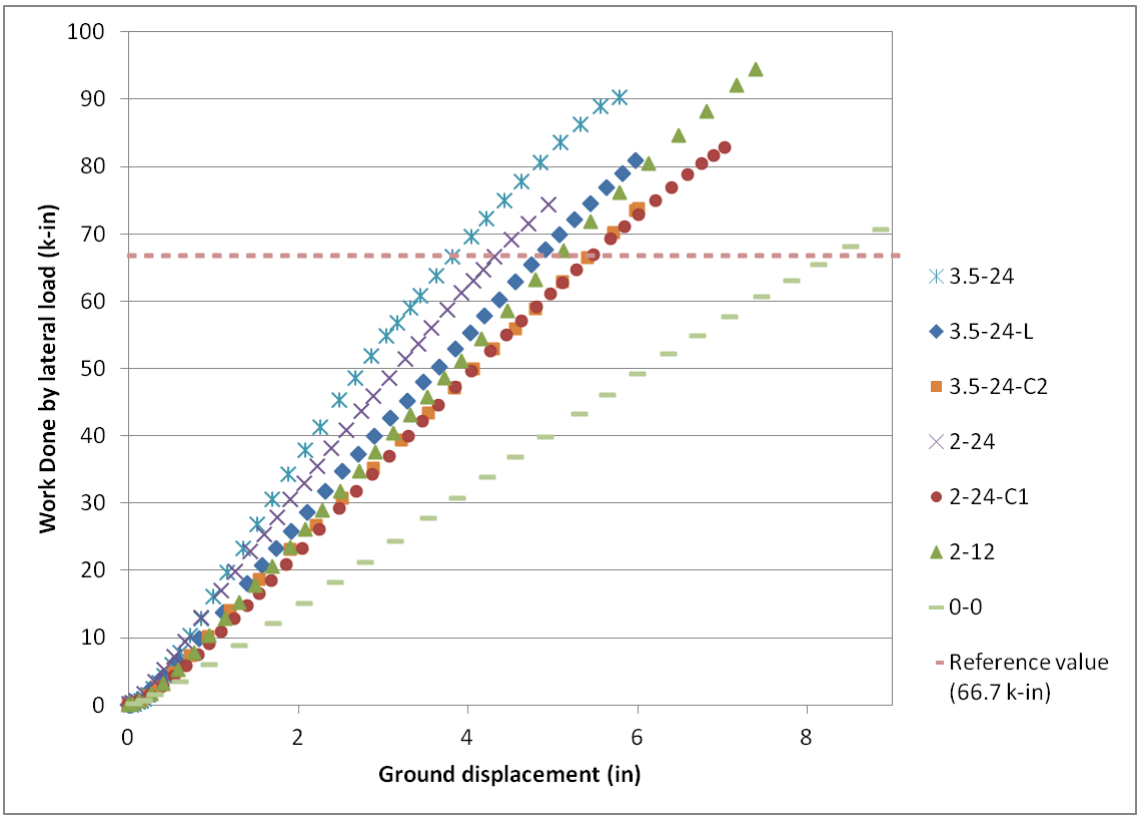

FIGURE 32

Relative performance of various mow strip configurations in terms of ground-level displacement for a specified value of work done.

Figure 33 shows a contour plot of ground displacement associated with the reference value of 66.7 kip-in work done in the system, which contains a wider range of dimensional (thickness and rear-distance) combinations than those found in the experimental program. The 4.9 inch target ground-level displacement of the post/mow strip incorporating a leave-out is indicated in the Figure. Values below this reference line may be expected to have satisfactory performance relative to the mow strip configuration incorporating a leave-out. Experimental data from Figure 32 are indicated in parentheses, showing reasonable agreement with the computational results.

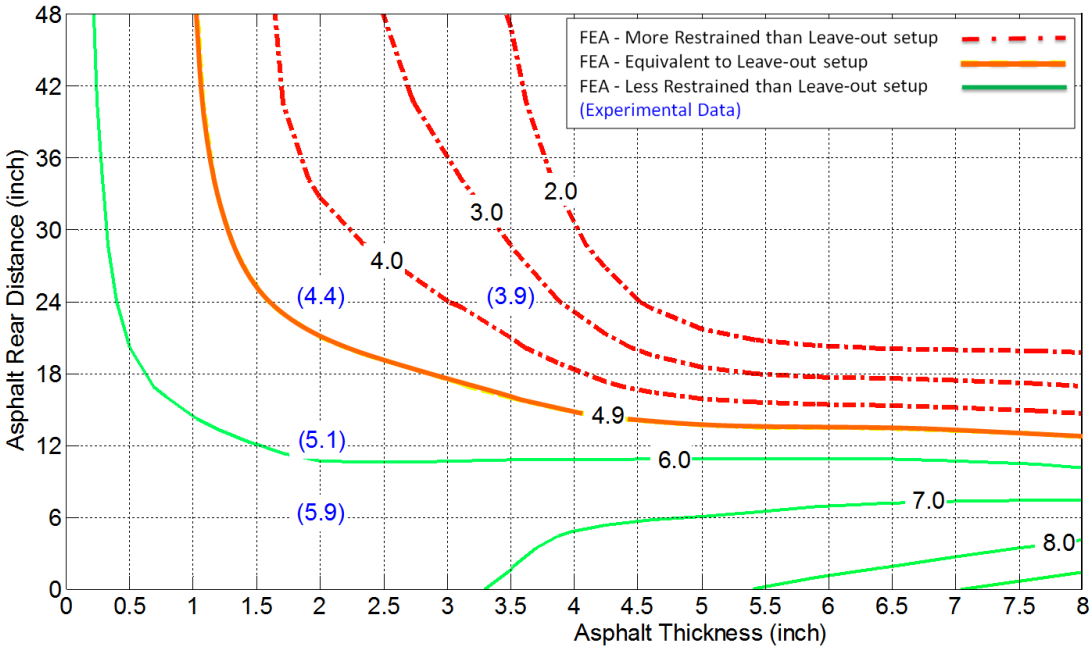

FIGURE 33

FEA Contour plot of ground-level displacement (inch) at a specified energy level in a guardrail post demonstrating the influence of mow strip geometric parameters.

Table 9 gives maximum longitudinal strains measured during the static test program for a number of post/mow strip configurations and their normalized strain assuming a yield strain of 0.00168 for the steel post. Based on the maximum strain

criterion described above, a given mow strip configuration could be expected to potentially perform well in dynamic testing if the normalized maximum strain did not exceed 1.0. As with the peak force and ground-level displacement criterion, alternative designs incorporating a reduced rear distance or pre-cutting the asphalt layer demonstrate a very similar or in some cases better performance than that of the mow strip incorporating a leave-out.

TABLE 9
Maximum strain and normalized strain with yield strain (static test)

Test designation	3.5-24	3.5-24-L	3.5-24-C2	2-24	2-24-C1	2-12	0-0
Maximum strain	0.00249	0.00165	0.00174	0.00222	0.00166	0.00156	0.00079
Normalized strain with yield strain	1.48	0.98	1.04	1.32	0.99	0.93	0.47

Figure 34 shows an FE simulation contour plot of normalized maximum strain, which contains a wider range of dimensional (thickness and rear distance) combinations than those found in the experimental program. The 0.98 target maximum normalized strain performance line of the post/mow strip incorporating a leave-out is indicated in the Figure. Values below this reference line may be expected to have satisfactory performance relative to the mow strip configuration incorporating a leave-out. Experimental data from Table 9 are indicated in parentheses, showing reasonable agreement with the computational results.

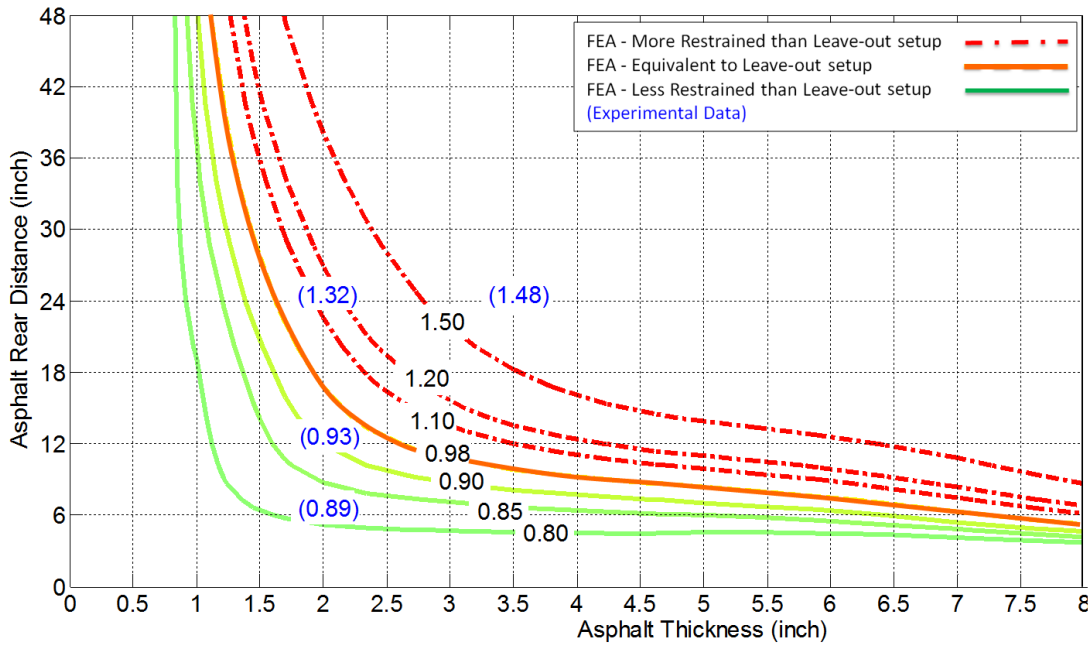

FIGURE 34

FEA Contour plot of normalized maximum strain in a guardrail post demonstrating the influence of mow strip geometric parameters.

5.3 Selection of preferred alternative mow strip designs

Based on the analysis of quantitative performance criteria given above, it is reasonable to assume that some of the alternative mow strip configurations evaluated in the current project could exhibit satisfactory performance under dynamic loading. Many of the proposed alternatives demonstrated measurably better performance under static loading conditions than the mow strip configuration incorporating a leave-out recommended by the *Roadside Design Guide*. While this is not a guarantee of satisfactory dynamic behavior, the criteria used in the current project provide an objective basis to move forward with dynamic testing on selected alternatives.

The results of this project indicate that four mow strip configurations may exhibit satisfactory performance under dynamic loading. These alternatives are:

- Mow strips of 2 inch thickness with a maximum 12 inch rear distance behind the post;
- Mow strips of 3.5 inch thickness with a maximum 12 inch rear distance behind the post;
- Mow strips of 2 inch thickness with a maximum 24 inch rear distance behind the post with the asphalt pre-cut prior to testing;
- Mow strips of 3.5 inch thickness with a maximum 24 inch rear distance behind the post with the asphalt pre-cut prior to testing;

These alternative configurations share a great deal of similarity with GDOT's current preferred mow strip configuration [35], and as such should be acceptable in terms of cost and constructability. They will be recommended by the project team for testing during Phase II of this research program. However, prior to the final decision of mow strip alternatives to test, all options will be presented to GDOT for review.

CHAPTER 6
CONCLUSIONS FROM PHASE I PROJECT AND RECOMMENDATIONS FOR PHASE II

6.1 Conclusions from Phase I Project

Phase I of this research program was broken down into five major tasks:

Task 1 – Synthesis of the state-of-the-art and current state-of-practice

Task 2 – Development of proposed alternative mow strip details

Task 3 – Static testing of guardrail posts installed using alternative procedures

Task 4 – Finite element simulation

Task 5 – Selection of alternative designs and installation procedures

These tasks have been completed. Based on the work completed in the Phase I project, the following conclusions may be drawn:

1) There is a wide variation in the use and implementation of asphalt mow strips by state Departments of Transportation. The results of an electronic and phone survey indicate that 11 states (20%) currently do not use mow strips, 18 states (36%) use mow strips without incorporating a leave-out, and 15 states (30%) use mow strips including a leave-out. No information was found for four states (9%), and two states (5%) stated that their practice is to pave up to the face of the post. Based on the information gathered, there does not appear to be a significant correlation between geographic location and the current state of practice for mow strip usage in the United States.
2) For those states that use mow strips, there is a broad variation in geometric parameters employed. The thickness of the mow strips used in the United States

varies from 1.5 to 8 inches, and the rear distance behind the post can vary from 6 to 48 inches.

3) Engineering and Construction professionals at the Georgia Department of Transportation are in consensus that the current mow strip and guardrail post installation method specified by their organization is optimal in terms of cost effectiveness, constructibility, and scheduling for both new construction and maintenance activities in Georgia. As such, any alternative mow strip designs that are identified for further evaluation should attempt to incorporate as many elements of the current GDOT preferred method as possible, and avoid unnecessary deviations.

4) Static experiments on 19 guardrail posts installed in a variety of different mow strip configurations demonstrated that the performance of the post was directly affected by the mow strip geometry as well as service conditions. Posts tested in summer conditions with relatively young asphalt demonstrated no excessive restraint. Results from identical tests under winter conditions with older asphalt indicated a much greater degree of restraint from the mow strip.

5) Prior FEA simulations of the performance of guardrail posts in which the asphalt layer was assumed as a rigid layer are capable of representing the response of cases where the asphalt layer does indeed provide excessive levels of restraint; however, such models are not capable of accounting for the influence of deformability and finite strength of general mow strip geometries. The finite stiffness and strength of the asphalt layer need to be included in the FEA in order to capture the general non-rigid response of this layer.

6) Given improvements in computational methods and speed that have occurred since the development of early numerical models of guardrail systems, it is now feasible to perform very refined FEA simulations of these systems to characterize the responses at a fundamental material level.

7) The use of a Mohr-Coulomb material model for the soil and the asphalt, used with element erosion based on a combined principal strain and principal stress criterion to capture the rupture of the asphalt layer and the modeling of the contact conditions between the post and the soil and asphalt media, provides for a very effective representation of the load-deflection response of the guardrail post, soil, and asphalt layer system over a broad range of material and geometric parameters.

8) Quantitative performance criteria can be developed to evaluate the performance of post/mow strip configurations under static lateral loads. By comparing to a specific reference configuration – in this case, the mow strip with leave-out specified by the *AASHTO Roadside Design Guide* – these criteria can be used as an indicator of potential satisfactory performance under dynamic loading.

9) Finite Element Analysis can be used effectively to perform parametric studies on pertinent geometric variables in terms of the quantitative performance criteria developed in this project. The analysis performed in this project indicates that there are definitive combinations of mow strip thickness and rear distance that are more likely to result in satisfactory static and dynamic performance.

10) Based on the static experimental program, finite element analysis, and assessment of quantitative criteria, the GDOT preferred mow strip with 3.5

inches thickness and 24 inches of rear distance behind the post is likely to demonstrate unsatisfactory performance under dynamic loading in comparison to a mow strip with a leave-out around the posts. A mow strip configuration with 2 inch thickness and 24 inches of rear distance appeared to cause more restraint than the leave-out configuration under static loading, but the results compared to the reference configuration were not so dissimilar as to preclude consideration of this setup.

11) Decreasing the mow strip rear distance behind the post appears to be an effective way to reduce the restraint imparted by a mow strip on a guardrail system. Experimental and finite element analysis indicated that posts embedded in mow strips with rear distances of 12 inches performed as well or better than posts embedded in mow strips with a leave-out.

12) Fabricating targeted full-depth cuts in the mow strip significantly reduces the amount of restraint the mow strip provides to a guardrail post. Post/mow strip configurations including cuts performed better than those with leave-outs under static loading. This technique may be very effective to ensure satisfactory performance in posts embedded in mow strips without a leave-out.

13) The following alternative mow strip configurations are recommended for further evaluation under dynamic loading in Phase II of this research program:

- Mow strips of 2 inch thickness with a maximum 12 inch rear distance behind the post;
- Mow strips of 3.5 inch thickness with a maximum 12 inch rear distance behind the post;

- Mow strips of 2 inch thickness with a maximum 24 inch rear distance behind the post with the asphalt pre-cut prior to testing;
- Mow strips of 3.5 inch thickness with a maximum 24 inch rear distance behind the post with the asphalt pre-cut prior to testing;

Prior to the final decision of mow strip alternatives to test, all options will be presented to GDOT for review.

6.2 Proposed Research Tasks for Phase II Program

A subset of the most promising alternative installation methods will be selected for further evaluation under subcomponent dynamic loading in the Phase II research project. The dynamic tests results will be used to refine and expand results of finite element analysis simulations already underway. Following the Phase II project, multiple installation procedures will be selected for full-scale crash testing in Phase III of the research program. The final objective of the overall research program is to provide support for a submittal to FHWA for approval of a more constructible and cost-effective detail than that recommended in the present *AASHTO Roadside Design Guide*. The Phase II project is divided into 4 major tasks as shown below:

<u>Task 1 – Selection of Alternatives for Dynamic Tests</u>

The static tests completed in the Phase I project were performed in a laboratory test bed constructed to adhere to the soil profile and compaction standards specified in the 2009 *MASH* Guidelines [21]. These test results were used to calibrate the FEA models developed in the Phase I project, and form the basis for the selection of the post installation alternatives that will be subjected to dynamic loading in Phase II. These

alternatives will be initially identified based on the static test results as well as the FEA results from the Phase I project.

Prior to final selection of alternative post installation methods and development of the dynamic test matrix, the results of the Phase I project will be presented to pertinent GDOT personnel in a Technical Workshop to be held at GDOT Headquarters. The research team will seek the input of GDOT on the constructability, economy, and overall viability of the alternative post installation techniques. It is expected that this Workshop will include participation from GDOT's Offices of Construction and Design, as well as other departments and personnel identified as by GDOT as warranted. The research team will incorporate this input from GDOT into its dynamic testing plan.

Task 2 – Laboratory Dynamic Testing on Post Installation Alternatives

This task will include the subcomponent dynamic testing of various guardrail post/mow strip configurations using a unique Hydraulic Velocity Generator available at the Georgia Tech CEE Structural Engineering Laboratory. The Velocity Generator, shown in Figure 35, produces an impulse by impacting the specimen with a mass in a controlled manner. This is accomplished using ultra-fast, computer-controlled hydraulic actuators with a combined hydraulic/high pressure nitrogen energy source. The desired loading is achieved through the precise timing of valve openings and pressures along with the design of appropriate loading fixtures. The experiments will be used to produce numerical data and qualitative observations to calibrate/validate the computational models, which will predict guardrail behavior.

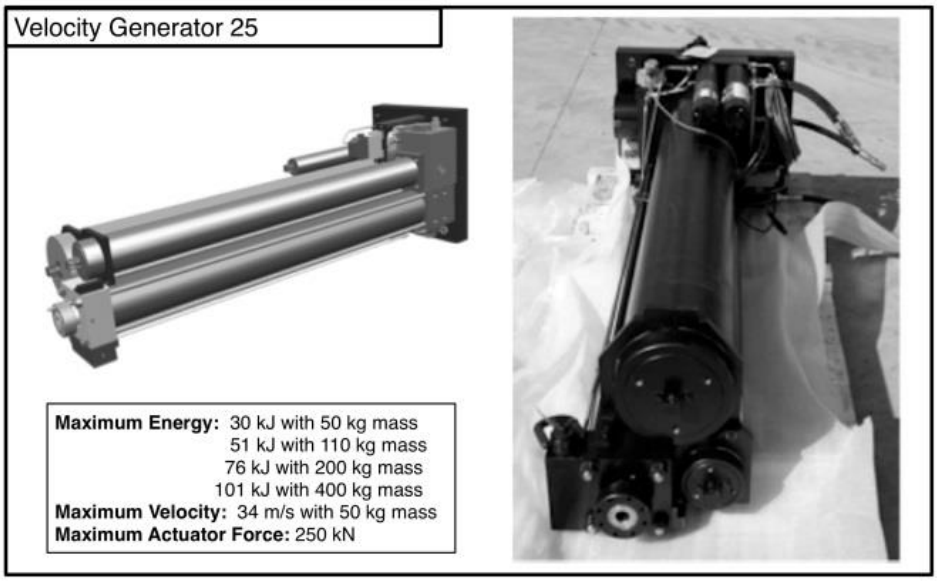

FIGURE 35

CEE Velocity Generator

This task will be completed as outlined in the following subtasks:

Development of Test Bed: The dynamic tests will be performed in the Structural Engineering Mechanics and Materials (SEMM) Laboratory on the Georgia Tech Campus. The Laboratory contains a strong wall that will be used as a reaction frame for the Velocity Generator. In order to provide the most flexibility for specimen preparation as well as the testing schedule, a moveable test bed will be constructed that can be moved in and out of the Laboratory area as needed. The moveable test bed will be fabricated using a steel roll-off container, with the posts embedded in soil placed and compacted in the container. Mow strip alternatives will also be constructed in the container. A basic illustration of the concept is shown in Figure 36.

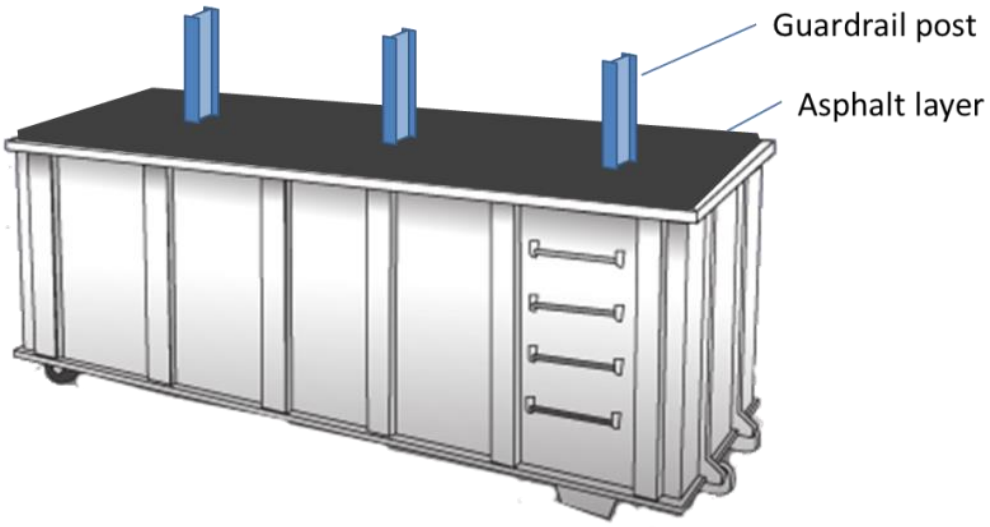

FIGURE 36

Basic concept for moveable test bed

The steel container will be modified to allow it to be towed into position, and then locked down to anchor points in the Laboratory Strong Floor. Load, strain, deflection, rotation, and acceleration sensors will be employed to provide a complete characterization of the dynamic behavior of the post system.

Initial Finite Element Model: A finite element model of the initial test setup and the hydraulic system will be developed utilizing calibrated material properties and models from Phase I. This model will be used to determine various parameters necessary for the test setup (i.e. impact mass, loading medium, instrumentation fixtures, etc.) Additionally, the model will be used to develop a reusable shakedown specimen.

Shakedown Testing: Because the loads imparted depend on the unique specimen and setup, calibration of valve settings, accumulator and deceleration chamber pressures, mass, and other parameters (shown in Figure 37) will be determined using data from tests conducted under conditions similar to those in the actual configuration. Utilizing the

reusable shakedown specimen developed in the previous task, experiments will be conducted to determine the appropriate valve parameters needed to achieve the loading desired. The loading will be calibrated for magnitude, rate, and duration. Calibration of loading duration larger than those achievable through valve manipulation alone will be combined with mechanical dampening systems, such as crushable foam, to extend the loading durations.

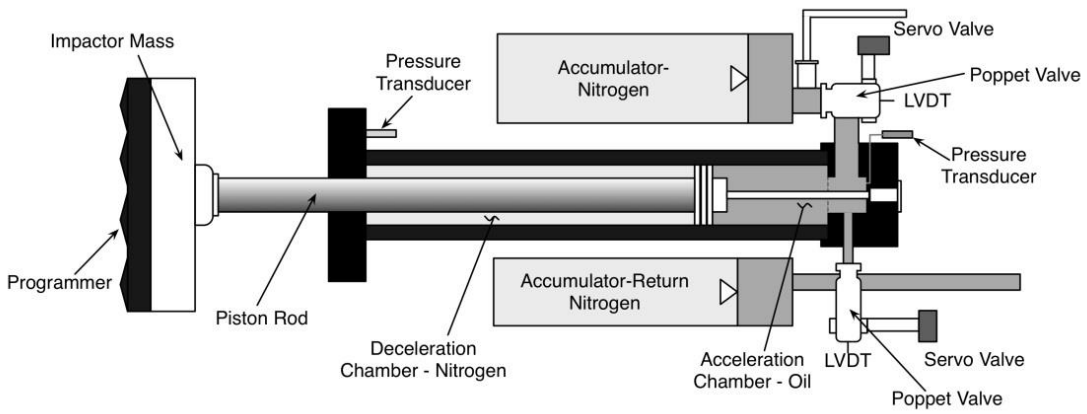

FIGURE 37

Schematic of hydraulic system including parameters for calibration

Dynamic Testing: Experiments on 14 specimens with various configurations will be conducted using the hydraulic actuator as shown in Figure 37. A tentative test matrix is given in Table 10. The tests will produce load-displacement data from load cells between the specimen and the impacting mass as well as velocity- and acceleration-time histories of the impacting mass. Additionally, high-speed photography recording at 5,000 frames/second will be utilized to provide detailed footage of various points on the guardrail. High-speed camera data will be analyzed with Track Eye Motion Analysis (TEMA) software in order to provide detailed displacement behavior of the guardrail and

surrounding asphalt. Hydraulic valve command and feedback data will be used to determine the loads imparted onto the specimen using algorithms developed by the research team.

Immediately following each experiment, analyzed data will be used to refine and calibrate the current finite element and hydraulic models for valve commands and specimen behavior. These models will be used to improve and determine parameters for any subsequent experiments.

TABLE 10
Proposed dynamic test matrix for evaluation of installation alternatives

Test Configuration	Repetitions	
	Repetition 1	Repetition 2
No mow strip	X	X
Grout leave-out	X	X
GDOT Standard Method	X	X
Reduced Strip Behind Post - 1	X	X
Reduced Strip Behind Post - 2	X	X
Pre-cut mow strip Section -1	X	X
Pre-cut mow strip Section - 2	X	X

Task 3 – Finite Element Analysis

This task involves the refinement of finite element models developed in Phase I of the research, with the final objective of providing a full-scale system simulation of a vehicle crash into a guardrail. The finite element simulations will be used in conjunction with the experimental results in Tasks 1 and 2 to select the most promising alternative post installation methodologies.

Three-dimensional finite element analysis will be performed using LS-DYNA V971 R8.0 throughout Phase II of this project. FE models will be calibrated and

validated using the data obtained from the dynamic loading tests described in Task 2. The material models used for the soil, asphalt, and steel in the static testing will be updated to account for strain rate effects under dynamic loading. A proper non-reflecting boundary condition will be used to avoid boundary effects in the dynamic tests. An appropriate boundary condition will be used to replicate the same loading condition applied by the velocity generator in Task 2. The verified dynamic model of a guardrail post will be used to conduct a parametric study to examine the impact of different mow strip details. Quantitative parameters will be measured during numerical simulations. These will include the dissipated energy in the guardrail post system, the peak force, the peak accelerations, the maximum ground-level displacement of the post, and the maximum tensile stresses, and strains in the post. The parametric study will help to ascertain the best alternatives to be used in the experimental tests. Moreover, the model sensitivity to each of these parameters will be checked.

Final models of a single post will be tuned to ensure a feasible simulation time and will be added to an available standard LS-DYNA model of a full guardrail setup including an impacting vehicle [48]. Numerical simulations of full-scale crash tests on the alternatives identified in the first series of dynamic subcomponent tests in Task 2 will be performed. The performance of the selected alternatives will be evaluated using numerical simulations of the standard full-scale crash test. If the alternatives are acceptable based on the *MASH* criteria, a selected number of them will be proposed for full-scale experimental crash tests by the *MASH* guidelines, during the subsequent Phase III project. If the selected alternatives fail in the numerical simulation of the full-scale crash tests, then changes to the guardrail post setup will be studied to ensure a greater

likelihood of success in the physical tests. These adjusted alternatives will be checked with numerical full-scale crash simulations and with subsequent experimental dynamic subcomponent tests to confirm their acceptable performance.

Task 4 – Project Deliverables and Dissemination of Results – Phase II

The major deliverable from the Phase II research project will be a report ranking the post installation alternatives in terms of dynamic structural performance. Once this ranking is established, the preliminary results will be presented to GDOT for review and input on the most viable post installation alternatives. Following this review by GDOT, the two most promising installation techniques from Phase II will be subjected to full-scale crash testing in the subsequent Phase III research project.

CHAPTER 7
REFERENCES

[1] Georgia Department of Transportation. Standard Specifications: Section 641 – Guardrail. http://www.dot.ga.gov/PartnerSmart/Business/Documents/GDOT_SpecBook_2013.pdf. Accessed Aug. 25, 2015

[2] American Association of State Highway and Transportation Officials (AASHTO), Roadside Design Guide, 4th Edition, Washington D.C., 2011.

[3] Bligh, et al, Dynamic Response of Guardrail Systems Encased in Pavement Mow Strips, Research Report FHWA/TX-04/0-4162-2, Texas Transportation Institute, Texas A&M University, 2004.

[4] Arrington, et al, Alternative Design of Guardrail Posts in Asphalt or Concrete Mowing Pads, Research Report 405160-14-1, Texas Transportation Institute, Texas A&M University, 2009.

[5] Pass, D., Office of Design Policy and Support, Georgia Department of Transportation, 2013 (personal communication).

[6] Ray, et al, Guardrail and Median Barrier Crashworthiness. No. project 20-5, NCHRP synthesis 244, Washington, D.C., 1997.

[7] Reid, LS-DYNA Simulation Influence on Roadside Hardware. Transportation Research Record: Journal of the Transportation Research Board, vol. 1890, no. 1, pp. 34–41, 2004.

[8] Atahan, Vehicle Crash Test Simulation of Roadside Hardware Using LS-DYNA: A Literature Review, International Journal of Heavy Vehicle Systems, vol. 17, no. 1, pp. 52–75, 2010.

[9] Atahan, Finite Element Simulation of a Strong-Post W-Beam Guardrail System, Simulation: Transactions of The Society for Modeling and Simulatio, vol. 78, no. 10, pp. 587–599, 2002.

[10] Borovinšek, et al, Simulation of Crash Tests for High Containment Levels of Road Safety Barriers, Engineering Failure Analysis, vol. 14, no. 8 SPEC. ISS., pp. 1711–1718, 2007.

[11] Ren, et al, Computational and Experimental Crash Analysis of the Road Safety Barrier, Engineering Failure Analysis, vol. 12, no. 6 SPEC. ISS., pp. 963–973, 2005.

[12] Hampton, et al, Crash Performance of Strong-Post W-Beam Guardrail with Missing Blockouts, International Journal of Crashworthiness, vol. 17, no. 1, pp. 93–103, 2012.

[13] Mohan, et al, Finite Element Modeling and Validation of a 3-strand Cable Guardrail System, International Journal of Crashworthiness, vol. 10, no. 3, pp. 267–273, 2005.

[14] Sicking, et al, Development of the Midwest Guardrail System, Transportation Research Record, vol. 1797, no. 1, pp. 44–52, 2002.

[15] Mak, et al, Testing of State Roadside Safety Systems—Volume XI: Appendix J—Crash Testing and Evaluation of Existing Guardrail Systems, Report FHWA-RD-98-046," Washington, D.C., 1998.

[16] Ross, et al, Recommended Procedures for the Safety Performance Evaluation of Highway Features. NCHRP Report 350." National Cooperative Highway Research Program, 1993.

[17] Plaxico, et al, Impact Performance of the G4(1W) and G4(2W) Guardrail systems: comparison under NCHRP report 350 test 3-11 conditions," Transp. Res. Rec., vol. 1720, no. 1, pp. 7–18, 2000.

[18] LS-DYNA Version V971 R8.0, Livermore Software Technology Corporation (LSTC), Livermore, CA, 2014.

[19] Gabauer, et al, Pendulum Testing as a Means of Assessing the Crash Performance of Longitudinal Barrier With Minor Damage," International Journal of Impact Engineering, vol. 37, no. 11, pp. 1121–1137, 2010.

[20] Bligh, et al, MASH Test 3-10 on 31-inch W-Beam Guardrail with Standard Offset Blocks, Report FHWA/TX-11/9-1002-4, Texas Transportation Institute, College Station, TX, 2011.

[21] American Association of State Highway and Transportation Officials (AASHTO), Manual for Assessing Safety Hardware (MASH), First Edition. AASHTO, Washington, D.C., 2009.

[22] Abu-Odeh, et al, Guardrail Deflection Analysis, Phase I: (2010-11), report 405160-24, Texas Transportation Institute, College Station, TX, 2011.

[23] Schrum, et al, Safety Performance Evaluation of the Non-Blocked Midwest Guardrail System (MGS) Report TRP-03-262-12/ RPFP-11-MGS-3," Lincoln, NE, 2013.

[24] Dewey, et al, A Study of the Soil-Structure Interaction Behavior of Highway Guardrail Posts, Research Report 3431, Texas Transportation Institute, College Station, TX, 1983.

[25] Ferdous, et al, Performance Limit Analysis for Common Roadside and Median Barriers Using LS-DYNA, International Journal of Crashworthiness, vol. 16, no. 6, pp. 691–706, 2011.

[26] LSTC, LS-DYNA® keyword user's manual–vol. 2–version 971 R8.0., Livermore Software Technology Corporation, Livermore, CA, 2015.

[27] Rohde, et al, Instrumentation for Determination of Guardrail-Soil Interaction, Transportation Research Record, vol. 1528, no. 1, pp. 109–115, 1996.

[28] Plaxico, et al, Finite Element Modeling of Guardrail Timber Posts and the Post-Soil Interaction, Transportation Research Record: Journal of Transportation Research Board, vol. 1647, no. -1, pp. 139–146, 2007.

[29] Wu, et al, A Study of the Interaction Between a Guardrail Post and Soil During Quasi-Static and Dynamic Loading, International Journal of Impact Engineering, vol. 34, no. 5, pp. 883–898, 2007.

[30] Tabiei, et al, Roadmap for Crashworthiness Finite Element Simulation of Roadside Safety Structures, Finite Elements in Analysis and Design, vol. 34, no. 2, pp. 145–157, 2000.

[31] Tabiei, et al, Validated Crash Simulation of the Most Common Guardrail System in the USA, International Journal of Crashworthiness, 2000.

[32] Souli, et al, Arbitrary Lagrangian Eulerian Formulation for Soil Structure Interaction Problems, Soil Dynamics and Earthquake Engineering, vol. 35, pp. 72–79, 2012.

[33] Jowza, et al, Safety Investigation and Guidance for Retrofitting Existing Approach Guardrail Transitions, MwRSF Research Report No. TRP-03-266-12, Midwest Roadside Safety Facility, Nebraska, 2012

[34] Rosenbaugh, et al, Development of Socked Foundations for S3x5.7 Posts, Research Report TRP-03-293-15, Midwest Roadside Safety Facility, Lincoln, NE, 2015

[35] Georgia Department of Transportation. Construction Standards and Details: No.4381 and S-4. http://mydocs.dot.ga.gov/info/gdotpubs/ConstructionStandardsAndDetails/Forms/AllItems.aspx. Accessed Aug. 25, 2015

[36] Scott, et al, Static Response of Steel Guardrail Posts Driven Through Asphalt Vegetation Barriers, Session 209, Transportation Research Board 94th Annual Meeting, Washington, D.C., 2015.

[37] Herbst, et al, “Rear Impact Test Methodologies: Quasistatic and Dynamic,” ESV 09-0533, 21st International Technical Conference on the Enhanced Safety of Vehicles, Stuttgart, Germany, June 15-18, 2009.

[38] Fwa, et al, Rutting Prediction of Asphalt Pavement Layer Using C-ϕ Model, Journal of Transportation Engineering, ASCE, Vol.140, pp. 675-683, 2004

[39] Zhang, et al, Characterization of Viscoplastic Yielding of Asphalt Concrete, Construction and Building Materials, Vol.47, pp.671-679, 2013.

[40] Bell, Summary Report on Aging of Asphalt-Aggregate Systems, Strategic Highway Research Program (SHRP) Report SR-OSU-A-003A-89-2, 1989

[41] Pellinen, T. K., and Xiao, S. Stiffness of Hot-Mix Asphalt. Joint Transportation Research Program (JTRP), Technical Report No. FHWA/IN/JTRP-2005/20. 2006

[42] Farrar, et al, Evolution of the Crossover Modulus with Oxidative Aging, Transportation Research Record, vol. 2370, no.1, pp. 76–83, 2013

[43] American Association of State Highway and Transportation Officials (AASHTO), Standard Specification for Materials for Aggregate and Soil-Aggregate Subbase, Base and Surface Courses (AASHTO M 147). 1990.

[44] American Association of State Highway and Transportation Officials (AASHTO), Standard Method of Test for Moisture-Density Relations of Soils Using a 4.54-kg (10-lb) Rammer and a 457-mm (18-in.) Drop (AASHTO T 180). 2010.

[45] Bowles, Foundation Analysis and Design, 1996.

[46] Budhu, Soil Mechanics and Foundations 3rd ed., Hoboken, NJ: John Wiley & Sons Inc, 2010.

[47] Davis, R.O., and Selvadurai, A.P., Plasticity and Geomechanics, Cambridge University Press, 2005.

[48] National Crash Analysis Center (NCAC) - George Washington University, Finite Element Model Archive, http://www.ncac.gwu.edu/vml/models.html, accessed May 22, 2015.

[49] Whitesel, D., Jewell, J., and Meline, R. “Development of weed control barrier beneath metal beam guardrail”. Technical Report FHWA/CA10-0515, California Department of Transportation, Sacramento, CA. 2011.

[50] Colorado Department of Transportation (CDOT), Standard Plan No.M-606-1, Guardrail Type 3 W-Beam (Sheet No.1 of 19), Project Development Branch, CDOT, Denver, CO. 2012.

[51] New Mexico Department of Transportation (NMDOT), Guardrail Post Details in Rock Formation and in Mow Strip Application, Drawing No.606-GR31-5/20, NMDOT, Santa Fe, NM. 2014.

[52] Idaho Transportation Department (ITD), Standard Drawing No.G-1-A-2, W-Beam Guardrail Installation Assemblies, ITD, Boise, ID. 2010.

[53] American Association of State Highway and Transportation Officials (AASHTO), *Construction Manual for Highway Construction* (AASHTO CM4) – Sections 304.05, AASHTO, 1990.

[54] American Association of State Highway and Transportation Officials (AASHTO), Standard Method of Test for Density of Soil In-Place by the Sand-Cone Method (AASHTO T191). 2014

[55] Faller, et al. "Midwest Guardrail System for Standard and Special Applications". Transportation Research Record: Journal of the Transportation Research Board, No. 1890, Transportation Research Board of the National Academies, Washington, D.C., 2004.

[56] American Society of Testing and Materials (ASTM), Standard Test Methods for Deep Foundations Under Lateral Load (ASTM D3966/D3966M-07), 2013

[57] Coon, et al, "Dynamic Impact Testing of Guardrail Posts Embedded in Soil". Technical Report TRP-03-77-98, Midwest Roadside Safety Facility (MwRSF), Lincoln, NE, 1999

[58] Lewis, B.A., Manual for LS-DYNA Soil Material Model 147. NO. FHWA-HRT-04-095, 2004.

[59] Reid, J. D., Coon, B. A., Lewis, B. A., Sutherland, S. H., & Murray, Y.D., Evaluation of LS-DYNA Soil Material Model 147. No. FHWA-HRT-04-094, 2004.

[60] American Society of Testing and Materials (ASTM), Standard Test Method for Compressive Strength of Bituminous Mixtures (ASTM D1074-09), 2009.

APPENDIX A
SURVEY OF OTHER STATE DOT PRACTICES

A.1 Mow Strip Survey

Different states in the U.S. use a variety of methods to install guardrail posts when vegetation control is a concern. The most common method employed for this purpose is the installation of an asphalt layer or mow strip. A comprehensive survey of State Departments of Transportation was performed in the current research project to obtain information on the current state of practice related to the installation of mow strips. Each state has a publically available electronic directory and database, which often (though not always) contains standard specifications and drawings for guardrail mow strip installation. An investigation of these databases was undertaken by the research team. In addition, phone calls were made to the Engineering and Construction Divisions for Each state DOT, to ascertain whether a state had additional information on mow strips that was not available in their public database.

As can be seen in Table A1, 18 states use a mow strip without leave-out (Type 1), 15 states use a mow strip with leave-out (Type 2), and two states pave up to the face of guardrail post (Type 3). Example drawings of other DOT's post installation details are given in Figure A1. In the other 15 states, no indication of using mow strip was found (which could mean either those states do not use mow strips or the proper documentation related to usage of mow strips was simply not found through the electronic survey). Excluding the states for which no indication of mow strip was found, most of the states (36%) are using mow strip without leave-out. The second popular method is using mow

strip with leave-out (30%), and the last method identified is paving up to the face of the guardrail post (4%). A summary of survey results and details are tabulated in Table A2.

TABLE A1
Classification of mow strip configuration from State DOT specifications.

Mow Strip Configuration	Classification	Number of States (percent)
Mow strip without leave-out (asphalt removed around post)	Type 1	18 (36%)
Mow strip with leave-out (asphalt adjacent to post)	Type 2	15 (30%)
Asphalt placed up to the face of the post	Type 3	2 (4%)
No mow strip use	-	15 (30%)

In 2011, the California Department of Transportation (CALTRANS) published a technical report named "Development of Weed Control Barrier beneath Metal Beam Guardrail" [49]. CALTRANS sought an alternative installation method for "mow strip with leave-out", with a more effective, less costly but still crashworthy system. CALTRANS also recognized the issues associated with regular roadside weed control such as worker exposure, cost and environmental concern (when herbicides are used). As a CALTRANS alternative, the mow strip around the guardrail posts were partially replaced by EFP (Expanded Polystyrene Foam) material of weaker strength than that of concrete mow strip, as shown in Figure A2. This alternative design passed the crash test criteria of the *NCHRP Report 350* (former guideline, equivalent to *MASH* criteria) and this result implies that sufficient crashworthiness of the guardrail post can be achieved by mow strip modification.

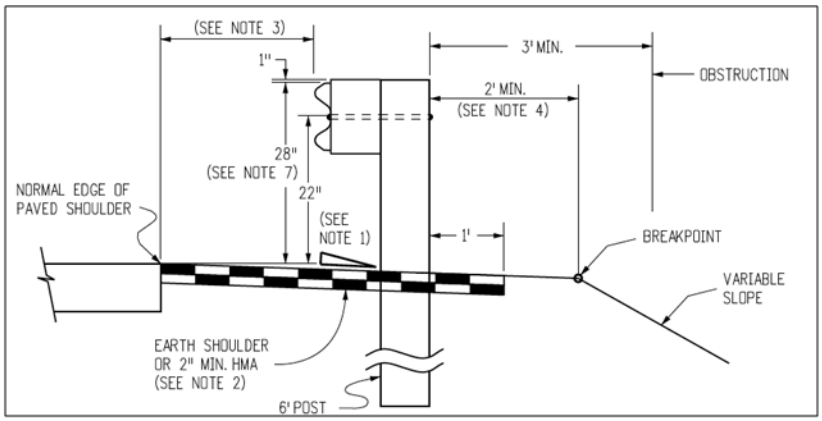

Type 1: Mow strip without leave out

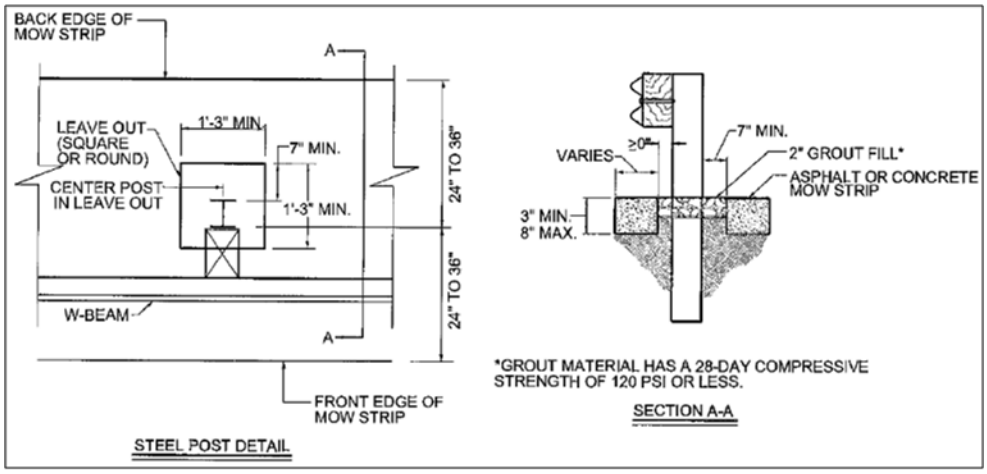

Type 2: Mow strip with leave out

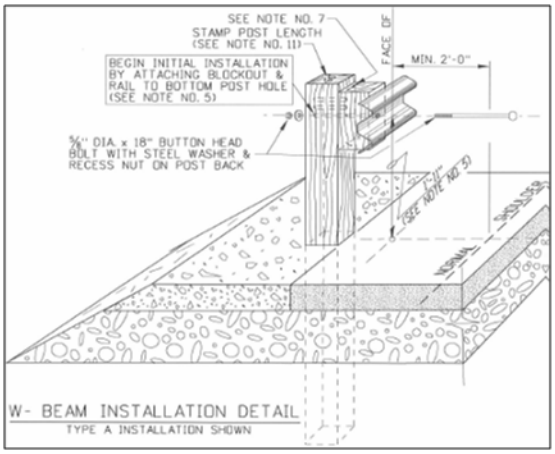

Type 3: Pavement placed up to the face of the post

FIGURE A1

Example drawings of other DOT's post installation detail [50,51,52].

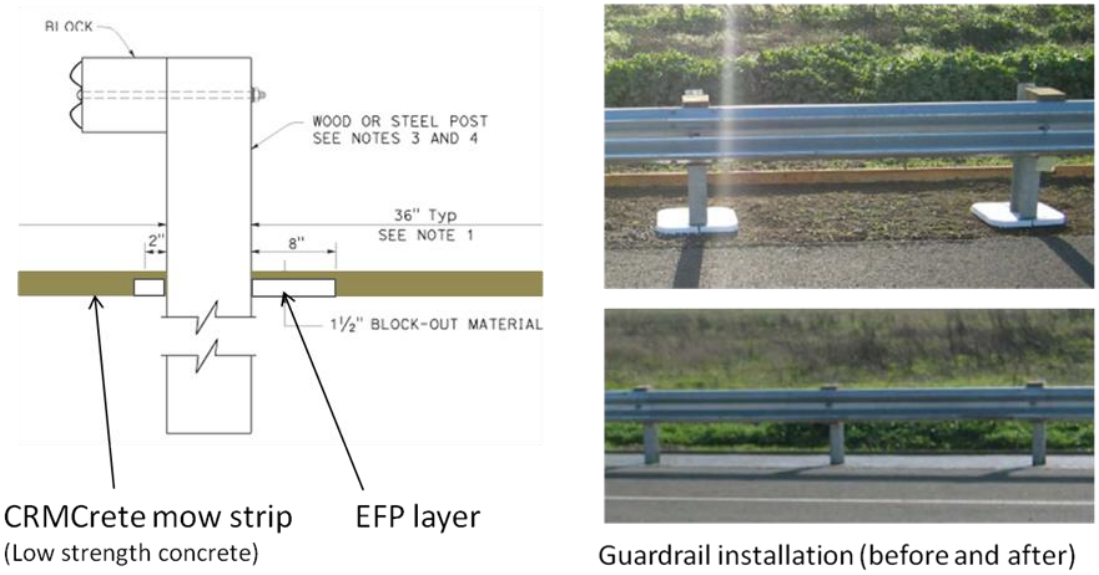

FIGURE A2

Alternative mow strip installation method by Caltrans [49].

A.2 Tabulated Survey Details

TABLE A2

Complete summary of mow strip survey.

States	Mow strip use	Leave-out use	Classification	Mow strip type	Leave-out type	Note 1	Note 2	Note 3	
50 intrastate states	(yes:0, no:x)	(yes:0, no:x)	(1, 2, 3)	(if mow strip is used)	(if leave-out is used)	about mow strip	about leave-out	Other relevant information from contacts	
Alabama	x	x						Soil compacted, no concrete or asphalt overlay, no weed control barrier	
Alaska	0	x	Type 1					Shoulder asphalt when driven through pavement. Otherwise no weed control. Weed mats were unsuccessful. Alaska has evaluated the use of leave-outs on Alaska roads and has issued a determination that leave-outs are not required. This is based on FHWA's 3/10/2004 Memorandum on the subject, the 2011 Roadside Design Guide guidance, and on Alaska experience in frozen soil conditions.	Alaska guardrail crash experience has not exhibited excessive guardrail rupture or failure to contain and redirect vehicles when struck. In addition, for many months each year the road structure is frozen solid which restricts post rotation entirely. Even with leave-outs, there is no method to enhance post rotation in frozen soil. Even with our climatic conditions, our guardrail has contained and redirected most strikes. As a result, there is no economic or pressing safety reason to require leave-outs in asphalt pavement shoulders.
Arizona	x	x						Posts may be drive/ or placed in manually or mechanically dug holes. If damage may occur, engineer is judge as to whether driving of posts will occur.	
Arkansas	0	x	Type 1			no leave-out for asphalt mow strip	leave-out if concrete pavement is mow strip	Driven through asphalt pavement, otherwise outside shoulder, 2" regular surface coat& aggregate base. For concrete, drill post and fill hole with grout	
California	0	0	Type 2	2" minor concrete	expanded polystyrene foam is an approved item	minor concrete must have 1400-1800psi strength, CRMCrete (concrete + recycled scrap tire crumb rubber). Weed control is not mandatory,	foam must have compressive strength of 8-18psi (according to ASTM D1621). Weed out is mandatory only if installed in pavement		

States	Mow strip use	Leave-out use	Classification	Mow strip type	Leave-out type	Note 1	Note 2	Note 3	
50 intrastate states	(yes:0, no:x)	(yes:0, no:x)	(1, 2, 3)	(if mow strip is used)	(if leave-out is used)	about mow strip	about leave-out	Other relevant information from contacts	
Colorado	0	x	Type 1	Extended pavement		extend a 2 in. minimum thickness paved surface to 1 ft behind the guardrail posts or to the erosion control curb		"We currently do not have a standard detail for "leave-outs;" however, I am aware that when positioning of the guardrail requires that the posts fall within proposed pavement areas that the local/regional designer has requested that "leave-outs" be utilized to better facilitate the installation of the guard rail as well as, create a point where the post can be more easily removed for maintenance removal or correction."	"It is my understanding that the same type of pavement is utilized to fill the holes with the exception that joint material is utilized around the "leave-outs" to more easily facilitate the pavement, surrounding the post, removal and replacement."
Connecticut	x	x				put it off 1 ft behind pavement, typically use weed control chemicals, in water reservoirs areas - 2"-3" asphalt (mulch)- no leave-out			
Delaware	0	x	Type 1	2" maintenance strip around guardrail		HMA			
Florida	0	x	Type 1	asphalt	2-sack grout fill - not in standard specs	2" thick asphalt mow strip is specified in drawing			making modifications currently to match new roadway standards, Although they are getting good performance with current guardrail (based on performance, not performed tests). Currently leave-out may have been a project specific detail.
Georgia	0	x	Type 1	asphalt					
Hawaii	0	0	Type 2	1.5" Asphalt	2sack grout in 8" max Asphalt/Concrete	contractors pave 1.5" of asphalt concrete and posts are driven into pavement, and then asphalt sealer around the post to fill cracks	used in PCC paved shoulders where concrete swale exists behind, rarely used for asphalt pavement		
Idaho	0 (up to post)	x	Type 3	Extended pavement		They extend the pavement up to the base of guardrail but they do not pave after and behind the guardrail. They only extend the asphalt pavement and if the pavement is concrete, they used asphalt to pave the shoulder to the base of guardrail. This information is obtained from the drawings.		guardrails are typically installed on compacted native material with no asphalt/ concrete overlay or with any weed control layers.	migrating towards the MidWest guardrail system.

States	Mow strip use	Leave-out use	Classification	Mow strip type	Leave-out type	Note 1	Note 2	Note 3	
50 intrastate states	(yes:0, no:x)	(yes:0, no:x)	(1, 2, 3)	(if mow strip is used)	(if leave-out is used)	about mow strip	about leave-out	Other relevant information from contacts	
Illinois	0	0	Type 2	pavement shoulder	3" thick HMA or grout (shall be same material as mow strip)	posts are driven through round blockouts or cored holes			
Indiana	x	x						drive guardrail posts through native material, but there *may* be a layer of aggregate above. They use the AASHTO design guide for certain details.	INDOT does not use mow strips or leave-outs. If shoulders are less than 14' INDOT paves to the face off the guardrail.
Iowa	0	0	Type 2	no weed control required if posts are installed in earth	must have the leave-out when paved mow strip is used		When posts are placed in solid material such as paved shoulder or rock, drill minimum 15 inch diameter holes for the depth of the material. Backfill holes with special backfill. Special backfill is given in 4132 on spec, 2102(spec) , 4" deep (depth of pvd shoulder)	Backfill material in 4132 of specs : Crushed stone, crushed PCC, crushed composite pavement, or reclaimed HMA,	
Kansas	x	x							
Kentucky	x	x				Only Paves to the face of the guardrail		no further information	
Louisiana	0	0	Type 2	concrete/ asphalt	2-sack non shrink grout mixture 4 inch thickness with max compressive strength of 120 psi		leave-out is mandatory, only grout used as leave-out material, no other materials		
Maine	0	x	Type 1					As per section 606.03 of specs, posts are either driven in or set plumb in holes. If they are driven, damaged area is repaired with approved bituminous patching.	Posts are set on stable foundations, and backfilled with suitable material-thoroughly tamped
Maryland	0	x	Type 1					Posts are driven in through asphalt-no mow strip or leave-out details. For weed control, spray chemical around guardrail posts.	

States	Mow strip use	Leave-out use	Classification	Mow strip type	Leave-out type	Note 1	Note 2	Note 3	
50 intrastate states	(yes:0, no:x)	(yes:0, no:x)	(1, 2, 3)	(if mow strip is used)	(if leave-out is used)	about mow strip	about leave-out	Other relevant information from contacts	
Massachusetts	x	x						driven or in mechanically dug holes, and backfilled with acceptable material placed in layers and thoroughly compacted. For bituminous surfacing, posts shall be erected prior to laying surrounding finished material	drive into shoulder- granular surface, dense aggregate surface, pave to face of guardrail, but not to face of post- 11 inches
Michigan	0	0	Type 2		shoulder rock			backfill for rock and leave-out for pvmt in Section 7.01.33 of RDM (link) Leave-out is generally just removal of 15 x 15 area and filled back with shoulder rock/ aggregate/ No mow strip, no fancy materials. Most times just native earth is compacted around guardrail if its neither hard rock nor pavement	http://mdotcf.state.mi.us/public/design/files/englishroadmanual/erdm07.pdf
Minnesota	0	0	Type 2		4-6" grout: 1 part cement, 14 parts sand, 5 parts water				
Mississippi	0	x	Type 1			Pave the shoulders with around 4-5 inches of asphalt and drive the guardrail post through asphalt layer		guardrail posts are driven into compacted earth and in some cases this earth in chemically treated. No leave-outs are used in Mississippi.	They do not put down any weed control but we do extent the top 2 layers of mainline asphalt out under the guard rail.
Missouri	0	x	Type 1	concrete or less than 2" asphalt	for concrete mow strip, coarse aggregate leave-out is used		Leave-out is used only for concrete mow strip		
Montana	x	x							
Nebraska	0	0	Type 2		3" Asphalt or 2" flowable fill concrete		16" diameter for flowable fill.	mow strip and leave-out detail mandatory around guardrails	
Nevada	x	x							
New Hampshire	x	x						no weed control is mandatory, only where post is driven into pvt. If installed in pvt/ concrete:, FHWA detail. 4" hole with no more than 3" of pvt.	drive into crushed stone compacted base. stone or grout as backfill material

States	Mow strip use	Leave-out use	Classification	Mow strip type	Leave-out type	Note 1	Note 2	Note 3	
50 intrastate states	(yes:0, no:x)	(yes:0, no:x)	(1, 2, 3)	(if mow strip is used)	(if leave-out is used)	about mow strip	about leave-out	Other relevant information from contacts	
New Jersey	0	x	Type 1	Allows "4" thick Hot Mixed Asphalt" as Non-vegetative surface (see 8.3.6)		on CD 808-1, and Table 8-5 in RDM. broken stone, HMA, non porous HMA, polyester matting (link).		Broken stone is not too popular because it can kick out, only if landscaper likes it. Rarely used on compacted earth without mow strip (although not banned). Leave-outs are not used.	http://www.state.nj.us/transportation/eng/documents/RDM
New Mexico	0	0	Type 2	asphalt/ RCC (wire mesh/ synthetic fiber)- min 3", max 8"	2" grout fill with compressive strength 120 psi or less		leave-out when posts are restrained by rock, asphalt or concrete..Posts may be driven into compacted earth as well. Mow strip is an option...but then leave-outs are mandatory.		
New York	0	x	Type 1	3" vegetation control strip		vegetation control strip is optional depending on if there is enough room to warrant the effort of mowing for aesthetic reasons . The vegetation control is either HMA or total herbicide (lesser recommended)			
North Carolina	0	x	Type 1					backfill and tamp holes using excavated material- note on sheet 862.01 only for wooden posts, but they are seldom used. Typically pave as close to the face of guard rail as possible for weed control.	Mostly posts driven through embankment or pavement. Sometimes upon discretion of engineer emulsified or thin pavement is used. Leave-outs are never used . (Sheets 2, 11 on 862.01)
North Dakota	0	0	Type 2					No information on mow strips. Posts drilled or placed in augured holes in bituminous pavement (from specs), and backfill with approved material.	No median guardrails, in asphalt shoulders, 2" HMA (bituminous)- section 764.04 a of spec and verified with DOT contact
Ohio	0	x	Type 1	max 3" thick asphalt (specified as type 1, PG64-22)		paving around posts is not advisable if the thickness of the pavement would prevent this rotation from occurring. Three inches of asphalt pavement is the maximum allowable thickness for paving under guardrail.		mow strip is not mandatory. Guardrails are never installed in regular pavement.	
Oklahoma	0	x	Type 1	Superpave		4" superpave type s4 is used to widen the shoulder. It is not a mow strip, but based on the drawing I think the pave under the guardrail and it is called superpave.- T-605		(superpave is additional paving on roadside after regular pavement)	

States	Mow strip use	Leave-out use	Classification	Mow strip type	Leave-out type	Note 1	Note 2	Note 3	
50 intrastate states	(yes:0, no:x)	(yes:0, no:x)	(1, 2, 3)	(if mow strip is used)	(if leave-out is used)	about mow strip	about leave-out	Other relevant information from contacts	
Oregon	0 (up to post)	x	Type 3					They extend the pavement up to the base of guardrail but they do not pave after and behind the guardrail-from drawings. Guardrails only used in compacted earth.	In medians, only concrete barrier is used. Over compacted subgrade, an aggregate layer (Spec'd in Section 6-40) / shoulder rock up to 2 ft behind the post. Thickness of this layer will depend on pvmt design
Pennsylvania	x	x						Information found in Publication 408-drill or punch holes, drive posts mechanically& use acceptable embank material for backfill if excavated.	In medians, fill with hot/cold bituminous wearing course. Fill voids with asphalt cement PG 64-22 or PG 58-28
Rhode Island	0	x	Type 1	bituminous millings crushed/ grounded to pass through 1" sieve(2.5" thickness)				but millings from cold planinig operations at guard rails < 2 ft from edge of existing pavement. Steel posts with exception of end anchor posts, they are mechanically driven. Wood posts are either driven in or set in drug holes.	
South Carolina	x	x				mow strip was discontinued after FHWA memo (1.5" HMA was used earlier)		driven through compacted earth, and backfilled using the same	
South Dakota	0	x	Type 1	2" asphalt over granular material		guardrails are also installed in native earth with weed control sprays (on sheet 630.01 :http://www.sddot.com/business/design/plates/docs/s63001.pdf)	no leave-out- 2" asphalt max is allowed. Only one instance where this reqmt was not met (8" thick concrete pavement) then used leave-out detail as in roadside design guide		
Tennessee	x	x						asphalt or concrete pavement is removed and filled with compacted earth, whether on medians (as specified on sheet) or on shoulders (not specified on sheet)	
Texas	0	0	Type 2	4" asphalt or RCC	2 sack grout	Mow strip is not mandatory. The detail is optional.			
Utah	0	0	Type 2		flowable backfill with max 28 day compressive strength of 50-100 psi	weed control is not mandatory. They have been using weed mats since early this year, again not mandatory		Details for installation through rock-cut hole and fill with native material. In pavement, flowable backfill to depth of pavement	

States	Mow strip use	Leave-out use	Classification	Mow strip type	Leave-out type	Note 1	Note 2	Note 3	
50 intrastate states	(yes:0, no:x)	(yes:0, no:x)	(1, 2, 3)	(if mow strip is used)	(if leave-out is used)	about mow strip	about leave-out	Other relevant information from contacts	
Vermont	x	x				do not install in paved shoulders/ any pavement. Aggregate shoulder material underneath that prevents weed control (the main purpose is base stability)		no standard detail / spec that says this material is esp. for guardrail.	
Virginia	0	x	Type 1			Limit maximum 2" or 3" thick (depends on asphalt type) - see p.206 of Volume 1, never installed in PCC		mow strip is not mandatory, and guardrails may also be installed on regular earth/ aggregate. Where there is paved shoulder, the shoulder is widened to install guardrail. The pavement effectively acts as a weed control barrier.	Although not currently in specs, planning on introducing a detail with aggregate leave-out only if guardrail is placed in concrete. If guardrails are installed in concrete, they are torn out and installed in grass/earth. http://www.extranet.vdot.state.va.us/LocDes/Electronic_Pubs/2008Standards/Section500/501_39.pdf
Washington	x	x						no overlay..guardrail in compacted soil	
West Virginia	0	0	Type 2	asphalt or concrete	granular fill 4" min depth			Guardrails installed by driving into compacted earth. No weed control / mow strip. Leave-out detail here http://www.transportation.wv.gov/highways/engineering/RevisedStandardDetails/wood%20blockout%2011-9-12.pdf"	
Wisconsin	0	0	Type 2	asphalt or concrete	controlled low-strength backfill or emulsified asphalt		4" thick, rectangular or circular leave-outs		
Wyoming	0	0	Type 2			asphalt or concrete	6" flowable backfill or 2" cold plant mix (lightly tamped) in 18" d or 18" square leave-out	when placed in rocks, excavate and replace with ASTM C33 curse aggregate size no 57. Details in Sheet 606-2. When guardrail is off shoulder, there is no weed control as of now	. But there have been reported problems, and state is considering switching to a mow-strip+ leave-out detail in the future. Leave-outs in pavements (asphalt/ concrete) are mandatory

APPENDIX B
STATIC TEST DETAILS

B.1 Test Site Preparation

Standardizing soil conditions and test dimensions is an essential process for when performing experiments on guardrail posts. Even if there is no directly relevant guideline for static testing of guardrail posts, the *AASHTO MASH* [21] specifies a standard soil condition and test dimensions. The *MASH* presents grading and compaction requirements for static soil strength tests. The test soil should meet *AASHTO M147* grading A or B requirements [43] and should be compacted in accordance with *AASHTO's Construction Manual for Highway Construction* [53]. The in-situ dry density of the compacted soil, determined by a sand cone test as given in *AASHTO T191* [54] or other specified methods, should exceed 95% of the maximum dry density of soil, determined by a Modified Proctor test (*AASHTO T180, Method D*) [44]. The test dimension given in Appendix B of *MASH* includes 25 inches of loading height, 32 inches of post height, and 40 inches of post embedment depth. The dimension corresponds to the standard post design of the Midwest Guardrail System (MGS) [55], which is one of the most widely used W-beam guardrail systems in the United States.

The outdoor test site is located at the Structural Engineering, Mechanics, and Materials Laboratory of the Georgia Institute of Technology, Atlanta, GA. The native soil was replaced with a graded aggregate base soil which satisfies *AASHTO M147* Grading B requirement (see Figure B1 for sieve test result) with a maximum dry density of 144 lb/ft^3 (22.7kN/m^3) as shown in Figure B2. A plate vibratory compactor was used to compact the imported soil and sand cone tests were performed to determine whether

the soil was adequately compacted or not. The in-situ dry density was 145 lb/ft^3 (22.9kN/m^3) and the *MASH* compaction requirement was met. Additionally, the thickness of every compacted soil layer was less than 8 inches as specified in requirements. Figure B3 shows the process of soil replacement and compaction.

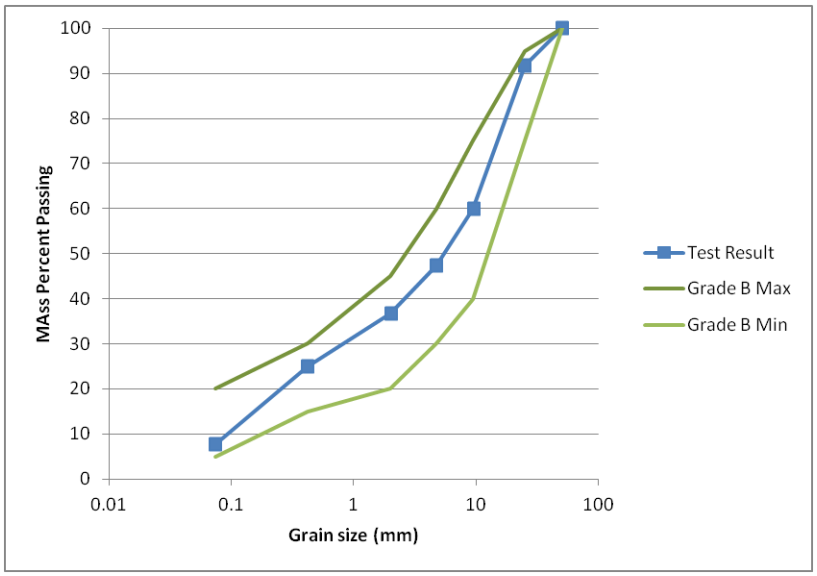

TABLE 1 Grading Requirements for Soil-Aggregate Materials

Sieve Designation		Mass Percent Passing					
Standard mm	Alternate	Grading A	Grading B	Grading C	Grading D	Grading E	Grading F
50	2 in.	100	100	—	—	—	—
25.0	1 in.	—	75-95	100	100	100	100
9.5	⅜ in.	30-65	40-75	50-85	60-100	—	—
4.75	No. 4	25-55	30-60	35-65	50-85	55-100	70-100
2.00	No. 10	15-40	20-45	25-50	40-70	40-100	55-100
0.425	No. 40	8-20	15-30	15-30	25-45	20-50	30-70
0.075	No. 200	2-8	5-20	5-15	5-20	6-20	8-25

FIGURE B1

Sieve test result in compliance with AASHTO M147.

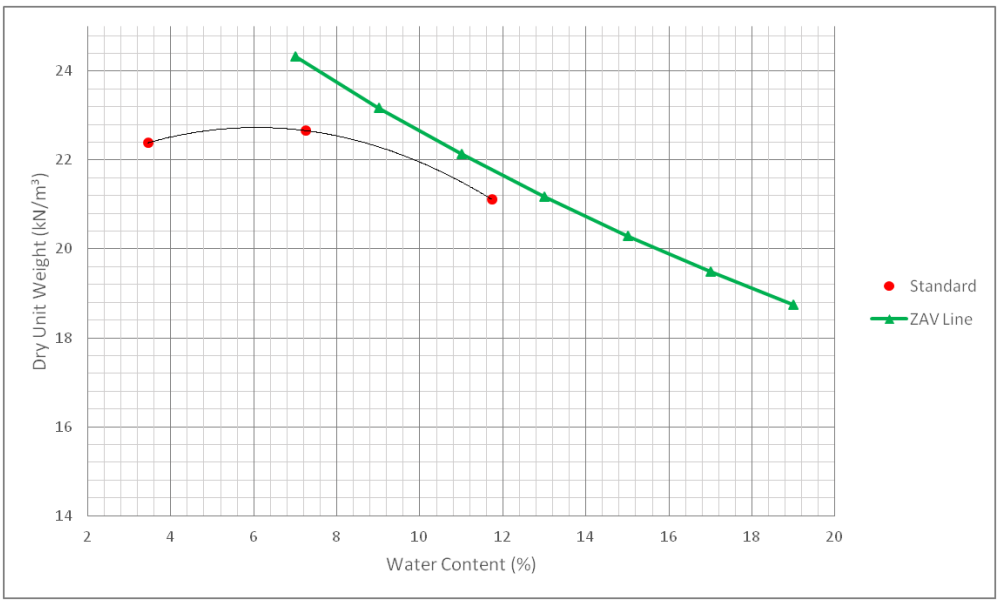

FIGURE B2

Modified Proctor test result in compliance with AASHTO T180, Method D.

FIGURE B3

Soil replacement with compaction.

B.2 Loading Fixture Design

There have been a number of experimental studies on testing guardrail posts. A representative study was published in 1983, by Texas Transportation Institute (TTI technical report: A study of the soil-structure interaction behavior of highway guardrail

posts) [24]. Researchers performed six static load tests and four dynamic load tests on guardrail posts with different test configurations. The lateral loading system of their static tests consisted of a hydraulic cylinder, a concrete anchor, and instrumentations. Selective test results from the study are shown in Table B1, and there was no significant difference but a slight correlation in maximum lateral load and dissipated energy (calculated from the load-displacement curve) among given test conditions. They concluded that steel posts performed similar to wood posts of the same embedment depth.

TABLE B1
Selective test results from TTI technical report [24].

	Static		Dynamic	
Test condition*	**Max. lateral load (kip)**	**Dissipated energy (ft-kip)**	**Max. lateral load (kip)**	**Dissipated energy (ft-kip)**
W-L	3.7	4.2	13.3 **	**
S-L	3.3	3.8	22.4	29.3
W-C	2.9	4.4	16.3	27.2
S-C	3.2	4.2	17.0	29.9

* W: Wood post, S: Steel post, C: Cohesive soil, L: Cohesionless soil
Loading height= 21", embedment depth= 38"
** Wood post broke during impact.

The load carrying capacity (maximum lateral load capacity of a guardrail post) was estimated by simple structural analysis. The ground was assumed to create a fixed boundary condition on the post similar to a cantilever beam. The W6x9 section was assumed to reach the plastic moment at the ground level. Finally, the post was assumed to be perfectly aligned with the loading direction. Using these assumptions, the maximum lateral load (P_{max}) is calculated as follows:

$$P_{\max} = \frac{M_p}{e} = \frac{311.5}{25} = 12.46\,\text{kip} \tag{B1}$$

Where M_p is the plastic moment in the post section and e is the load eccentricity (25 inches). These assumptions are not always valid in actual testing. Since both the mow

strip and the soil are not rigid and permit displacement/rotation of the post in the ground, the maximum lateral load in actual testing would not be expected to exceed 12.5 kip prior to the formation of plastic hinge. Therefore in the loading fixture design, all components were designed to carry a minimum capacity of 20 kips so that the post-yielding behavior of guardrail posts could be captured safely.

There were two different ways of reaction wall design in the literature. Either the anchor method or the friction method (see Figure B4) can be adopted as long as the system can provide the necessary reaction capacity for the anticipated maximum load. Considering the test site condition, the research team selected a friction method system including large concrete blocks, steel tube sections, and post-tension bars. Steel sections and bars were used for fastening the blocks together in both horizontal and vertical directions (see Figure B5). The total weight of the reaction wall system was 54 kips. A conservative estimate of 0.5 for the static coefficient of friction resulted in an estimated lateral load reaction capacity of at least 27 kips.

B.3 Measurement Plan and Installation

A lateral load on the guardrail post was induced by the retraction of a hydraulic cylinder. Lateral load on the post, displacement of the post, and longitudinal strains along the post flange were measured and recorded through a data acquisition system. A reader can find visual details in Figures 9, 10, and 11 in Chapter 3.

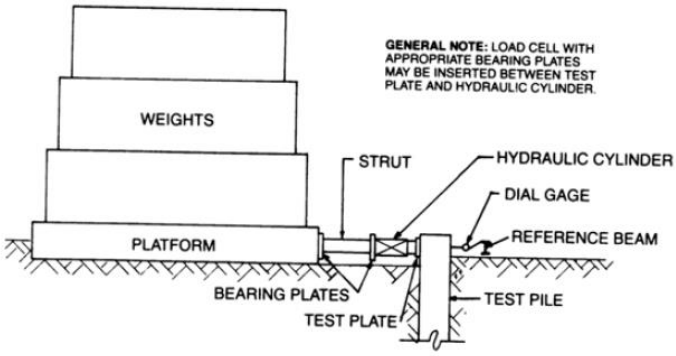

(a)

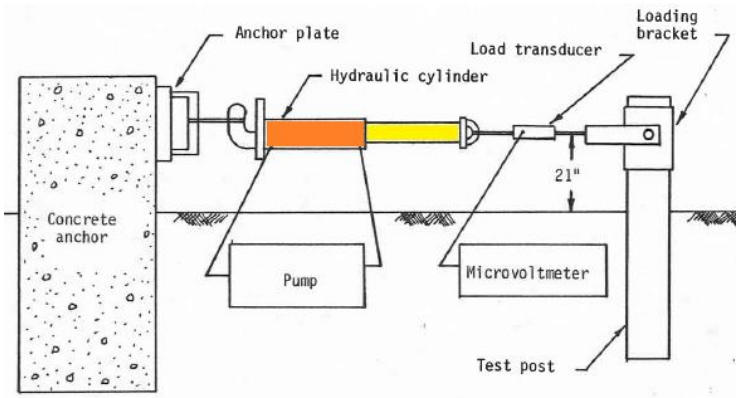

(b)

FIGURE B4

Lateral loading system described in: (a) ASTM D3966 [56], (b) TTI report [24].

FIGURE B5

Reaction wall system.

Load cell

The S-type load cell was linked on one side with the retracting arm of the hydraulic cylinder and on the other side with a loading bracket that transmitted the lateral load to the testing post. In order to prevent potential damage during testing, threaded bearing rod ends were attached on both sides of the load cell to prevent the occurrence of bending moment and torsion along the load axis. The maximum capacity of the load cell was 20 kips.

String Potentiometers

Two string potentiometers were mounted on the reference pole with a fixed stand-off distance from the testing post. One string potentiometer was located at the level of the lateral loading arm (to record the load-displacement curves) and another potentiometer was located at ground level (to measure ground level displacements). The maximum extension of the string potentiometer was 50 inches.

Strain Gages

For the initial baseline tests, strain gages were positioned as recommended by previous researchers [57]. Once the asphalt mow strips were incorporated into the testing program, nine strain gages were used as shown in Figure B6. This modification was made because the ground level of the post was expected to reach or exceed yielding during the testing due to the restraint provided by asphalt mow strips. A metal shim was attached at the bottom of the flange and covered all gages and wires under the ground level to prevent the damage during post-driving (Figure B7).

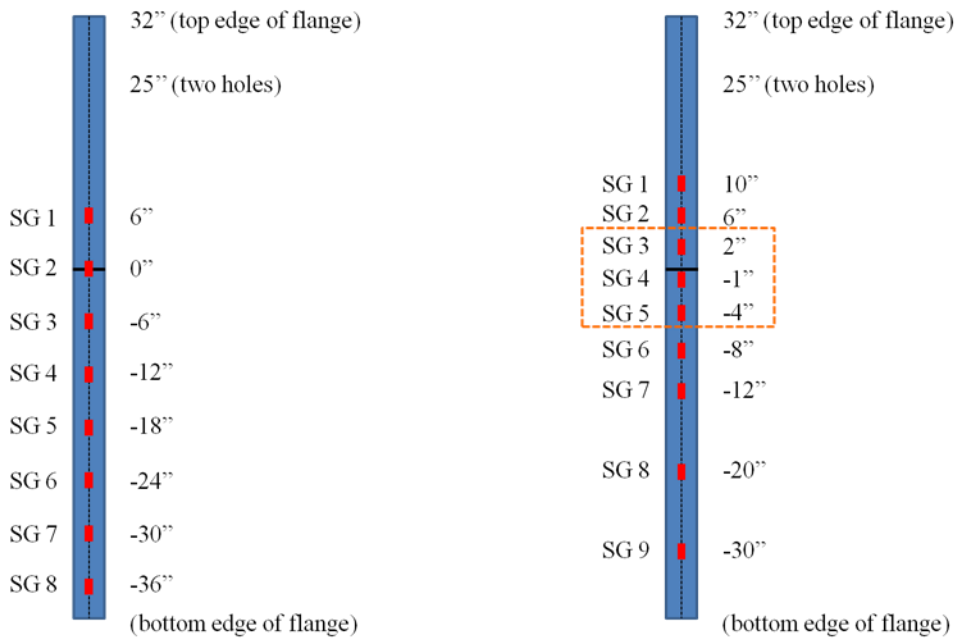

FIGURE B6

Modification in strain gage instrumentation:
(a) initial gage locations, and (b) modified gage location.

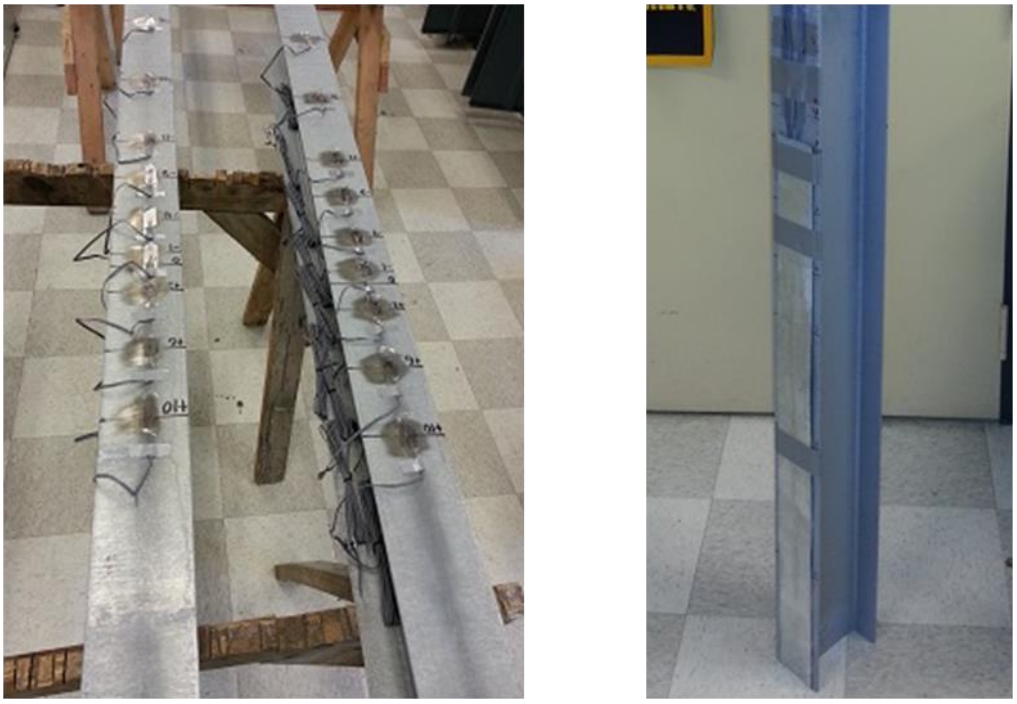

FIGURE B7

Strain gage installation: (a) attachment, and (b) protection.

B.4 Test Protocol and Safety Considerations

Each test was mainly controlled by manual retraction of the hydraulic cylinder on the loading fixture. The test was considered over when (1) the lateral movement of the cylinder exceeds 20 inches or (2) yielding was measured in the steel post. The following static test protocol was employed:

- Assemble all components of loading system (loading bracket, load cell, hydraulic cylinder and cable system).
- Check all fasteners/connection on the loading system.
- Setup the string potentiometers and the reference pole.
- Start the data acquisition.
- Start the hydraulic cylinder retraction (by using hydraulic pump unit).
- Take pictures of testing post of laterally displaced (if available).
- Stop pumping the hydraulic pump unit when the test end condition is satisfied.
- Stop the data acquisition.
- Perform visual inspection as needed.
- Remove the fasteners/connection of the loading system and move each component to the next post location.

Test configuration drawings for the static test program are given in Figures B8 –B12.

Test result reports of all 19 posts are presented in Figures B13–B31. Each report includes the following information:

- Test description
- Mow strip configuration
- Test condition and background information
- Test drawings with dimensions
- Test pictures taken at test start and test end
- Load vs. displacement curve
    - Peak load and displacement at peak load
- Work (energy dissipation) vs. ground level displacement curve
    - Ground level displacement at 66.7 kip-in work done
- Strain vs. displacement curves
    - Maximum strain values and their percentages to yield strain

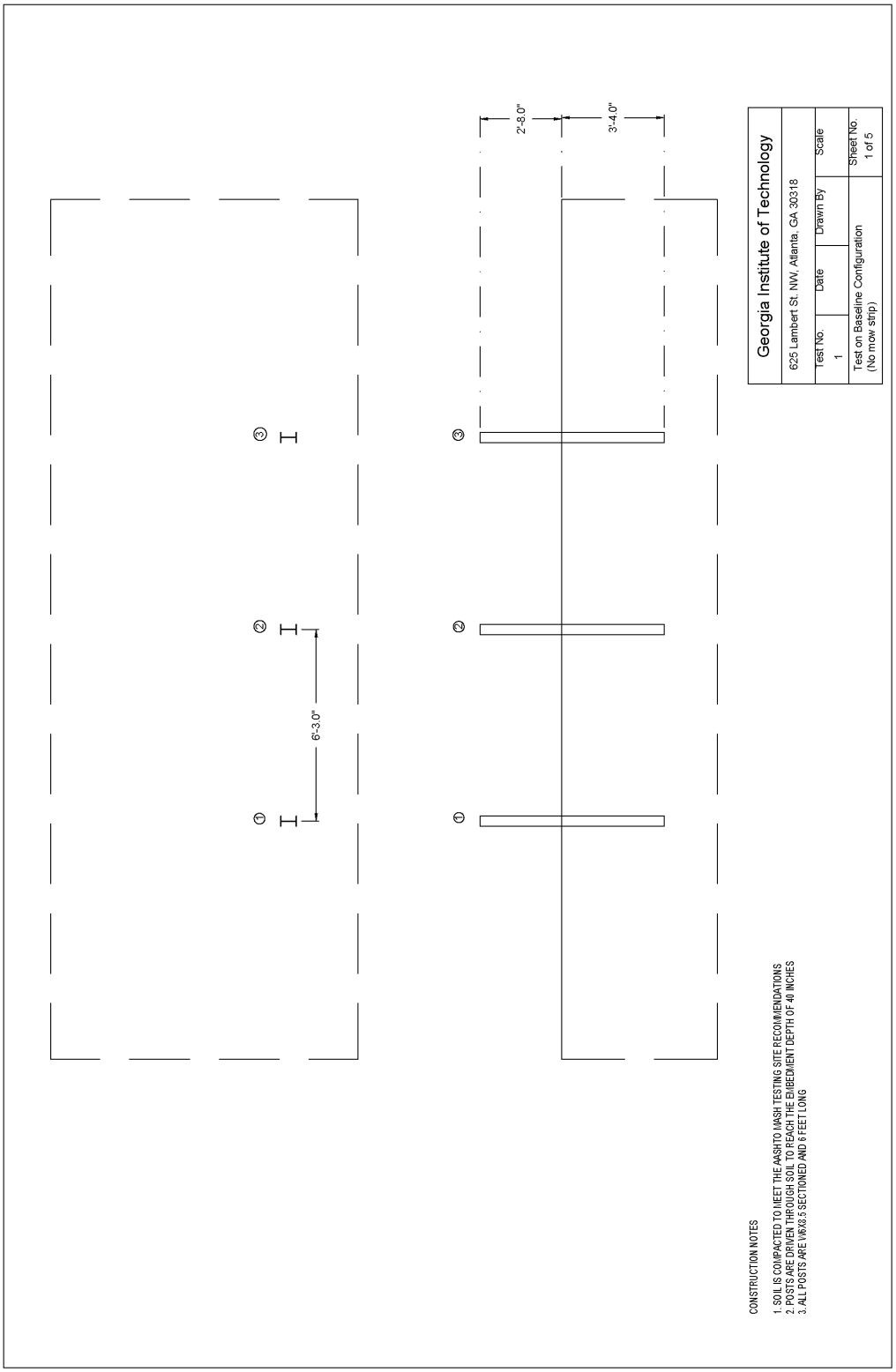

FIGURE B8

Test configuration drawing: Set 1

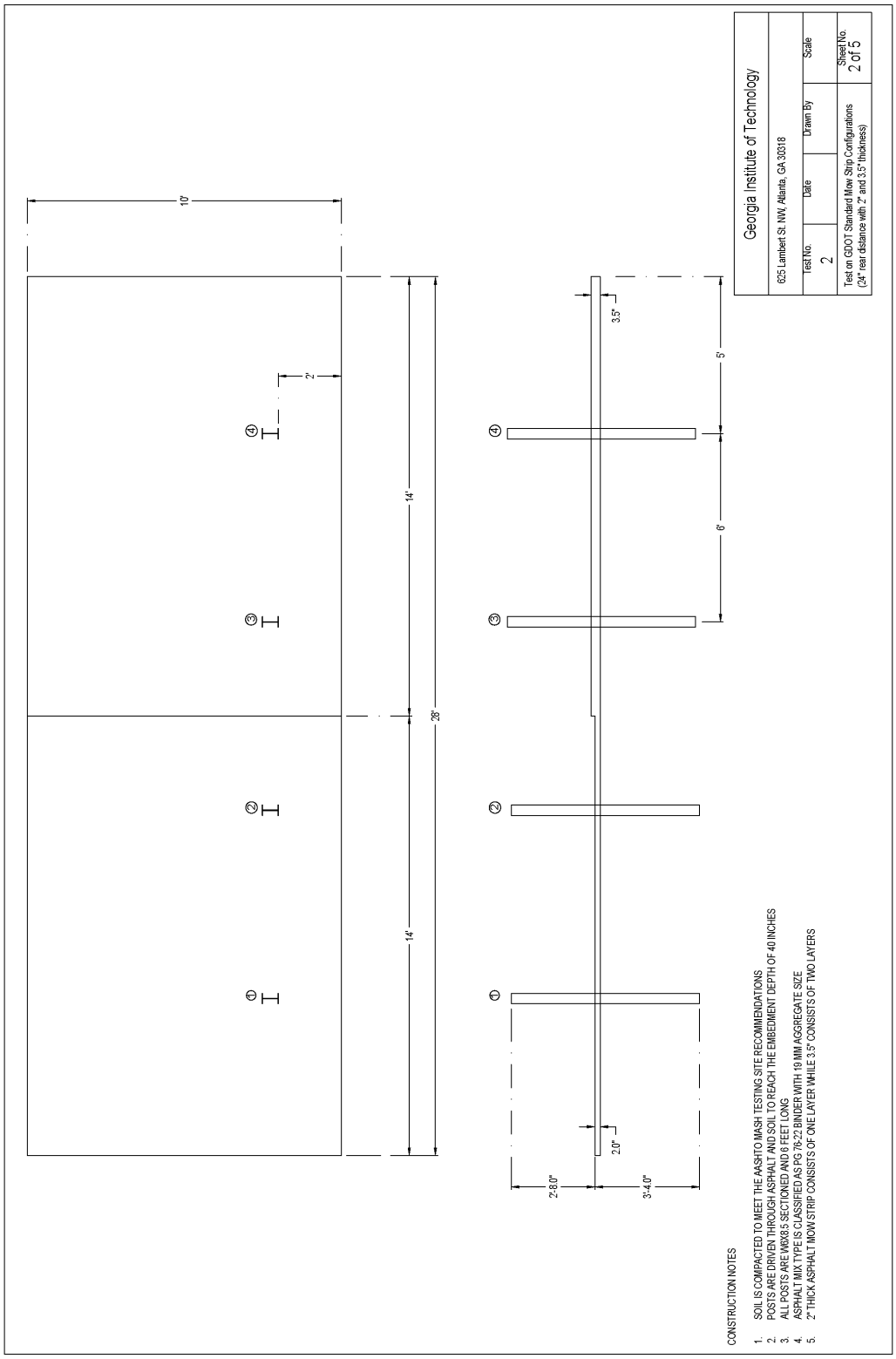

FIGURE B9

Test configuration drawing: Set 2

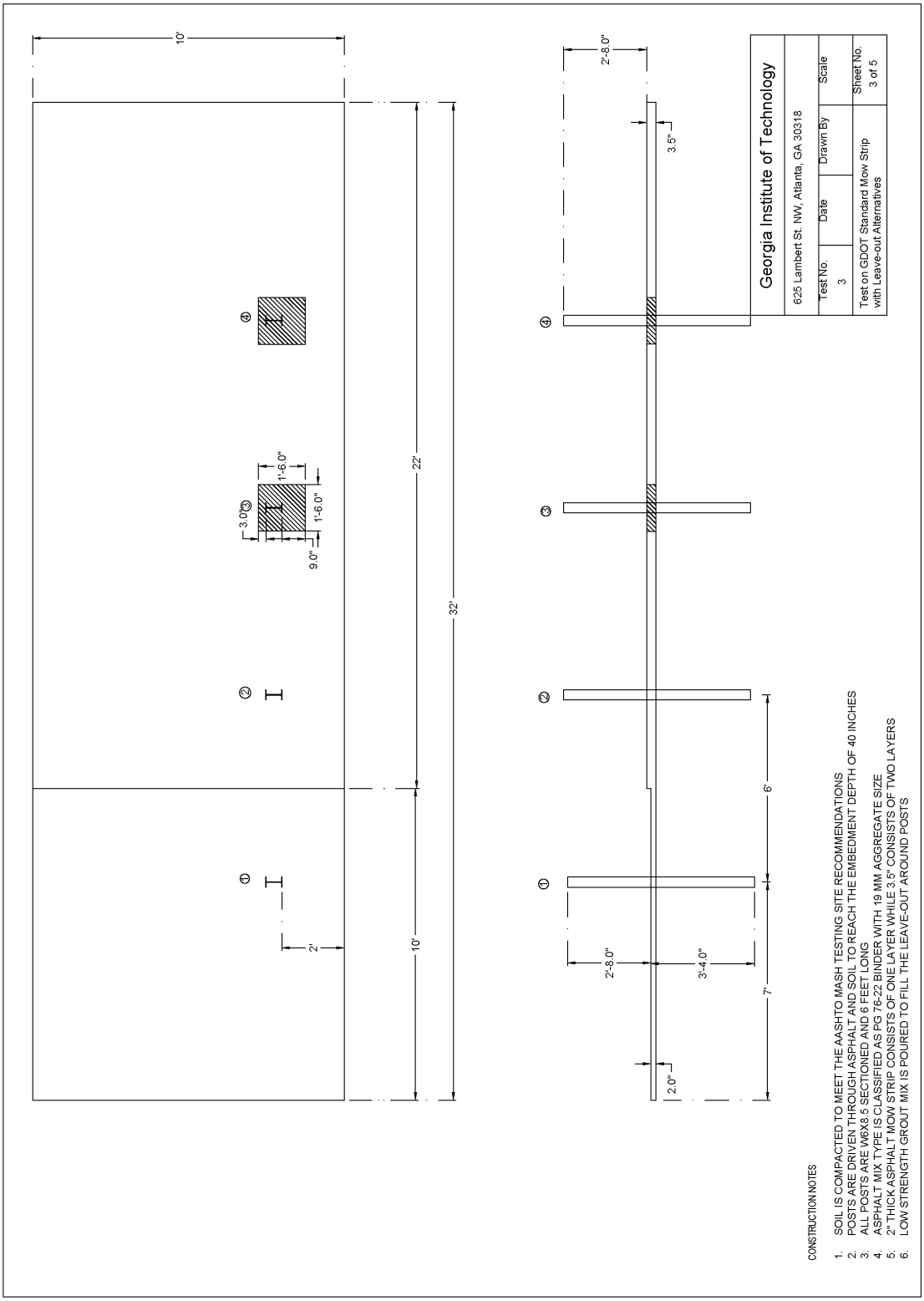

FIGURE B10

Test configuration drawing: Set 3

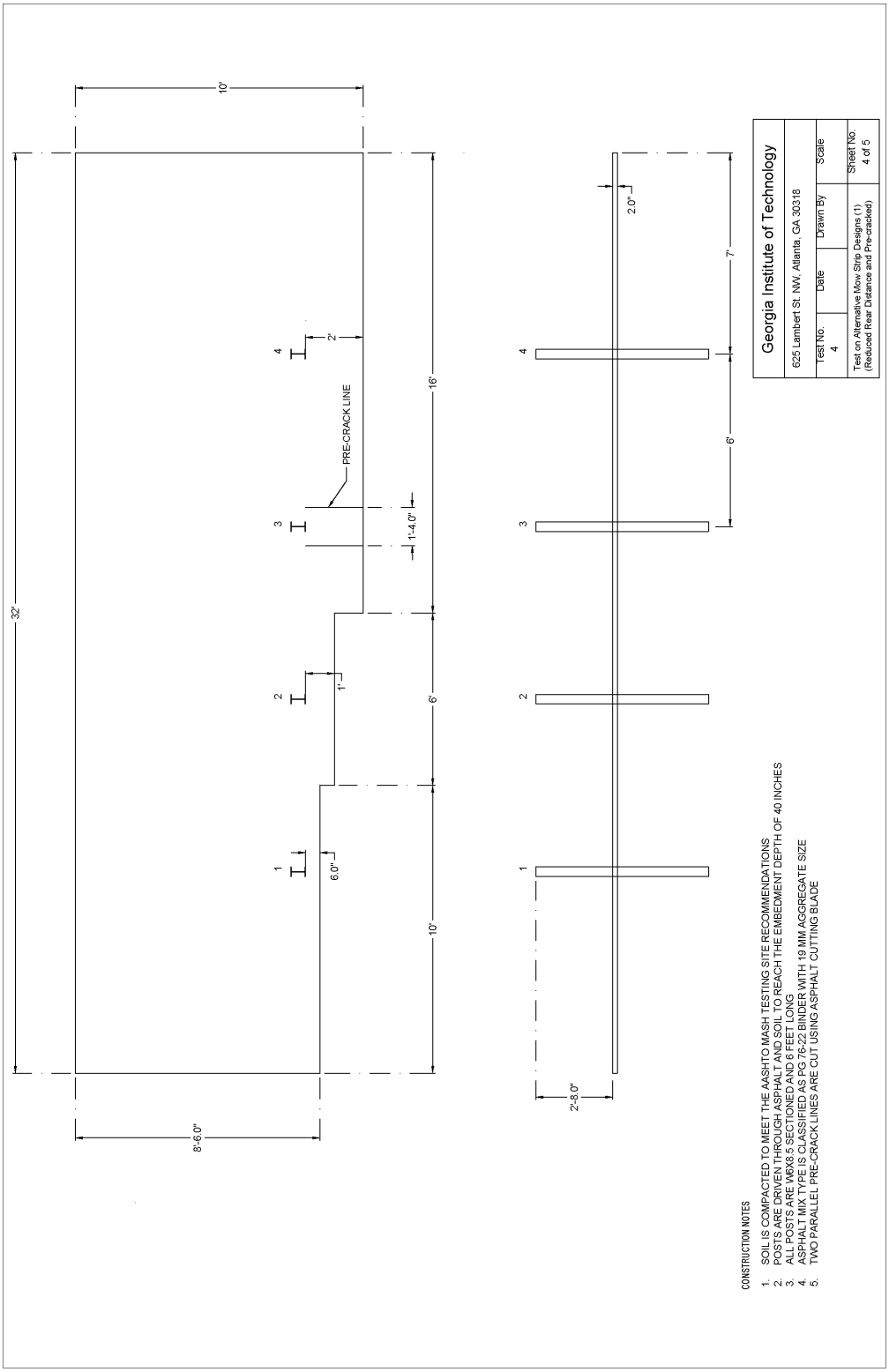

FIGURE B11

Test configuration drawing: Set 4

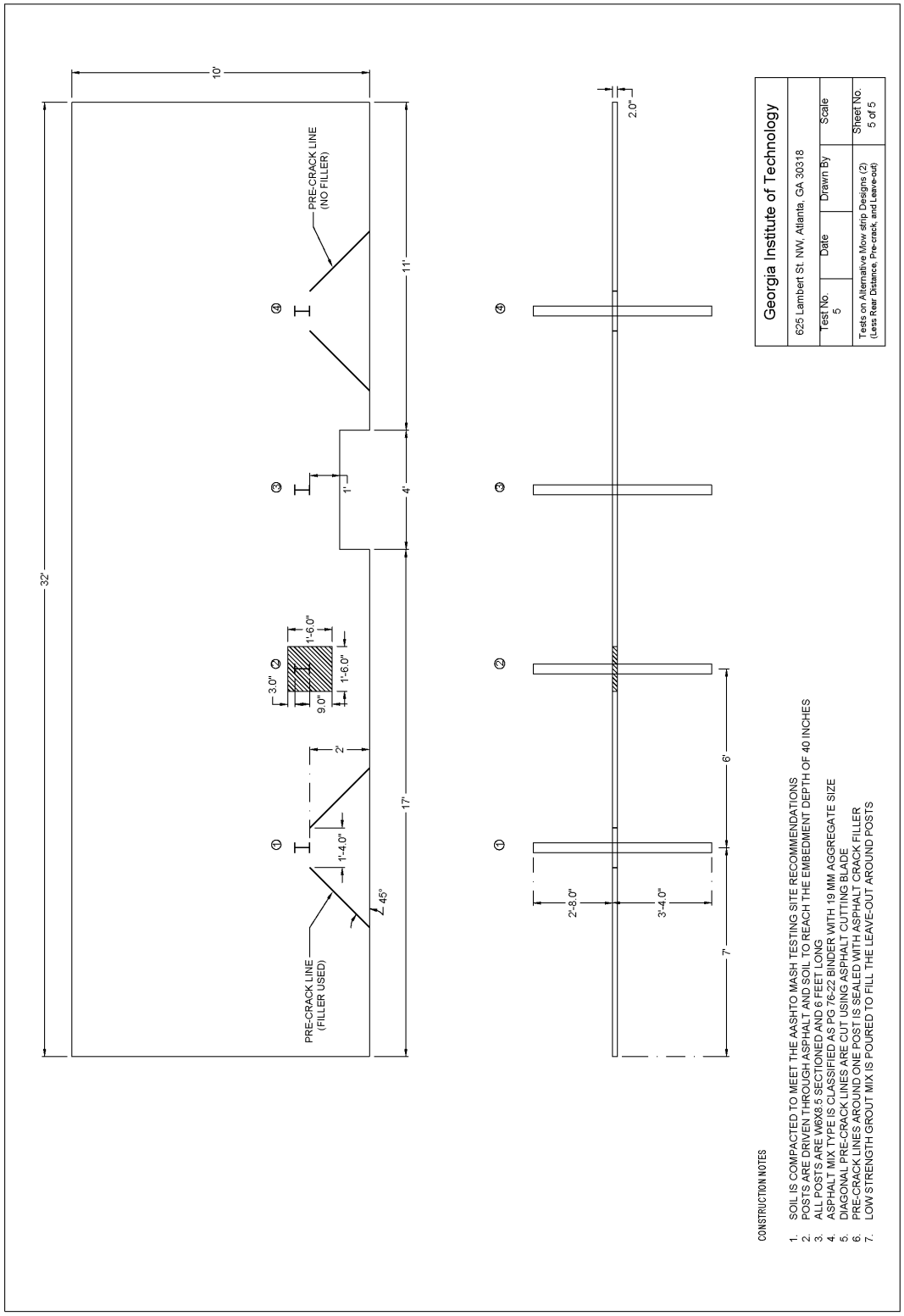

FIGURE B12

Test configuration drawing: Set 5

B.5 Test Result Reports

Test 1-1 0-0

- Baseline configuration
- No mow strip
- Temperature recording not needed

Mow strip configuration	Thickness	0 inch
	Rear Distance	0 inch
	Modification	N.A.

Location	Structural Lab, Georgia Tech, Atlanta, GA 30318
Test date	6/3/2014
Temperature	degrees F
Asphalt age	N.A. days from placement

Test drawings

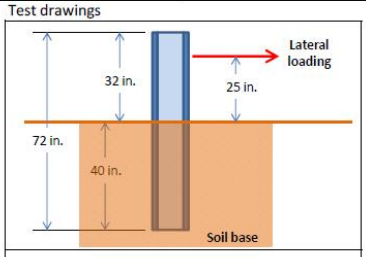

Test pictures

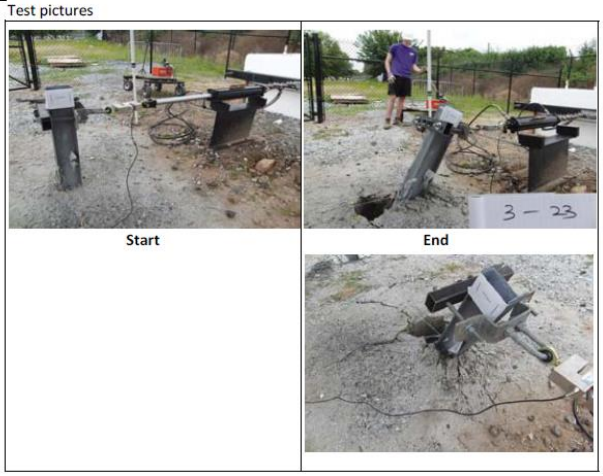

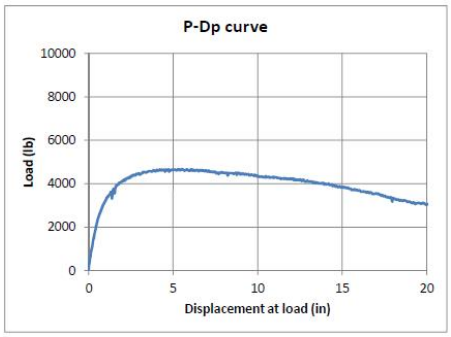

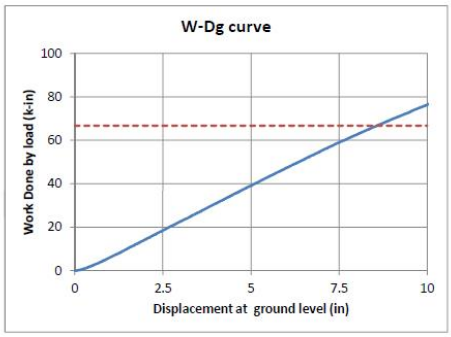

Peak load (lb)	4673.34
Dp at peak load (in)	5.51764

Dg at 66.7 k-in work (in)	8.57615

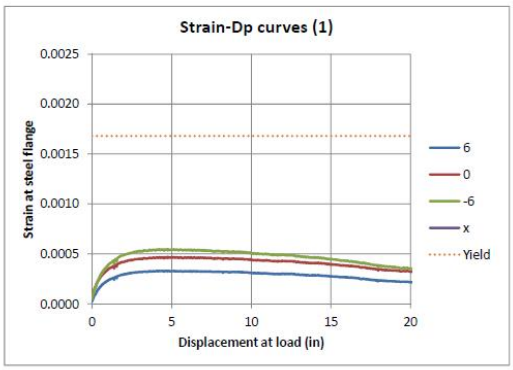

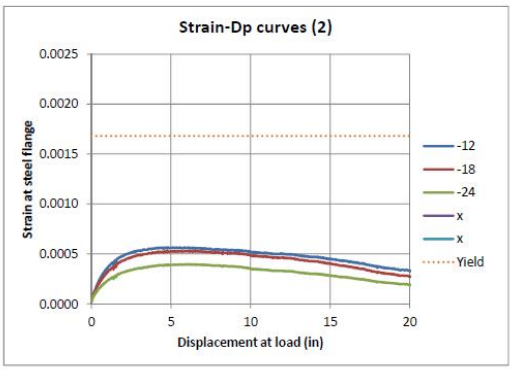

Gage location (in)	6	0	-6	x	-12	-18	-24	x	x
Maximum strain	0.00033	0.00047	0.00054	0	0.00056	0.00053	0.0004	0	0
Yield %	19.6083	27.7692	32.4298	0	33.6289	31.5467	23.5713	0	0

FIGURE B13

Test result report: Post 1-1

Test 1-2	0-0	
* Baseline configuration		
* No mow strip		
* Temperature recording not needed		
Mow strip configuration	Thickness	0 inch
	Rear Distance	0 inch
	Modification	N.A.

Location	Structural Lab, Georgia Tech, Atlanta, GA 30318	
Test date	6/3/2014	
Temperature		degrees F
Asphalt age	N.A.	days from placement

Test drawings

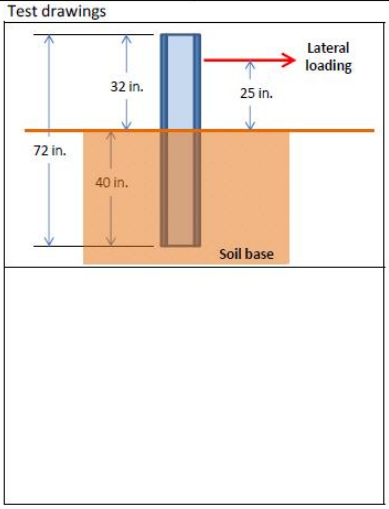

Test pictures

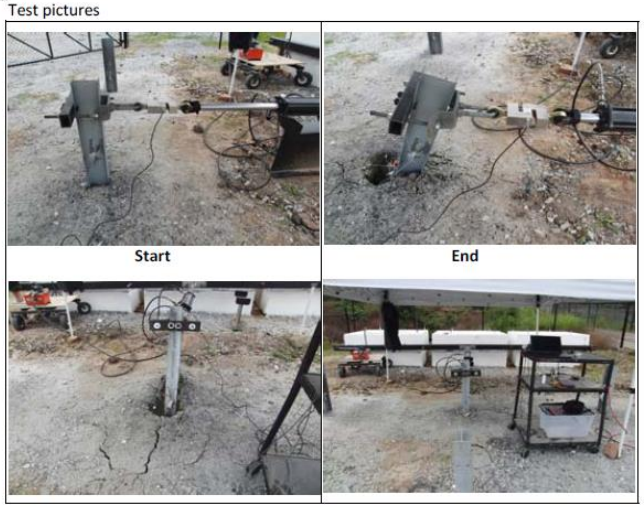

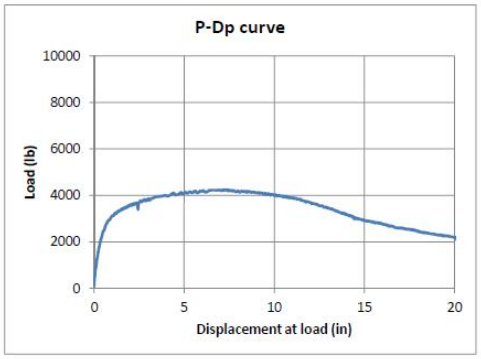

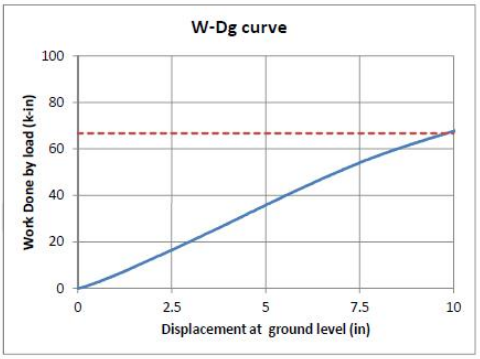

Peak load (lb)	4247.29
Dp at peak load (in)	7.11042

Dg at 66.7 k-in work (in)	9.83429

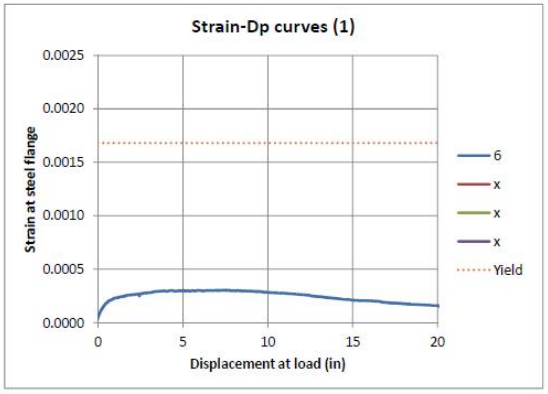

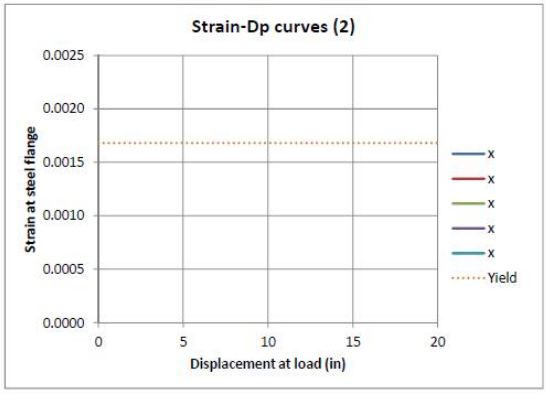

Gage location (in)	6	x	x	x	x	x	x	x	x
Maximum strain	0.00031	0	0	0	0	0	0	0	0
Yield %	18.2008	0	0	0	0	0	0	0	0

FIGURE B14

Test result report: Post 1-2

Test 1-3	0-0	
* Baseline configuration		
* No mow strip		
* Temperature recording not required		
Mow strip configuration	Thickness	0 inch
	Rear Distance	0 inch
	Modification	N.A.

Location	Structural Lab, Georgia Tech, Atlanta, GA 30318	
Test date	6/3/2014	
Temperature		degrees F
Asphalt age	N.A.	days from placement

Test drawings

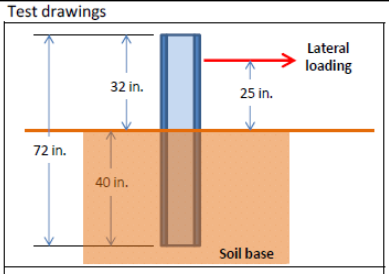

Test pictures

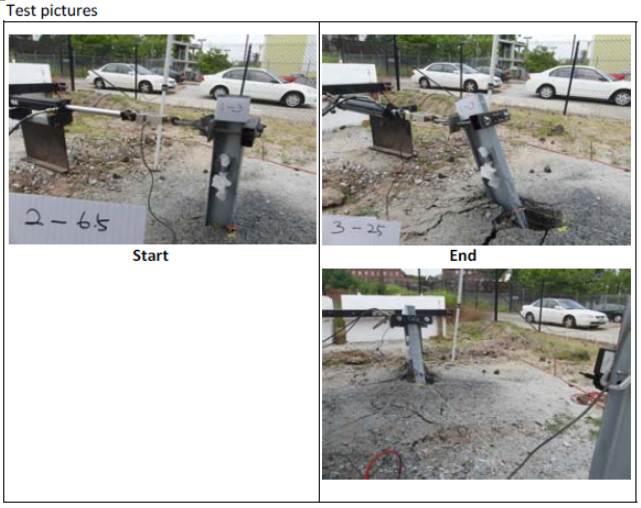

Start End

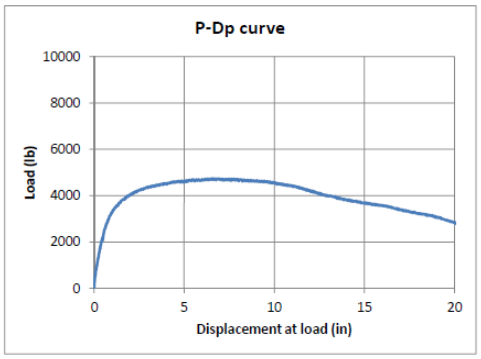

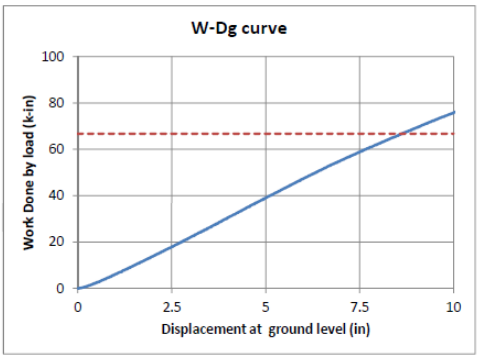

Peak load (lb)	4743.67
Dp at peak load (in)	6.59314

Dg at 66.7 k-in work (in)	8.62428

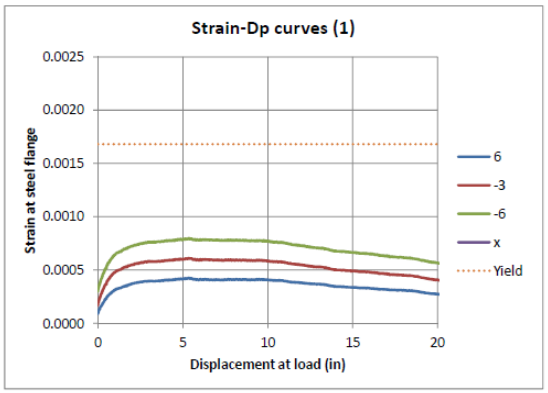

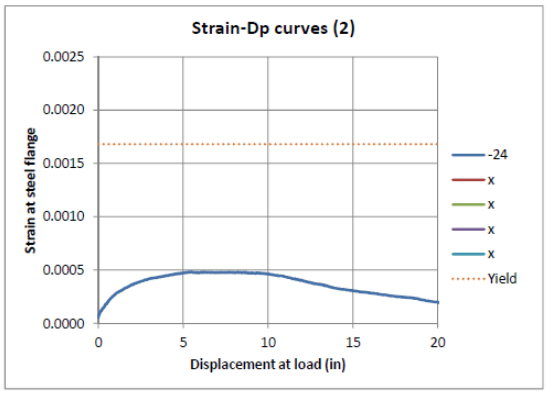

Gage location (in)	6	-3	-6	x	-24	x	x	x	x
Maximum strain	0.00041	0.0006	0.00079	0	0.00048	0	0	0	0
Yield %	24.5481	35.6867	46.7811	0	28.6182	0	0	0	0

FIGURE B15

Test result report: Post 1-3

Test 2-1	2-24	
* GDOT typical mow strip practice		
* 2" thickness and 24" rear distance behind the post		
*		
Mow strip configuration	Thickness	2 inch
	Rear Distance	24 inch
	Modification	N.A.

Location	Structural Lab, Georgia Tech, Atlanta, GA 30318
Test date	7/8/2014
Temperature	90 degrees F
Asphalt age	18 days from placement

Test drawings

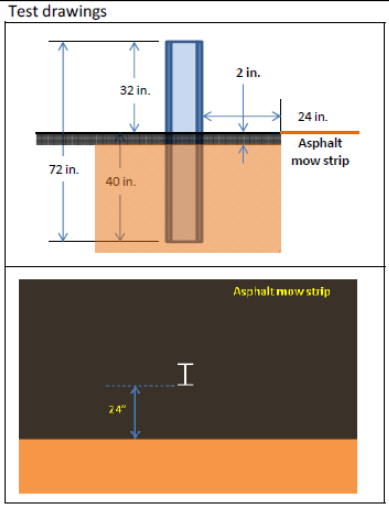

Test pictures

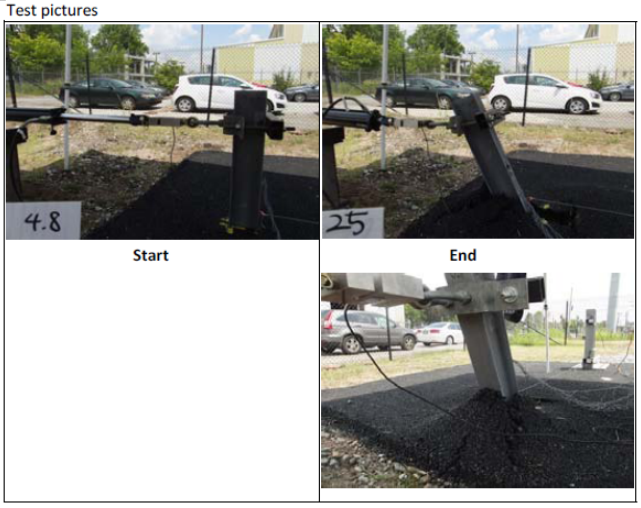

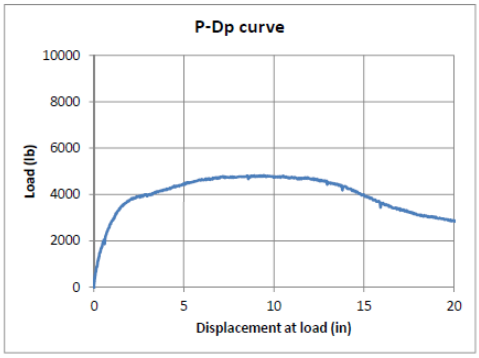

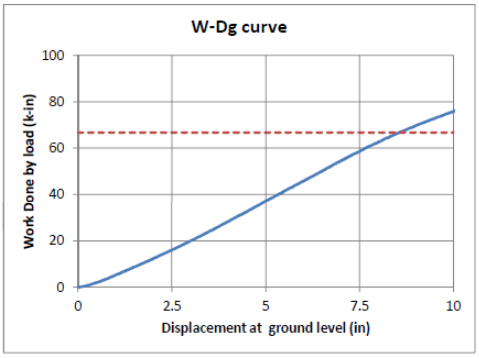

Peak load (lb)	4827.28
Dp at peak load (in)	9.42257

Dg at 66.7 k-in work (in)	8.5604

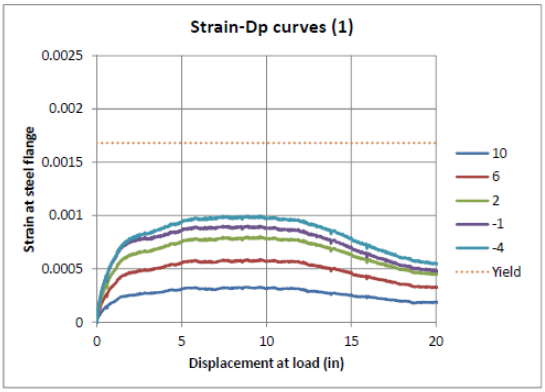

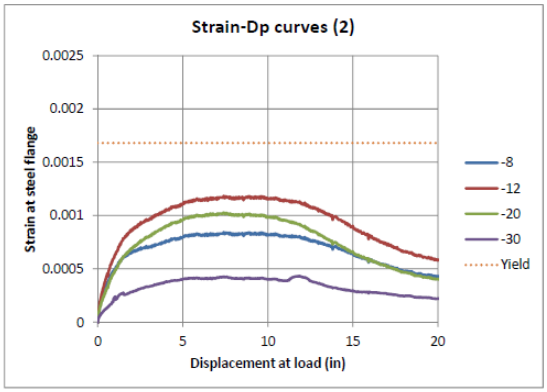

Gage location (in)	10	6	2	-1	-4	-8	-12	-20	-30
Maximum strain	0.00033	0.00059	0.0008	0.0009	0.001	0.00084	0.00118	0.00101	0.00042
Yield %	19.6697	35.0916	47.7676	53.76	59.334	50.0199	70.3348	60.0454	24.7642

FIGURE B16

Test result report: Post 2-1

Test 2-2	2-24	
* GDOT typical mow strip practice		
* 2" thickness and 24" rear distance behind the post		
*		
Mow strip configuration	Thickness	2 inch
	Rear Distance	24 inch
	Modification	N.A.

Location	Structural Lab, Georgia Tech, Atlanta, GA 30318
Test date	7/8/2014
Temperature	90 degrees F
Asphalt age	18 days from placement

Test drawings

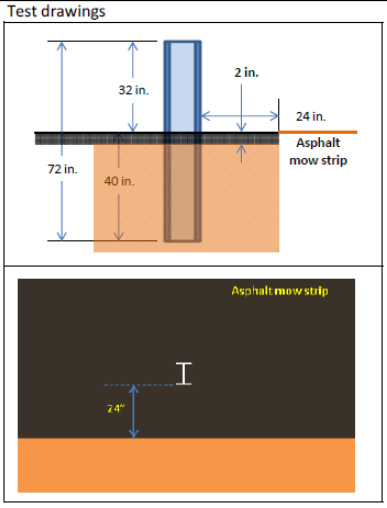

Test pictures

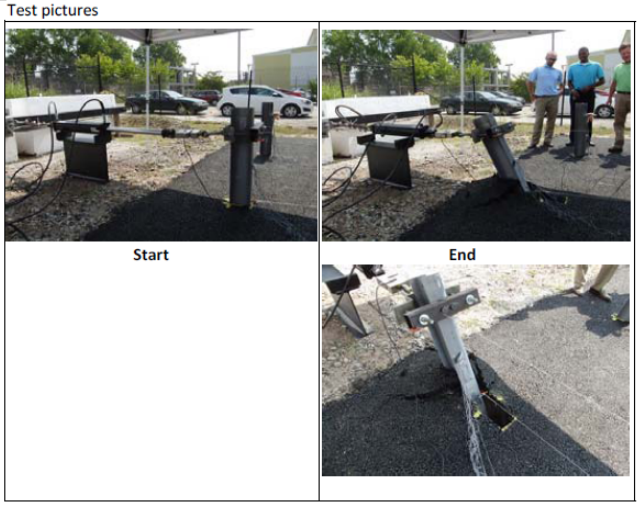

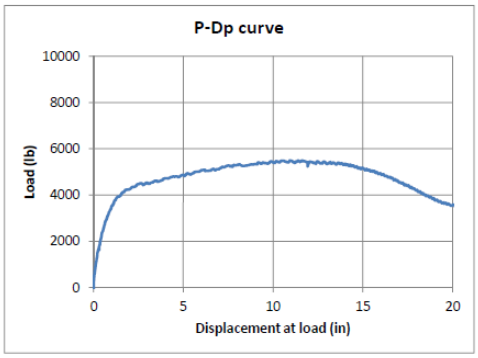

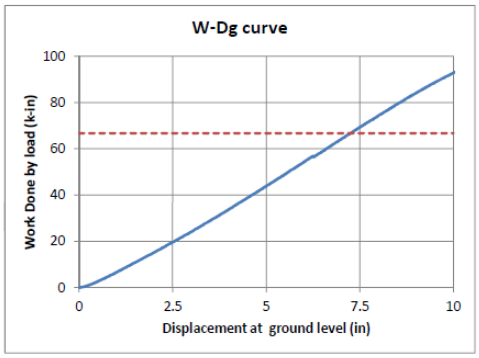

Peak load (lb)	5490.62
Dp at peak load (in)	10.9583

Dg at 66.7 k-in work (in)	7.25718

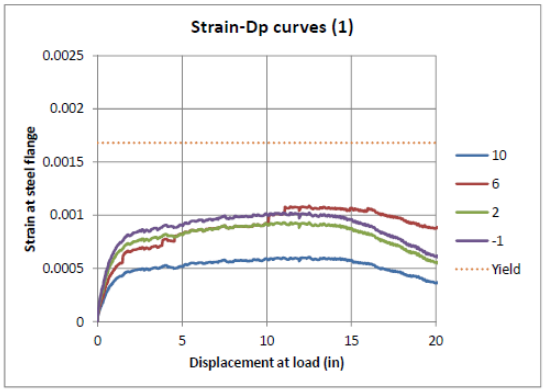

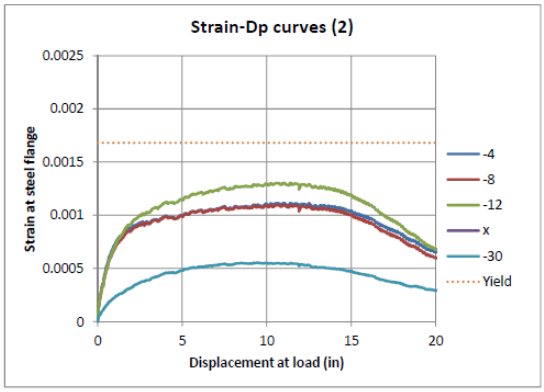

Gage location (in)	10	6	2	-1	-4	-8	-12	x	-30
Maximum strain	0.0006	0.00108	0.00093	0.00102	0.00111	0.0011	0.0013	0	0.00055
Yield %	35.7011	64.2276	55.4098	60.8635	66.3624	65.3165	77.5668	0	32.6457

FIGURE B17

Test result report: Post 2-2

Test 2-3	3.5-24	
* GDOT typical mow strip practice		
* 3.5" thickness and 24" rear distance behind the post		
*		
Mow strip configuration	Thickness	3.5 inch
	Rear Distance	24 inch
	Modification	N.A.

Location	Structural Lab, Georgia Tech, Atlanta, GA 30318
Test date	7/8/2014
Temperature	90 degrees F
Asphalt age	18 days from placement

Test drawings

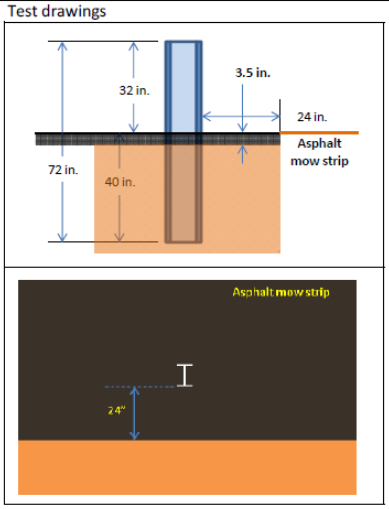

Test pictures

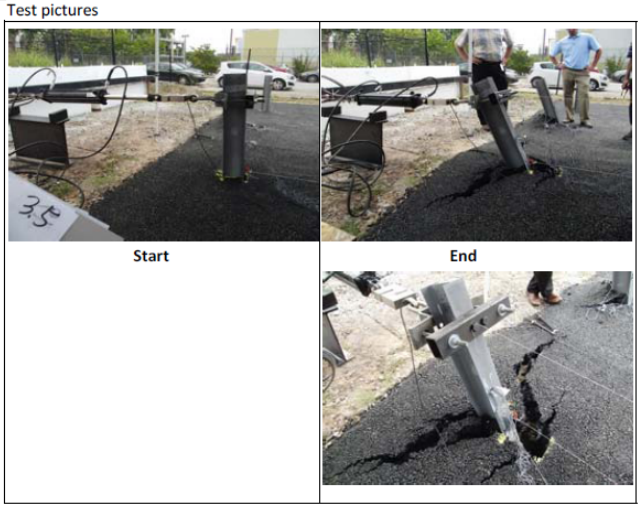

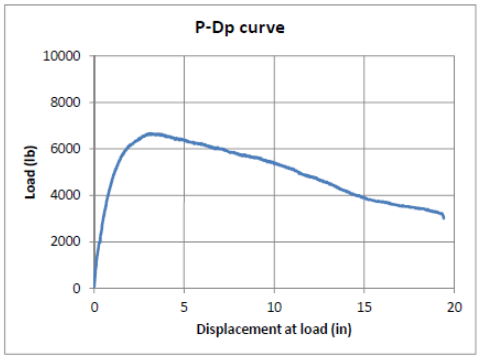

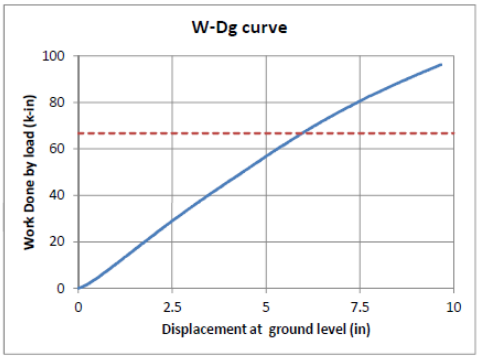

Peak load (lb)	6662.83
Dp at peak load (in)	3.10825

Dg at 66.7 k-in work (in)	5.97238

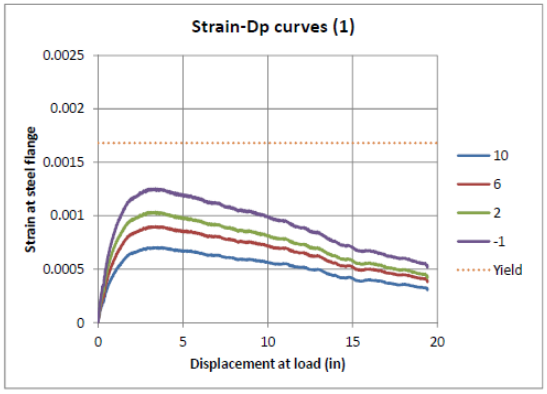

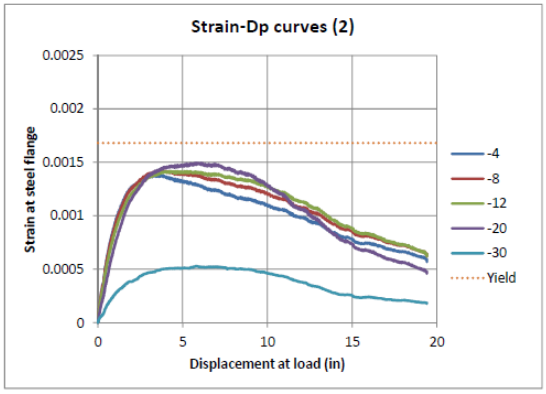

Gage location (in)	10	6	2	-1	-4	-8	-12	-20	-30
Maximum strain	0.0007	0.0009	0.00104	0.00125	0.00138	0.00142	0.00139	0.00142	0.00048
Yield %	41.9517	53.6604	61.6733	74.6974	82.3979	84.2487	82.9148	84.5858	28.6401

FIGURE B18

Test result report: Post 2-3

Test 2-4	3.5-24	
* GDOT typical mow strip practice		
* 3.5" thickness and 24" rear distance behind the post		
*		
Mow strip configuration	Thickness	3.5 inch
	Rear Distance	24 inch
	Modification	N.A.

Location	Structural Lab, Georgia Tech, Atlanta, GA 30318
Test date	7/8/2014
Temperature	90 degrees F
Asphalt age	18 days from placement

Test drawings

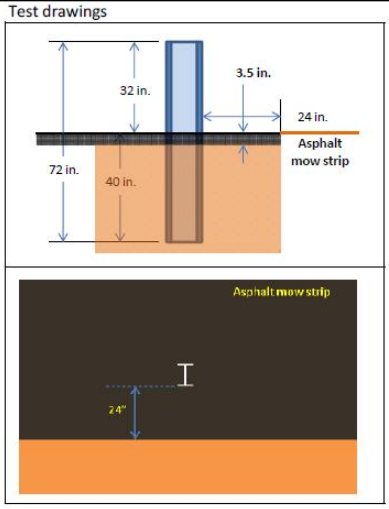

Test pictures

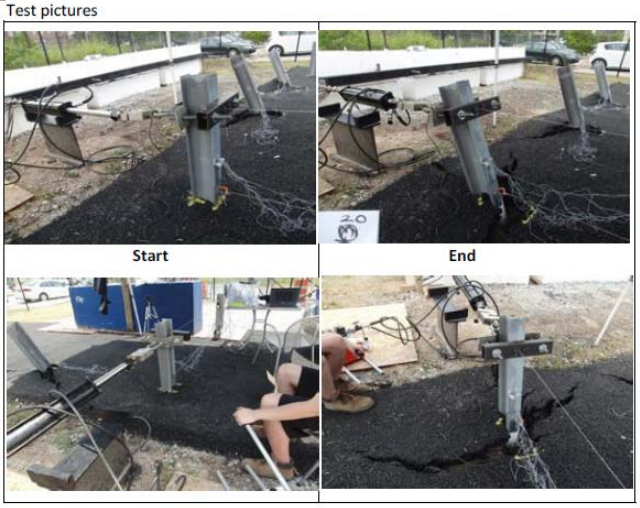

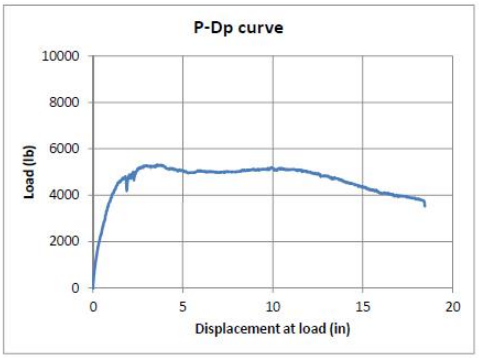

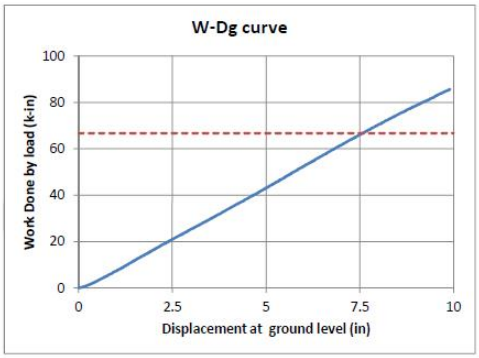

Peak load (lb)	5317.55
Dp at peak load (in)	3.54968

Dg at 66.7 k-in work (in)	7.57823

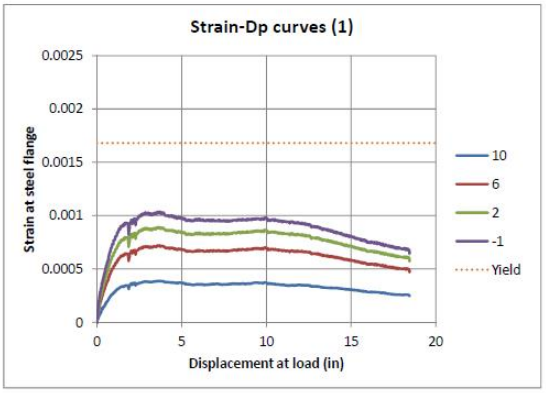

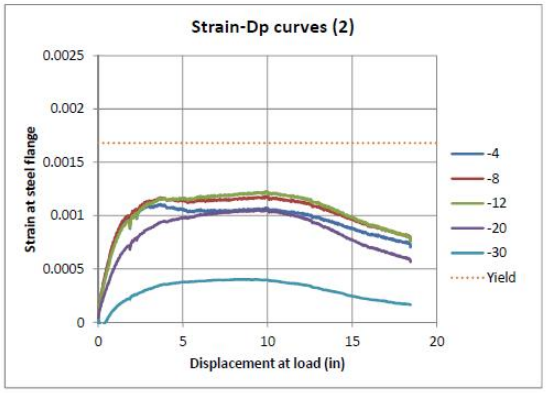

Gage location (in)	10	6	2	-1	-4	-8	-12	-20	-30
Maximum strain	0.00039	0.00072	0.00089	0.00104	0.00111	0.00117	0.00116	0.00095	0.00036
Yield %	23.1902	43.0443	53.1858	61.7358	65.9654	69.6195	69.1799	56.3096	21.1445

FIGURE B19

Test result report: Post 2-4

Test 3-1	3.5-24-L	
* The GDOT mow strip with typical leave-out application		
* 18"x18" low strength grout as leave-out material		
* Recommended by the AASHTO Roadside Design Guide		
Mow strip configuration	Thickness	3.5 inch
	Rear Distance	24 inch
	Modification	Typical grout leave-out

Location	Structural Lab, Georgia Tech, Atlanta, GA 30318
Test date	2/12/2015
Temperature	50 degrees F
Asphalt age	118 days from placement
Grout strength	105.6 psi (28-day comp. strength less than 120 psi)

Test drawings

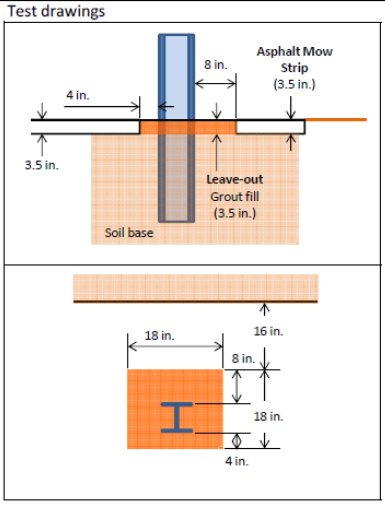

Test pictures

Start | End

The 3-1 test was terminated earlier than expected due to the malfunction of hydraulic cylinder.

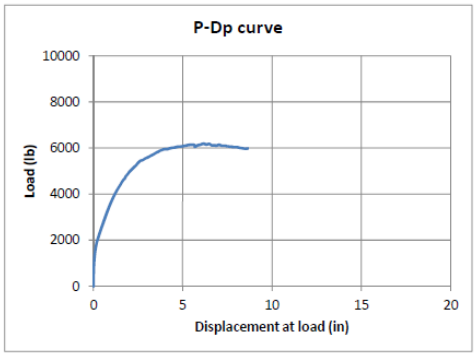

Peak load (lb)	6181.34
Dp at peak load (in)	6.18023

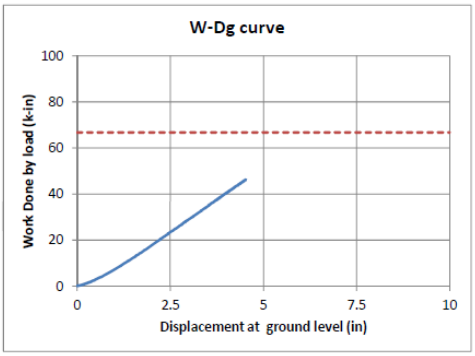

Dg at 66.7 k-in work (in)	6.353	* expected value

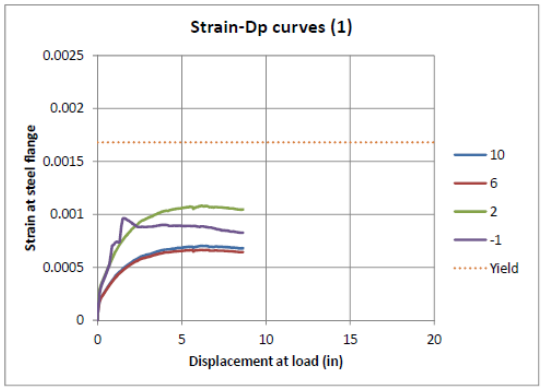

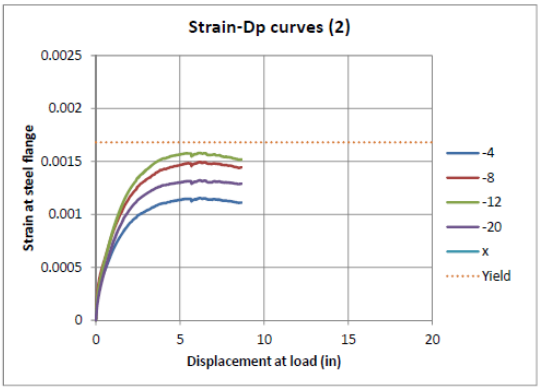

Gage location (in)	10	6	2	-1	-4	-8	-12	-20	x
Maximum strain	0.0007	0.00067	0.00108	0.00089	0.00115	0.0015	0.00158	0.00132	0
Yield %	41.8429	39.6952	64.3996	52.882	68.7326	89.0248	94.1108	78.6882	0

FIGURE B20

Test result report: Post 3-1

Test 3-2	3.5-24-L	
* The GDOT mow strip with typical leave-out application		
* 18"x18" low strength grout as leave-out material		
* Recommended by the AASHTO Roadside Design Guide		
Mow strip configuration	Thickness	3.5 inch
	Rear Distance	24 inch
	Modification	Typical grout leave-out

Location	Structural Lab, Georgia Tech, Atlanta, GA 30318
Test date	2/12/2015
Temperature	50 degrees F
Asphalt age	118 days from placement
Grout strength	105.6 psi (28-day comp. strength less than 120 psi)

Test drawings

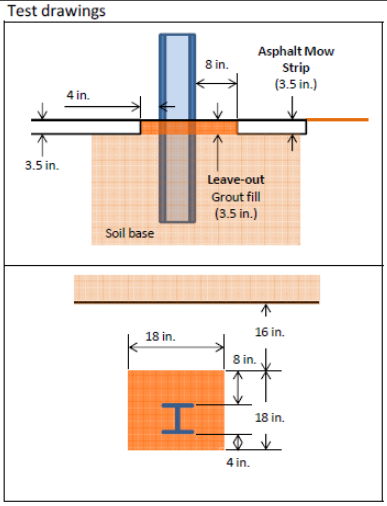

Test pictures

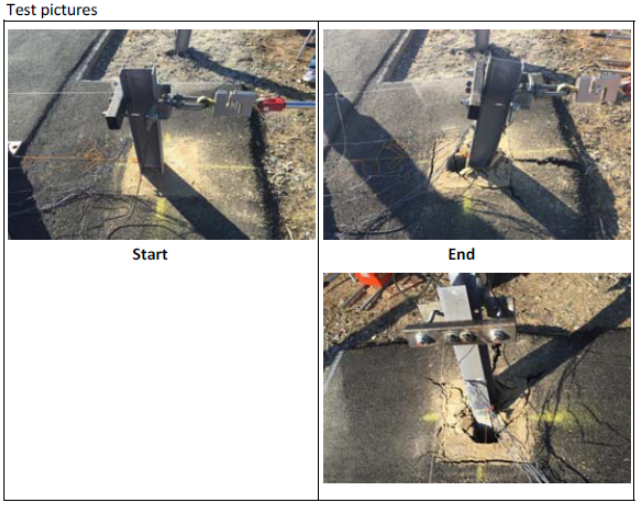

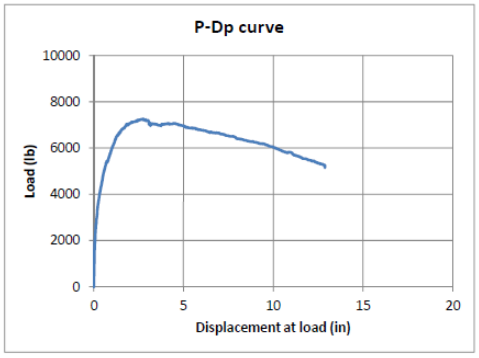

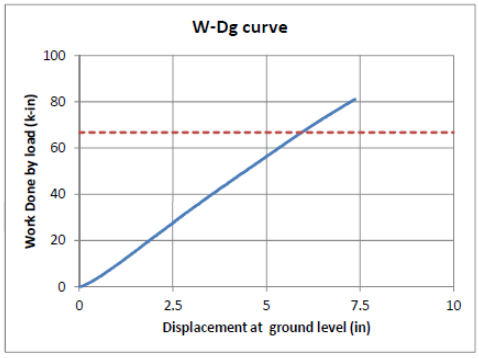

Peak load (lb)	7261.61
Dp at peak load (in)	2.75339

Dg at 66.7 k-in work (in)	5.94963

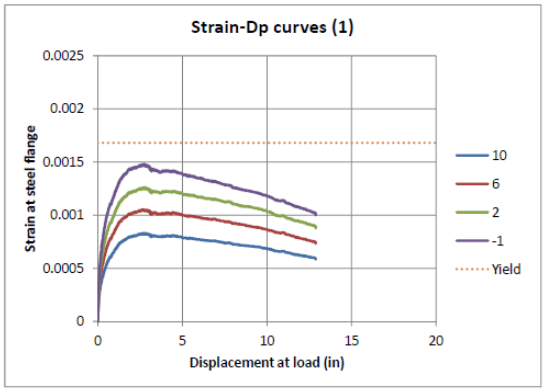

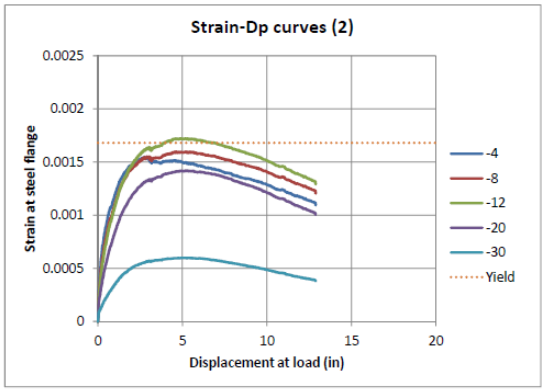

Gage location (in)	10	6	2	-1	-4	-8	-12	-20	-30
Maximum strain	0.00083	0.00105	0.00126	0.00148	0.00155	0.00155	0.00164	0.00134	0.00057
Yield %	49.4776	62.6427	75.1579	88.1061	92.1419	92.3488	97.5743	79.6913	34.0482

FIGURE B21

Test result report: Post 3-2

Test 3-3	3.5-24	
* GDOT typical mow strip practice		
* 3.5" thickness and 24" rear distance behind the post		
*		
Mow strip configuration	Thickness	3.5 inch
	Rear Distance	24 inch
	Modification	N.A.

Location	Structural Lab, Georgia Tech, Atlanta, GA 30318
Test date	2/12/2015
Temperature	50 degrees F
Asphalt age	118 days from placement

Test drawings

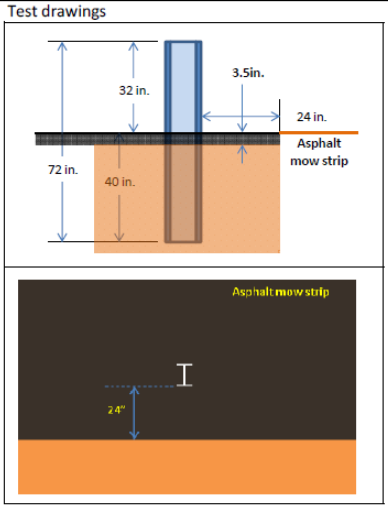

Test pictures

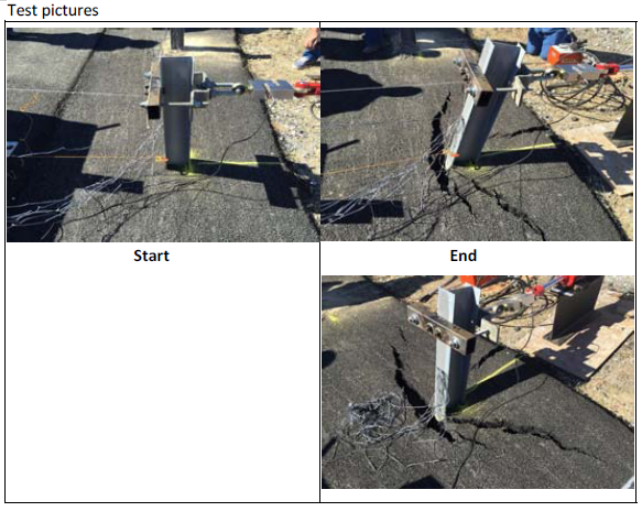

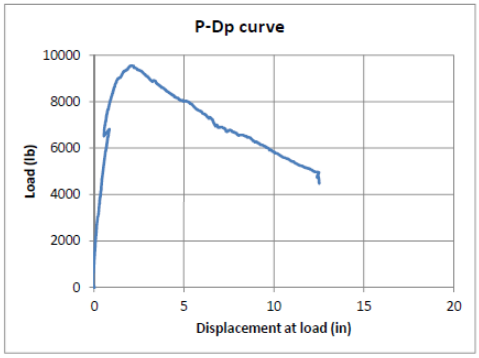

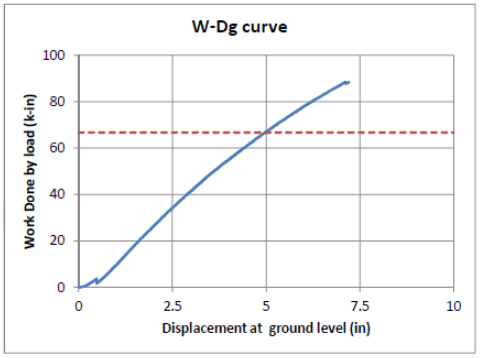

Peak load (lb)	9553
Dp at peak load (in)	2.05051

Dg at 66.7 k-in work (in)	4.98156

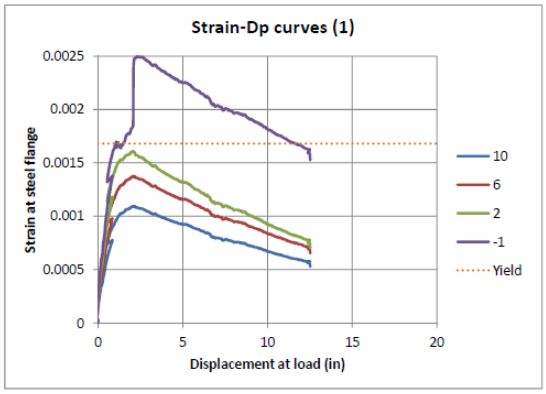

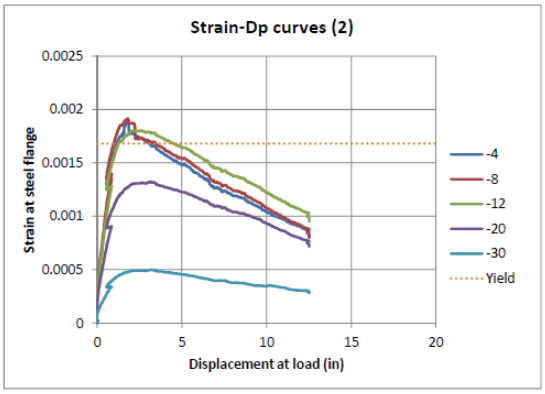

Gage location (in)	10	6	2	-1	-4	-8	-12	-20	-30
Maximum strain	0.00109	0.00137	0.00161	0.00248	0.00178	0.00187	0.00181	0.00131	0.00049
Yield %	65.1432	81.8267	95.8487	147.813	105.989	111.495	107.487	77.8692	29.2843

FIGURE B22

Test result report: Post 3-3

Test 3-4	2-24	
*	GDOT typical mow strip practice	
*	2" thickness and 24" rear distance behind the post	
*		
Mow strip configuration	Thickness	2 inch
	Rear Distance	24 inch
	Modification	N.A.

Location	Structural Lab, Georgia Tech, Atlanta, GA 30318
Test date	2/12/2015
Temperature	50 degrees F
Asphalt age	118 days from placement

Test drawings

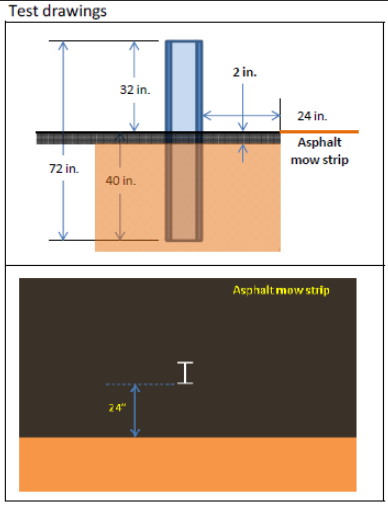

Test pictures

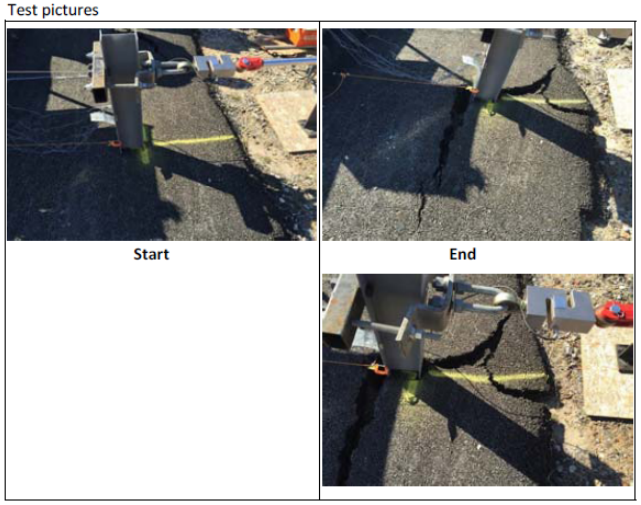

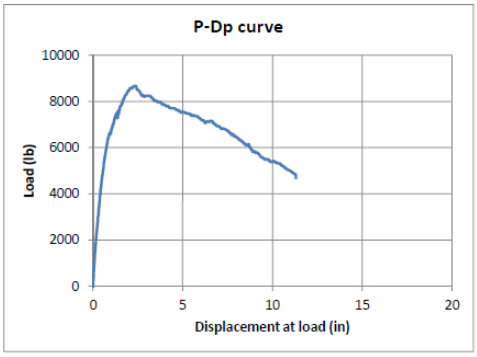

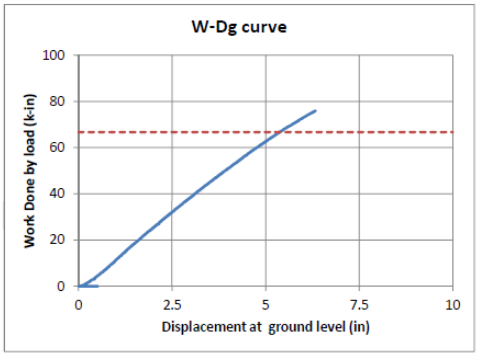

Peak load (lb)	8671.75
Dp at peak load (in)	2.30698

Dg at 66.7 k-in work (in)	5.37385

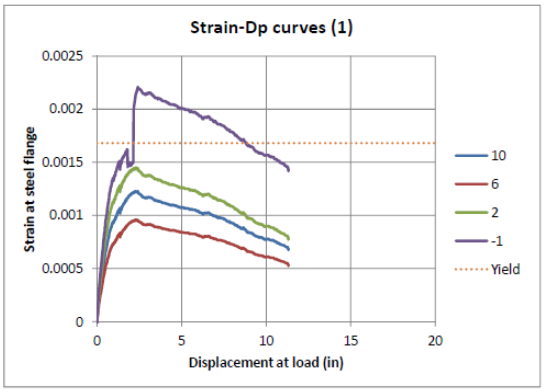

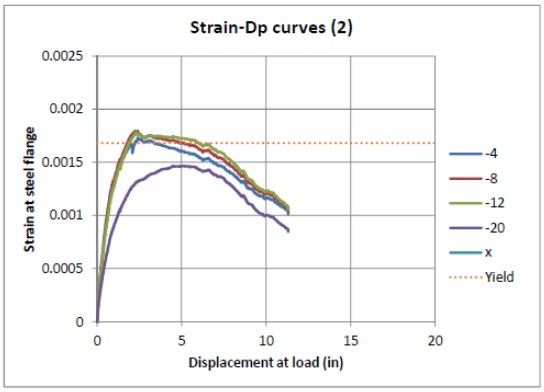

Gage location (in)	10	6	2	-1	-4	-8	-12	-20	x
Maximum strain	0.00123	0.00096	0.00145	0.00221	0.00173	0.00179	0.00178	0.00133	0
Yield %	73.087	57.1501	86.2891	131.6	103.224	106.794	105.912	79.2438	0

FIGURE B23

Test result report: Post 3-4

Test 4-1	2-12	
*	Reduced rear distance design	
*	2" thickness and 12" rear distance behind the post	
*		
Mow strip configuration	Thickness	2 inch
	Rear Distance	12 inch
	Modification	N.A.

Location	Structural Lab, Georgia Tech, Atlanta, GA 30318
Test date	5/5/2015
Temperature	75 degrees F
Asphalt age	40 days from placement

Test drawings

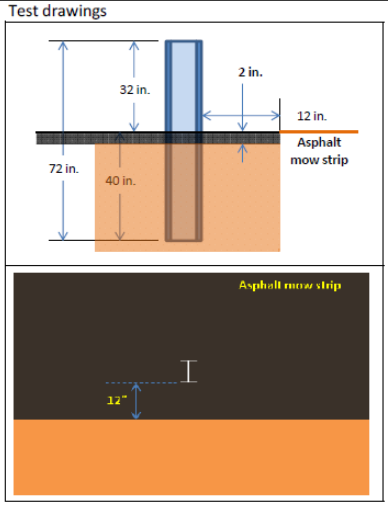

Test pictures

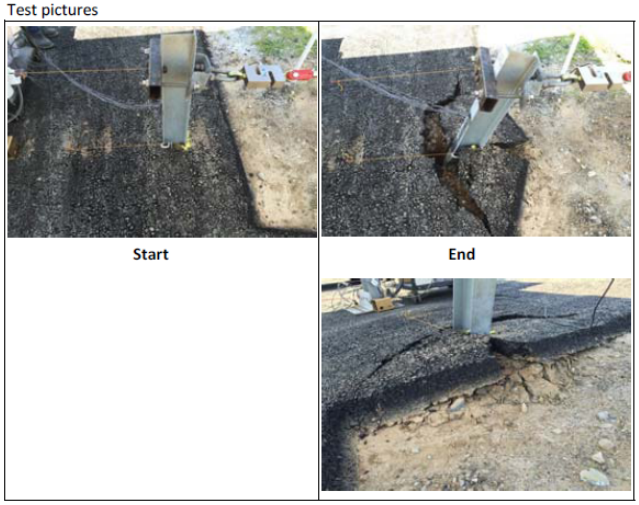

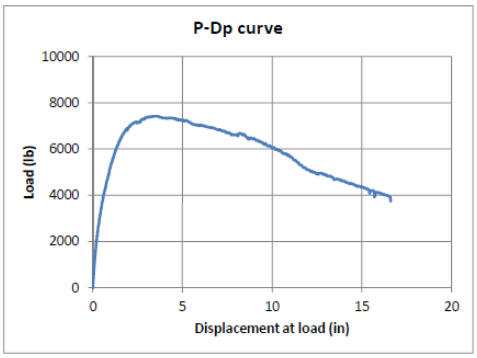

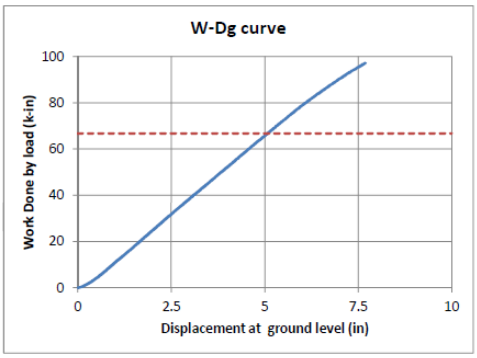

Peak load (lb)	7429.3
Dp at peak load (in)	3.32903

Dg at 66.7 k-in work (in)	5.07019

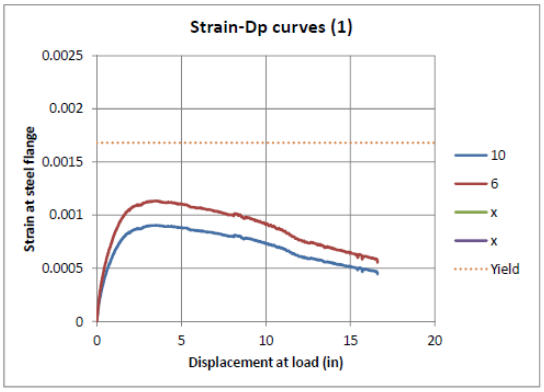

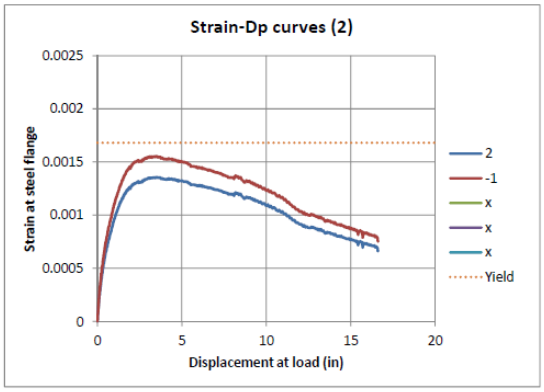

Gage location (in)	10	6	x	x	2	-1	x	x	x
Maximum strain	0.00091	0.00114	0	0	0.00136	0.00155	0	0	0
Yield %	53.9698	67.5909	0	0	80.7721	92.4324	0	0	0

FIGURE B24

Test result report: Post 4-1

Test 4-2	2-24-C1	
* Pre-cut mow strip design		
* 2" thickness and 24" rear distance behind the post		
* Parallel pre-cut pattern		
Mow strip configuration	Thickness	2 inch
	Rear Distance	24 inch
	Modification	Pre-cutting

Location	Structural Lab, Georgia Tech, Atlanta, GA 30318
Test date	5/5/2015
Temperature	75 degrees F
Asphalt age	40 days from placement

Test drawings

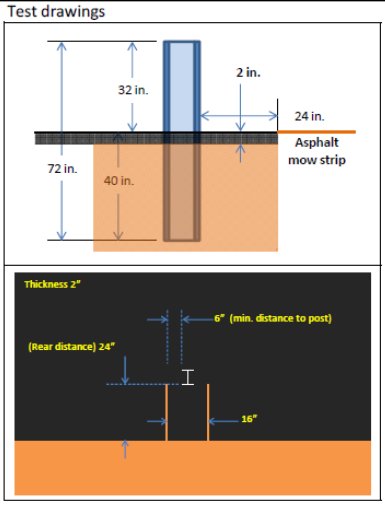

Test pictures

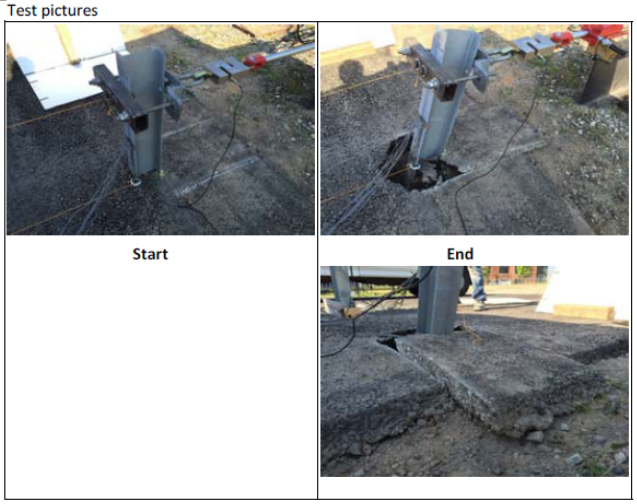

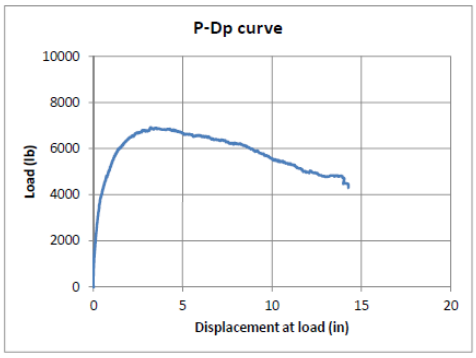

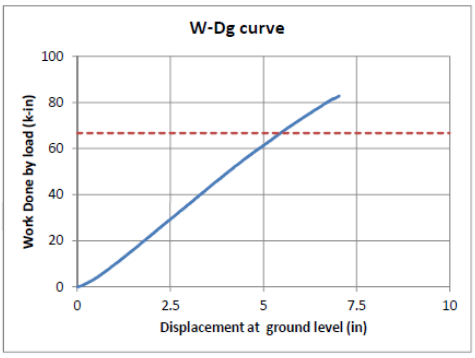

Peak load (lb)	6912.15
Dp at peak load (in)	3.22068

Dg at 66.7 k-in work (in)	5.4621

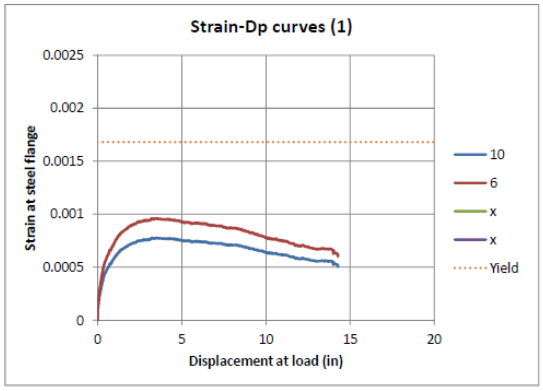

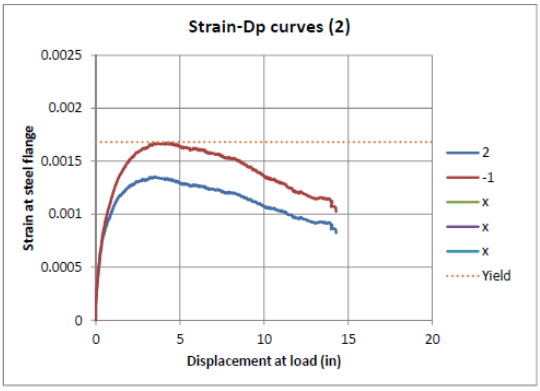

Gage location (in)	10	6	x	x	2	-1	x	x	x
Maximum strain	0.00078	0.00096	0	0	0.00135	0.00166	0	0	0
Yield %	46.2572	57.2108	0	0	80.5143	98.8407	0	0	0

FIGURE B25

Test result report: Post 4-2

Test 4-3	2-24	
* GDOT typical mow strip practice		
* 2" thickness and 24" rear distance behind the post		
*		
Mow strip configuration	Thickness	2 inch
	Rear Distance	24 inch
	Modification	N.A.

Location	Structural Lab, Georgia Tech, Atlanta, GA 30318
Test date	5/5/2015
Temperature	75 degrees F
Asphalt age	40 days from placement

Test drawings

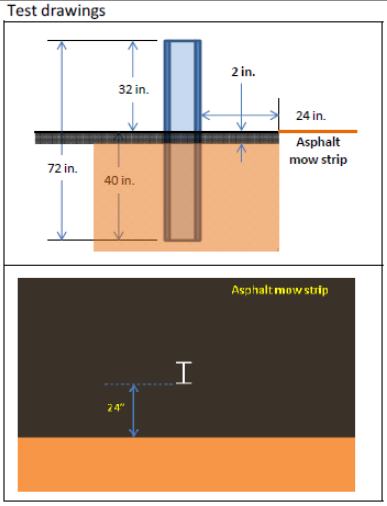

Test pictures

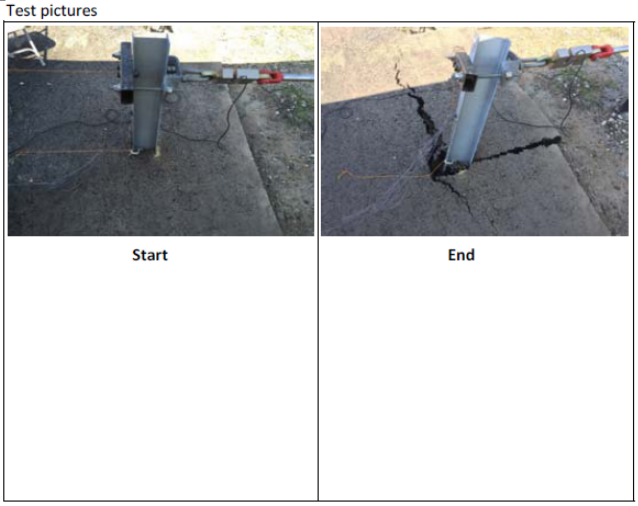

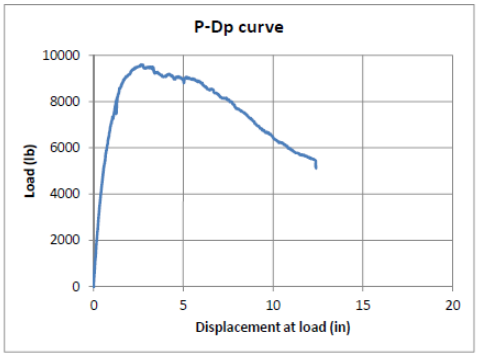

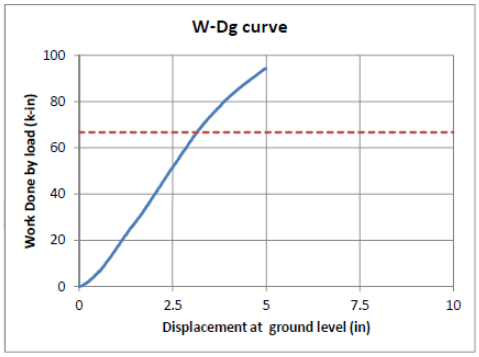

Peak load (lb)	9597.54
Dp at peak load (in)	2.64982

Dg at 66.7 k-in work (in)	3.15299

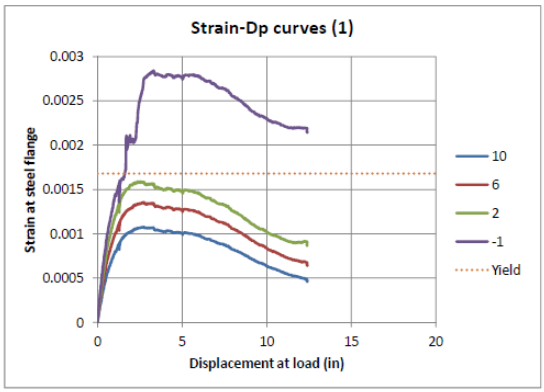

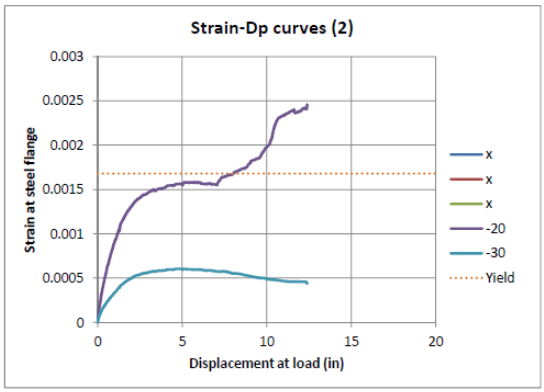

Gage location (in)	10	6	2	-1	x	x	x	-20	-30
Maximum strain	0.00108	0.00135	0.00158	0.00277	0	0	0	0.00145	0.00056
Yield %	64.1437	80.6329	94.2888	164.953	0	0	0	86.1657	33.1768

FIGURE B26

Test result report: Post 4-3

Test 4-4	2-6
*	Reduced rear distance design
*	2" thickness and 6" rear distance behind the post
*	

Mow strip configuration	Thickness	2 inch
	Rear Distance	6 inch
	Modification	N.A.

Location	Structural Lab, Georgia Tech, Atlanta, GA 30318
Test date	5/5/2015
Temperature	75 degrees F
Asphalt age	40 days from placement

Test drawings

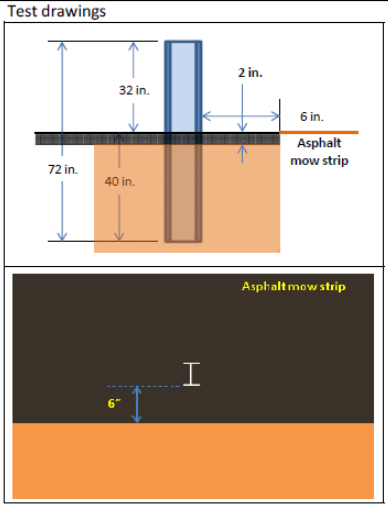

Test pictures

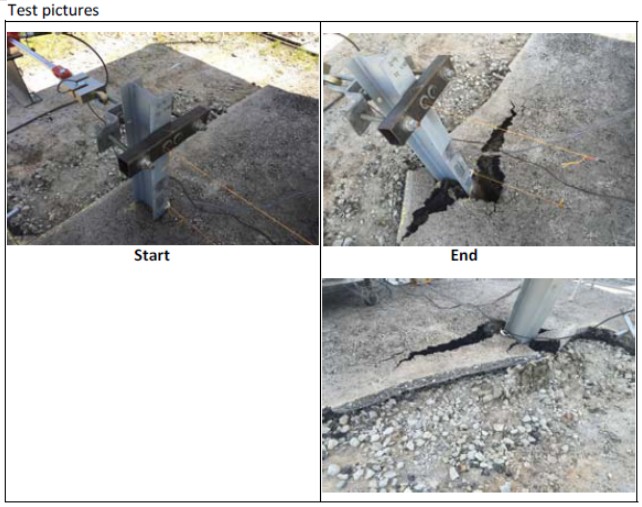

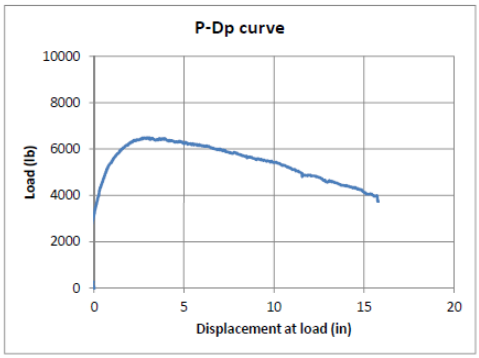

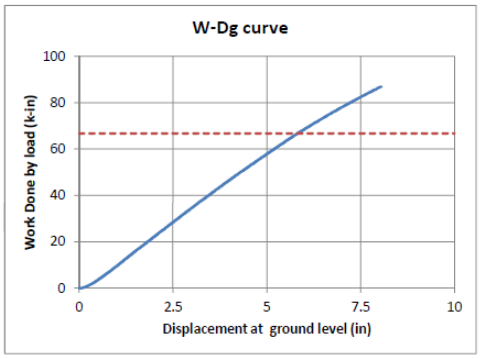

Peak load (lb)	6492.32
Dp at peak load (in)	2.9432

Dg at 66.7 k-in work (in)	5.81722

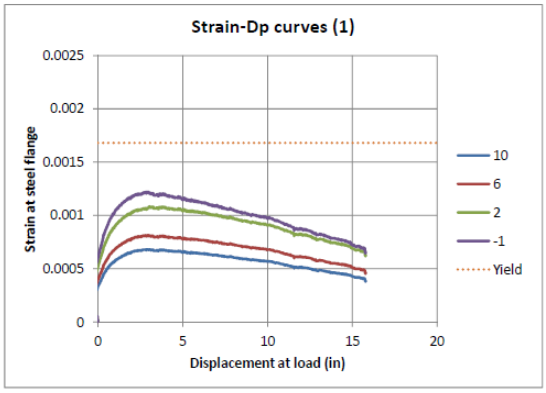

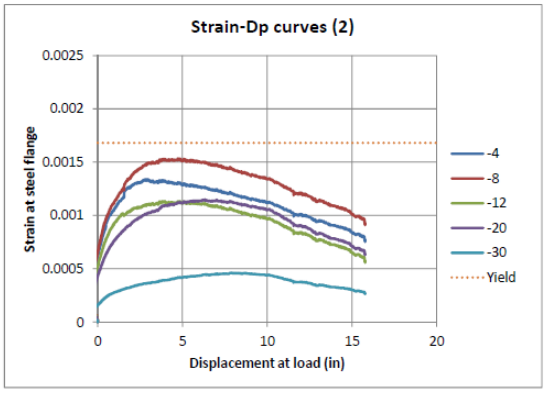

Gage location (in)	10	6	2	-1	-4	-8	-12	-20	-30
Maximum strain	0.00068	0.00081	0.00109	0.00122	0.00134	0.0015	0.00111	0.00104	0.00037
Yield %	40.6276	48.393	64.5871	72.5552	79.7033	89.104	66.0126	61.6086	22.1296

FIGURE B27

Test result report: Post 4-4

Test 5-1	3.5-24-C2	
* Pre-cut mow strip design		
* 3.5" thickness and 24" rear distance behind the post		
* Diagonal pre-cut pattern		
Mow strip configuration	Thickness	3.5 inch
	Rear Distance	24 inch
	Modification	Pre-cutting

Location	Structural Lab, Georgia Tech, Atlanta, GA 30318
Test date	7/14/2015
Temperature	70 degrees F
Asphalt age	32 days from placement

Test drawings

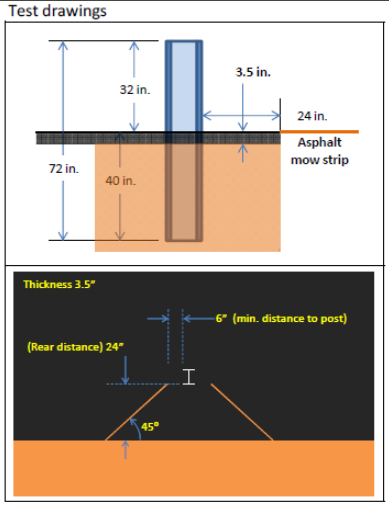

Test pictures

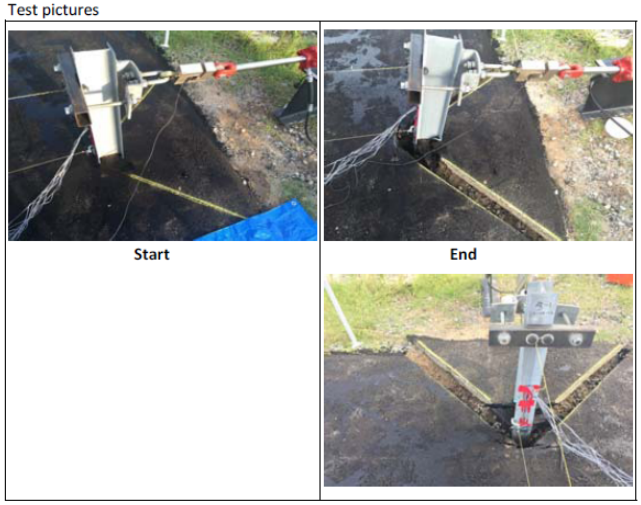

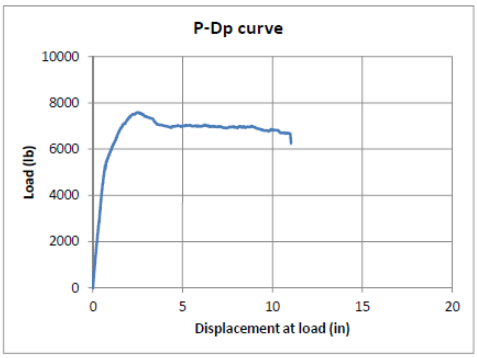

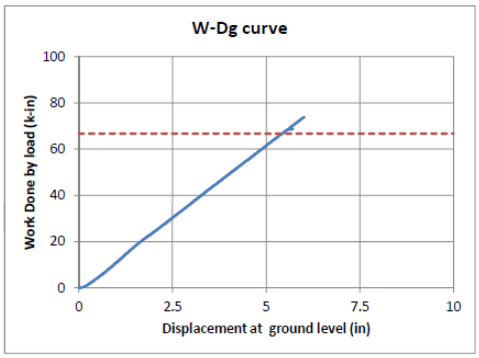

Peak load (lb)	7577.12
Dp at peak load (in)	2.49957

Dg at 66.7 k-in work (in)	5.42932

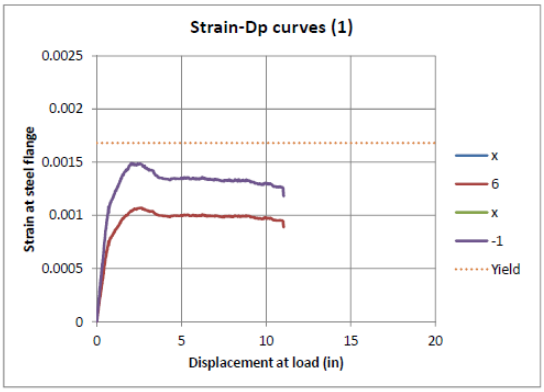

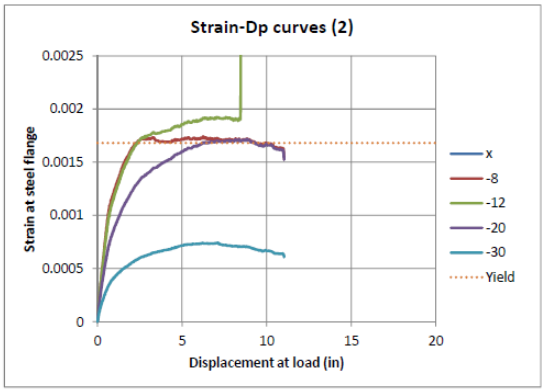

Gage location (in)	x	6	x	-1	x	-8	-12	-20	-30
Maximum strain	0	0.00107	0	0.00148	0	0.00173	0.00174	0.00138	0.00062
Yield %	0	63.687	0	88.2912	0	102.808	103.851	82.1412	36.86

FIGURE B28

Test result report: Post 5-1

Test 5-2	3.5-12	
* Reduced rear distance design		
* 3.5" thickness and 12" rear distance behind the post		
*		
Mow strip configuration	Thickness	3.5 inch
	Rear Distance	12 inch
	Modification	N.A.

Location	Structural Lab, Georgia Tech, Atlanta, GA 30318
Test date	7/14/2015
Temperature	70 degrees F
Asphalt age	32 days from placement

Test drawings

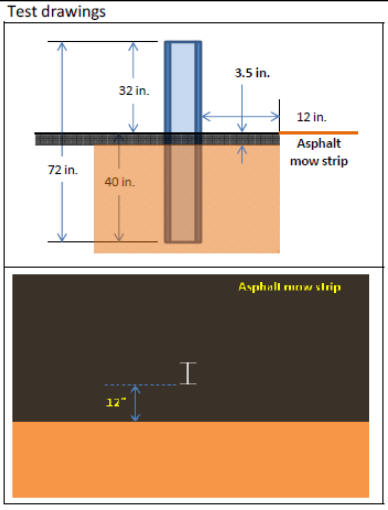

Test pictures

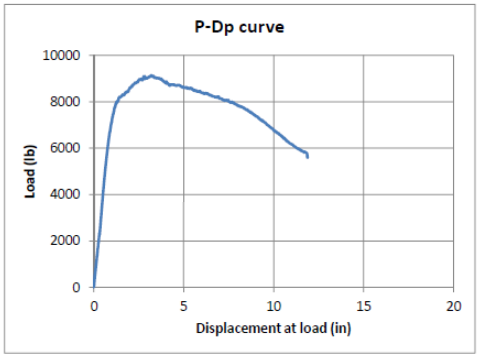

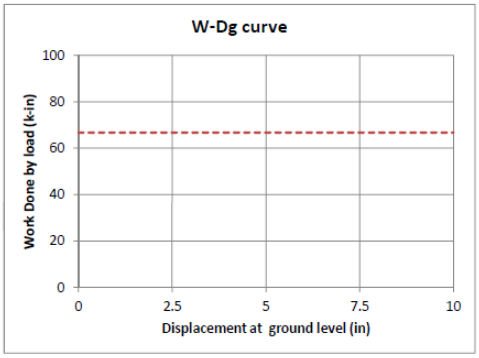

Peak load (lb)	9135.48
Dp at peak load (in)	3.18312

Dg at 66.7 k-in work (in)	Dg record is not available

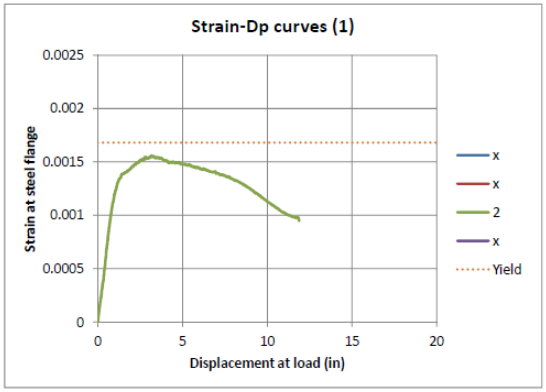

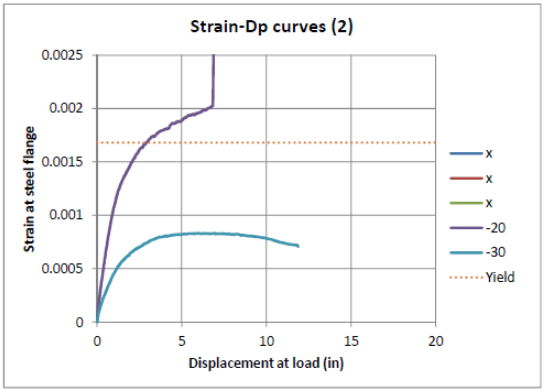

Gage location (in)	x	x	2	x	x	x	x	-20	-30
Maximum strain	0	0	0.00156	0	0	0	0	0.00173	0.00077
Yield %	0	0	92.8315	0	0	0	0	102.939	45.553

FIGURE B29

Test result report: Post 5-2

Test 5-3	3.5-24-L	
* The GDOT mow strip with typical leave-out application		
* 18"x18" low strength grout as leave-out material		
* Recommended by the AASHTO Roadside Design Guide		
Mow strip configuration	Thickness	3.5 inch
	Rear Distance	24 inch
	Modification	Typical grout leave-out

Location	Structural Lab, Georgia Tech, Atlanta, GA 30318
Test date	7/14/2015
Temperature	70 degrees F
Asphalt age	32 days from placement
Grout strength	55.23 psi (28-day comp. strength less than 120 psi)

Test drawings

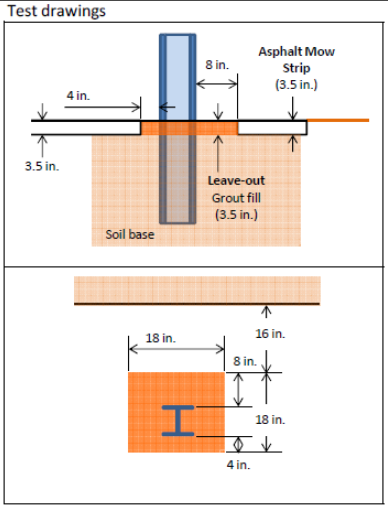

Test pictures

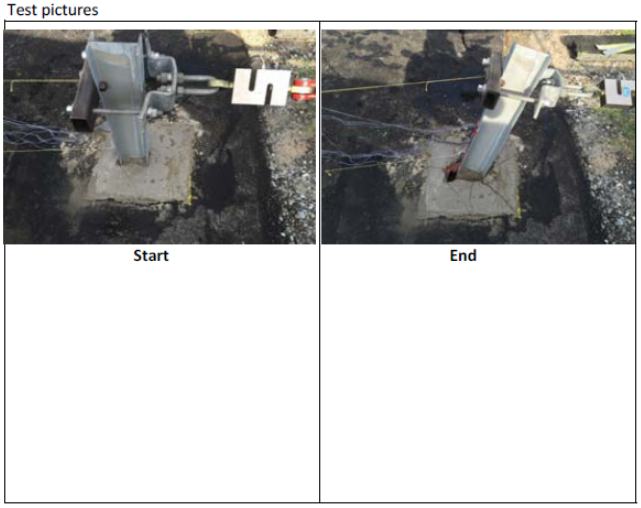

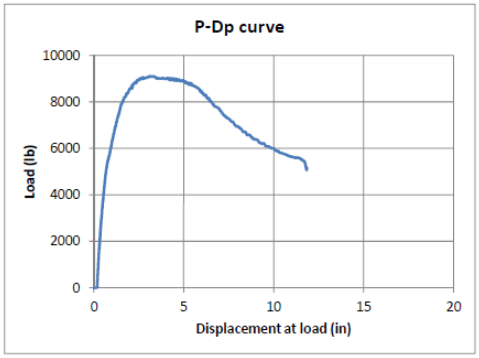

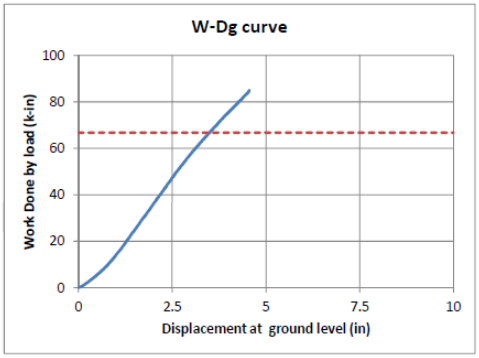

Peak load (lb)	9096.22
Dp at peak load (in)	3.11161

Dg at 66.7 k-in work (in)	3.49738

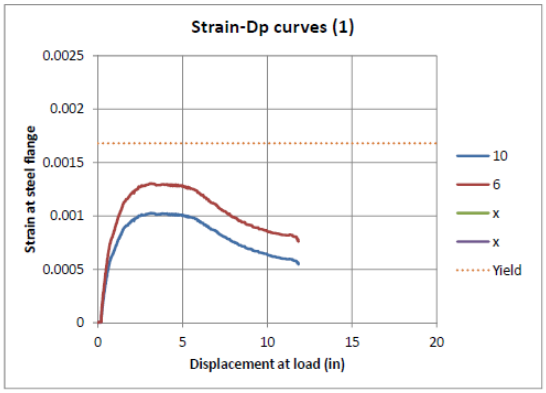

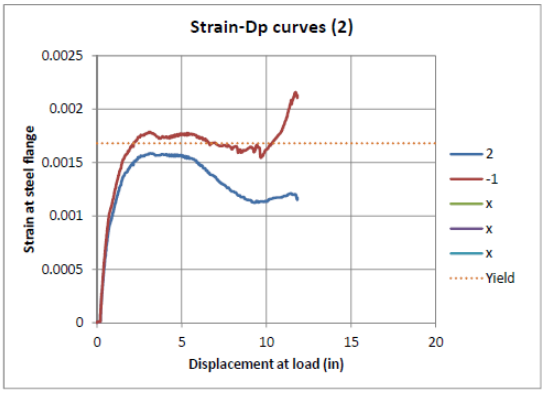

Gage location (in)	10	6	x	x	2	-1	x	x	x
Maximum strain	0.00103	0.0013	0	0	0.00159	0.00179	0	0	0
Yield %	61.1098	77.5495	0	0	94.3672	106.359	0	0	0

FIGURE B30

Test result report: Post 5-3

Test 5-4	3.5-24-C2a	
* Pre-cut mow strip design		
* 3.5" thickness and 24" rear distance behind the post		
* Diagonal pre-cut pattern with asphalt sealer application		
Mow strip configuration	Thickness	3.5 inch
	Rear Distance	24 inch
	Modification	Pre-cutting and sealing

Location	Structural Lab, Georgia Tech, Atlanta, GA 30318
Test date	7/14/2015
Temperature	70 degrees F
Asphalt age	32 days from placement

Test drawings

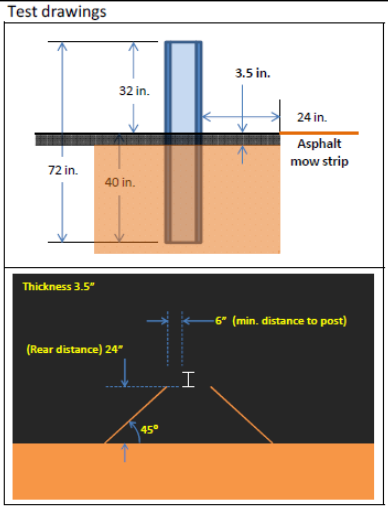

Test pictures

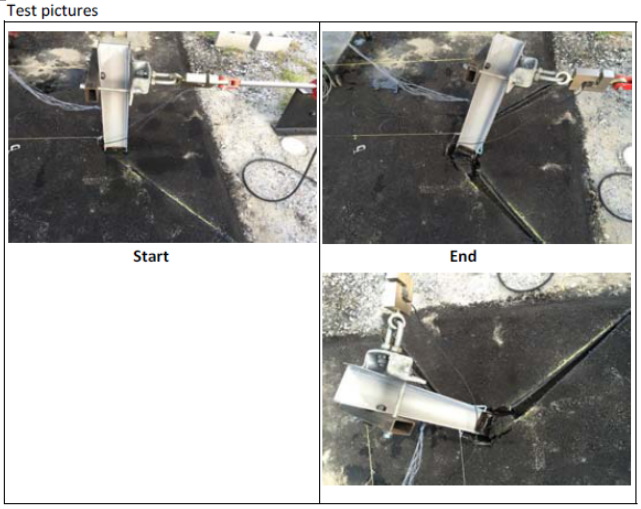

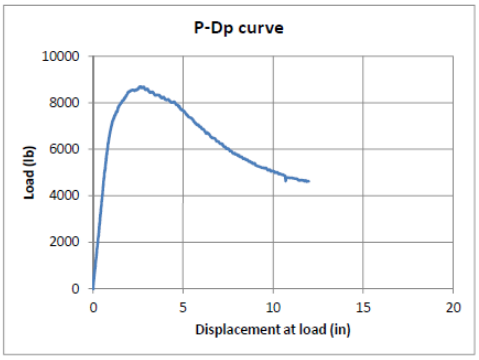

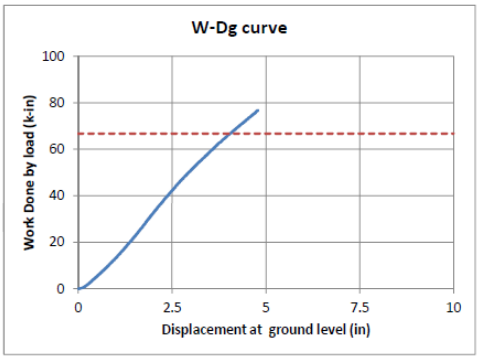

Peak load (lb)	8688.91
Dp at peak load (in)	2.63087

Dg at 66.7 k-in work (in)	4.04827

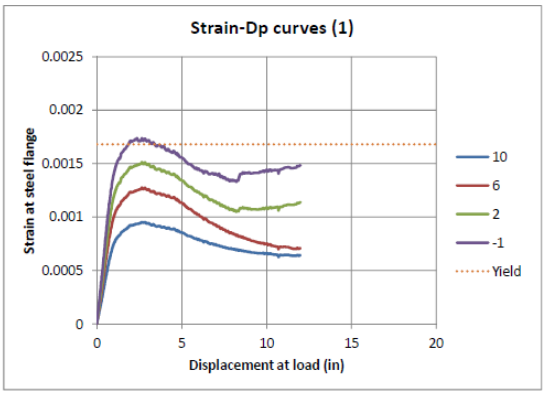

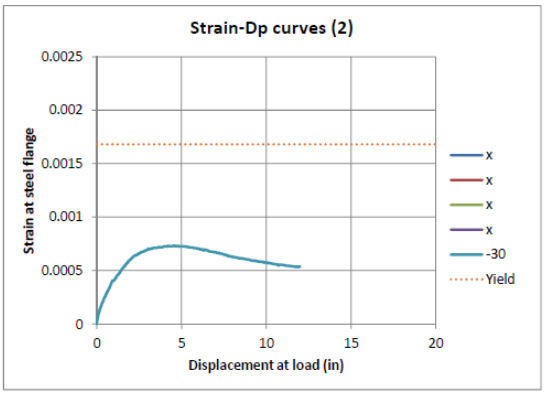

Gage location (in)	10	6	2	-1	x	x	x	x	-30
Maximum strain	0.00096	0.00127	0.00151	0.00174	0	0	0	0	0.00069
Yield %	56.9026	75.8693	90.121	103.347	0	0	0	0	40.9573

FIGURE B31

Test result report: Post 5-4

APPENDIX C

DETAILED DESCRIPTION OF THE FINITE ELEMENT MODEL AND MATERIAL TESTING

C.1 Lagrangian vs. Eulerian Mesh

In soil structure interaction, it is expected that the soil material fails and is substantially deformed. It is known that Lagrangian meshes become unstable when severe distortion occurs. Therefore, the simulation of soil-post dynamic interaction behavior can be carried out alternatively based on an Eulerian mesh. Mesh distortion is not an issue with the Eulerian formulation. The formulation allows material to transfer. Thus, soil material can be deformed with no mesh distortion. There is no need to define contact surfaces between the post with a Lagrangian mesh and the soil with an Eulerian mesh. Interactions between the two materials occur through the viscous stresses and no contact surface with friction is defined. It is important to note that the Eulerian mesh requires a much finer mesh near boundaries of the Lagrangian-Eulerian interaction. Another solution for mesh distortion problem is using Arbitrary Lagrangian-Eulerian (ALE) formulation. This method has been used successfully in problems such as modeling of fluid-structure interaction with significant structure movement where high mesh distortions occur [32]. Eulerian and ALE formulations are built in LS-DYNA software and are supported by some material models. Because the Lagrangian solution is more commonly used in civil engineering problems, the Lagrangian formulation is used to model the soil, asphalt, and steel in the current study. Eulerian and ALE formulations can be used for soil in a case that the Lagrangian mesh proves to be incapable of finishing the simulation, or a negative volume problem occurs for an element in the mesh.

C.2 Interface between the Post and Soil

Different approaches exist for modeling of the interface between the soil and post using a Lagrangian mesh as follows:

1) Nodes from the soil elements are tied to the nodes of the post elements. No contact definition between the post and the soil is necessary when this approach is used. This method assumes infinite friction between the soil and the post, which is not a correct physical representation. In addition, the soil elements on the sides of the post undergo high shear distortions that cause finite element shear locking problems for large deformations. Because of these reasons, this method yields a stiffer behavior than reality and is not recommended.
2) Nodes from the soil elements are not tied to the nodes of the post elements, and eroding contact is used to simulate the soil failure. This model demands very dense mesh and yields incorrect results. The failed elements are removed, and a gap is created between the soil and the post. Therefore, application of a negligible force in the axial direction can pull out the post. This behavior is observed even using a friction coefficient larger than one [30].
3) Nodes from the soil elements are not tied to the nodes of the post elements. Automatic surface-to-surface contact is defined between the post and the soil. In this method, the friction between the post and soil has an influence on the behavior [3].

In this study, the contact between soil and steel post were modeled using the automatic surface-to-surface contact model. Static and dynamic friction coefficients were set equal to 0.6, which is typical for an interface between the soil (a mixture of gravel, sand, and

clay) and a driven smooth steel pile. Null shell elements were added as a numerical treatment on the top of the soil and between soil and post contact surface in order to avoid negative element volume and element penetrations for large post displacements. Because the stiffness of steel is significantly greater than the stiffness of the soil, pinball segment based (soft 2) contact was used to avoid contact related problems and element penetration. The thickness of the hole in the soil where the post is placed is set properly to account for the thickness of the steel shell elements to avoid initial element penetrations. The SHLTHK parameter in the Control_Contact card is set to two to turn on shell thickness consideration in the surface to surface contact. FRCENG is set to one to enable sliding energy calculations. The frictional energy is important to consider because some part of the energy during steel post movement in the soil is dissipated by friction. Moreover, this energy has to be checked to make sure its value is positive and negative sliding energy, which is an indication of an erroneous slide between two contact surfaces, does not occur during simulations.

C.3 Soil Material Model

There are different material models provided in LS-DYNA for modeling of soil, asphalt, and steel. Each material model is appropriate for a particular problem. Therefore, these material models were examined to find the most appropriate model to use for modeling of these components. Lewis [58] provided a discussion on available materials in LS-DYNA that are suitable for soil. From these materials, soil and foam (material number 5), soil and foam with failure (material number 14), Mohr-Coulomb (material number 173), Drucker-Prager (material number 193), and FHWA (material number 147) soil material models were chosen to be evaluated in this project for

modeling of soil. The "FHWA-147" material model manual [58] and the document associated with verification of the model with experimental results [59] were reviewed. The FHWA soil model captures damage evolution, strain softening, pore water pressure effect, strain rate effect, and moisture content effect. However, the model has many parameters, some of which cannot be determined from experiment. This material model is developed because of the need for a new material model for highway safety simulations. The most important reason for developing this model was that the other material models in LS-DYNA, which represent soil, are unstable under low confining pressure. Therefore, the research team first used the other simpler material models to check their stability for modeling of the guardrail post. The other reason for not using this material model is the fact that this study is not focused on the effect some of parameters for soil (such as pore water pressure and moisture content effect). After running the simulations with different materials, soil and foam model and Mohr-Coulomb model both proved to be stable under the desired displacement for the current problem. Both material models work with the Eulerian formulation and ALE formulation as well.

The Mohr-Coulomb yield criterion is written as

$$\tau = \sigma \tan(\phi) + C \tag{C1}$$

where τ is the shear strength, σ is the normal stress, C is cohesion or the intercept of the failure envelope with the τ axis, and ϕ is the angle of the internal friction or the slope of the failure envelope. The Mohr–Coulomb yield criterion can then be evaluated for the six planes of maximum shear stress. Moreover, the Drucker-Prager yield criterion is written as

$$J_2 = \left(d + eI_1\right)^2 = \left(d + 3ep\right)^2 = d^2 + 6dep + 9e^2p^2 \tag{C2}$$

where I_1 is the first invariant of the Cauchy stress, p is the pressure, J_2 is the second invariant of the deviatoric part of the Cauchy stress, and d and e are constants determined from experiments [47]. Drucker–Prager yield surface is a smooth version of the Mohr–Coulomb yield surface. Therefore, it can be expressed in terms of the angle of internal friction ϕ and the cohesion C, which are utilized to define the Mohr–Coulomb yield surface. If the Drucker–Prager yield surface circumscribes the Mohr–Coulomb yield surface, then constants e and d can be defined as

$$d = \frac{6C\cos(\phi)}{\sqrt{3}\left(3+\sin(\phi)\right)} \tag{C3}$$

$$e = \frac{2\sin(\phi)}{\sqrt{3}\left(3+\sin(\phi)\right)} \tag{C4}$$

Another pressure dependent yield criterion available in LS-DYNA is soil and foam material (material number 5), which is written as [26]

$$J_2 = a_0 + a_1 p + a_2 p^2 \tag{C5}$$

By comparing equations C2 and C5, the constants in soil and foam yield criterion can be related to the constants in Drucker-Prager. This relation is expressed as

$$a_0 = d^2 \quad ; \quad a_1 = 6de \quad ; \quad a_2 = 9e^2 \tag{C6}$$

Therefore, given cohesion C and internal angle of friction ϕ, the other constants (i.e. d, e, a_0, a_1, a_2 and) can be obtained. Based on the simulation results, the Drucker-Prager model showed an unstable behavior for large mesh distortion and the simulation stopped with negative volume error. The soil and foam material model is an easier option to work with, and it only has three constitutive parameters for the yield surface and one for pressure cut off. It is also possible to give a volumetric strain versus stress curve as an

input. This model was stable for large displacements. However, the yield surface in the deviatoric stress plane is circular and smooth. This material model does not capture the difference in soil behavior in extension and compression. Many experiments in the past have been proved that soil behaves differently in extension and compression [47]. Therefore, the Mohr-Coulomb model was employed to model the soil behavior. This material model is widely used for soil. In addition to elastic parameters including shear modulus and Poisson's ratio, the strength constitutive parameters (cohesion and internal friction angle) can be obtained from laboratory tests. This material model can also capture the decrease in the friction angle for large plastic strains. This feature is especially useful to model the softening behavior of the soil. A curve for friction angle as a function of plastic strain can be given as input. This is very useful for modeling compacted sands that usually have peak friction angle associated with peak strength and critical friction angle for large strains.

To identify the soil type used in the experiment and find out the range of acceptable soil material properties in literature, the grain size distribution was obtained using sieve analysis. The following is the process used to identify the soil type using two commonly used methods.

C.4 Hourglass Energy and Kinetic Energy Checks

To prevent high hourglass energy during simulations, hourglass control number 9 in LS-DYNA, which is enhanced assumed strain stiffness form for three-dimensional hexahedral elements was used for the soil elements and the hexahedral mesh part of the asphalt. Hourglass coefficient equal to 0.004 and 0.1 were used for the soil elements and the hexahedral mesh part of the asphalt respectively. Because of the type of the elements

used for the steel post and tetrahedral mesh part of the asphalt, these two parts do not have any hourglass energy and do not need an hourglass control. Hourglass energy was monitored and compared to the internal energy. The hourglass energy in the soil and the hexahedral mesh part of the asphalt was approximately 3 percent of the internal energy, which is acceptable. Kinetic energy was less than 0.5 percent of the total energy that shows that the rate of loading is a good representation of a quasi-static loading.

C.5 Interface between the Asphalt and the Soil

The contact between the soil and the asphalt was modeled using the automatic surface-to-surface contact model. The static coefficient of friction was set equal to one to account for the fact that bitumen in the asphalt is bonded to the soil surface and provides a relatively high static friction between two surfaces. However, after this connection breaks and the asphalt layer starts to slip over the soil, friction substantially decreases. The kinetic coefficient of friction was assumed to be negligible and equal to zero to avoid large forces at the free edge of the asphalt behind the post. This allows the asphalt to move easily on the soil and avoids mesh distortions at the edge of the asphalt layer where there is no confinement pressure. Pinball segment based contact was used. SBOPT and DEPTH parameters set to four and five to prevent negative sliding energy. The same contact properties were used for the contact between asphalt and steel.

C.6 Mesh Transition in the Asphalt

The mesh around the post is made of tetrahedral elements, and hexahedral elements are used at further distances from the post. These two different meshes need to be connected to make a continuum part for the asphalt. A tied surface to surface contact

model was used to make this connection between the two meshes. A representation of the model is shown in Figure C1.

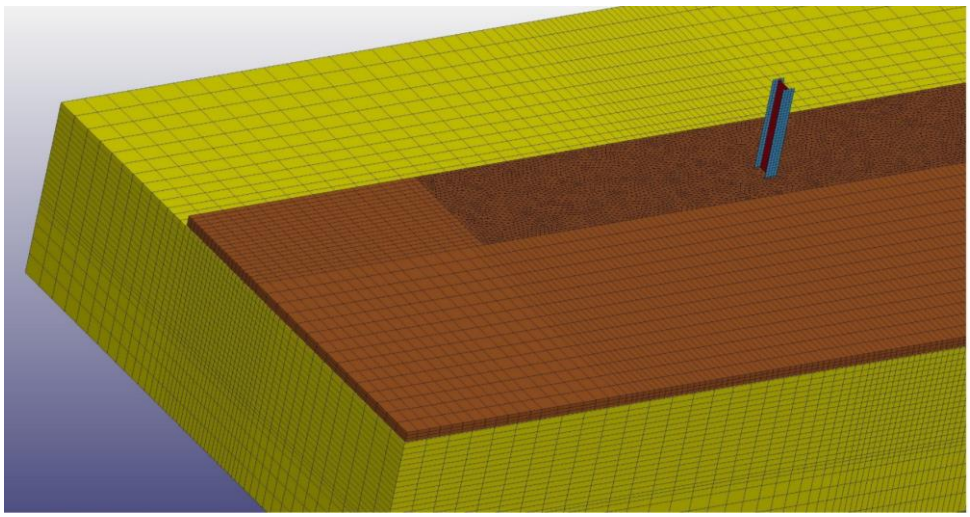

FIGURE C1

A representation of the FE model

C.7 Importance of Gravity Loading and Dynamic Relaxation

The soil and foam material (material model number 5) has been used in the past by investigators [30, 31]. By choosing specific values for the parameters, it can be assumed that the yield surface is not a function of the pressure, i.e. similar to Von-Mises yield surface. However, physically, the soil is known to be a pressure dependent material, and that is the reason for using soil and foam material model or Mohr-Coulomb material model. If the values of the soil and foam material model are set in a way that it behaves like a von-Mises material model, then the soil is not modeled correctly. Moreover, the soil's behavior changes at different depths because of the change in the pressure as the depth increases. To capture this important aspect of the soil behavior, a gravity loading must be applied, and stresses have to be initialized before the start of the main simulation. This is done in this study by applying a "load body" in the z direction

to all parts of the model. Because applying gravity loading during the real-time simulation causes dynamic waves that can contaminate the results, the gravity load was applied in the sudo time before the main simulation. Gravity loading was applied using a ramp load to minimize dynamic waves, and dynamic relaxation was utilized in the pseudo time to damp the waves caused by applying gravity. After the waves were damped, and the material reached a static equilibrium, the main simulation was conducted in real time. Applying a gravity loading also ensures the proper capture of friction forces on the surfaces that are in contact with each other. As it can be seen in Figure C2, applying gravity and using dynamic relaxation is very critical to properly model the guardrail post system. If the gravity load is applied without dynamic relaxation phase, large dynamic waves contaminate the result. Moreover, if the gravity loading is not applied in the model, the soil material shows significantly lower strength and the contact between the soil, the asphalt, and the post does not work correctly.

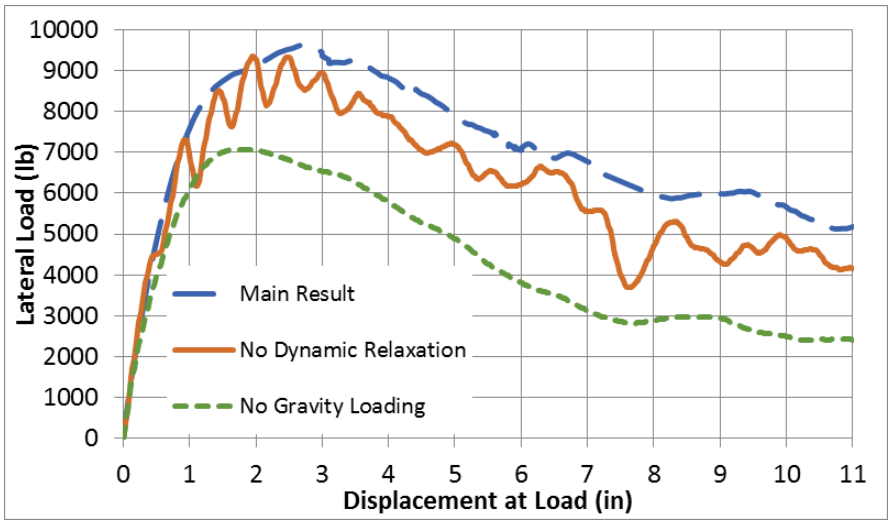

FIGURE C2

Comparing the load-displacement curve with and without using dynamic relaxation or gravity loading for a post embedded in soil with 3.5" Asphalt mow strip

C.8 Soil Classification

Unified Soil Classification System

The USCS uses symbols for the particle size groups. These symbols and their representations are G for gravel, S for sand, M for silt, and C for clay. These are combined with other symbols expressing gradation characteristics, W for well graded and P for poorly graded. USCS is used to classify the compacted soil that is deposited around the guardrail post. Grain size distribution was obtained using laboratory sieve test. Less than 50% (47%) of the grains passed sieve #4. Therefore, the soil is gravel. Then it is necessary to understand that if the soil is poorly graded or well graded. From the grain size distribution the sieve opening size that 10% of the soil sample mass passes through defined as D_{10}, the sieve opening size that 30% of the soil sample mass passes through defined as D_{30}, and the sieve opening size that 60% of the soil sample mass passes through defined as D_{60} were obtained equal to 0.093 mm, 0.81 mm, and 9.5 mm respectively. Using these values, the coefficient of uniformity and coefficient of curvature were computed as 102.15 and 0.75 respectively [46]. The soil is poorly graded because the coefficient of curvature is less than one. There are 8% fine grains (grains that pass sieve #200) in the soil sample. The fine grains are assumed to be silt (M), so the soil is graded as GP-GM. Moreover, 40% of the soil mass is sand and, therefore, the soil is classified as "poorly graded gravel with silt and sand".

AASHTO Soil Classification System

The AASHTO soil classification system is used to determine the suitability of soils for earthworks, embankments, and roadbed materials (subgrade: natural material below a constructed pavement; subbase: a layer of soil above the subgrade; and base: a

layer of soil above the sub-base). Using the grain size distribution, 37% of the soil mass passes sieve #10, 25% passes sieve #40, and 8% passes sieve #200. According to AASHTO soil classification system, the soil is graded as A-1-a, which is the best rating for soils being used as a subgrade. The soil name is "Stone Fragments, Gravel, and Sand".

After finding the soil type based on the grain size distribution, the typical range of mechanical properties of soil can be obtained to verify the numbers obtained from FEA calibration [45]. The soil mechanical properties obtained from FEA calibration were in the typically recommended range of values for the soil sample.

C.9 Experimental Determination of Asphalt Strength

Test Description

It is known that asphalt strength can vary significantly based on a number of different factors. Temperature change and physical aging are two important factors which increase or decrease the strength of asphalt. Prior studies have reported that asphalt strength is sensitive to both temperature [38, 39] and age [40,41,42]. One of most widely-used material models for asphalt concrete is the Mohr-Coulomb failure criterion model which is defined by two parameters: c for cohesion and φ for internal friction angle. This Mohr-Coulomb model was first adopted by pavement researchers in the early 1950s to evaluate asphalt performance. Later, Fwa [38] suggested a modified triaxial test method to determine the c-φ relationship at various temperature conditions. The cylindrical specimens were 4 inches in diameter, 8 inches in height, and were tested less than 24 hours after asphalt compaction. However, this method is not adequate to evaluate c-φ for in-situ asphalt samples taken from mow strip since it is nearly impossible to

retrieve a specimen with the necessary 8-inch height from roadside asphalt layers whose thickness typically range from 2 to 4 inches. Additionally, experimental results on short-term aged laboratory specimens are unlikely to be indicative of asphalt properties in actual roadway conditions.

A series of compression tests were performed to attempt to estimate the effect of temperature and physical aging on asphalt strength for the specific material used in this research program. Three levels of temperature and eight levels of age condition were evaluated. Test samples were cored from the asphalt pavement layer and were trimmed to approximately 4 inches in diameter and 4 inches in height as shown in Figure C3. A total of 35 compression tests were performed to investigate the effect of aging. A total of 18 compression tests were performed to investigate the effect of ambient temperature.

FIGURE C3

Asphalt test bed and cored specimen

Mohr-Coulomb Model Parameters

An unconfined compression test result can be expressed with a Mohr circle in a shear-normal plane. Figure C4 shows a Mohr-Coulomb failure envelope line drawn from the Mohr circle of an unconfined compression test. By selecting the internal friction angle of asphalt φ to be 0.35 (which is considered a typical value for the asphalt

concrete), the cohesion value of asphalt C can be estimated as approximately 26 percent of unconfined compression strength:

$$C = \frac{f_c'}{2}(\tan\phi)\left(\frac{1}{\sin\phi} - 1\right) = 0.2603 f_c' \qquad \text{(C7)}$$

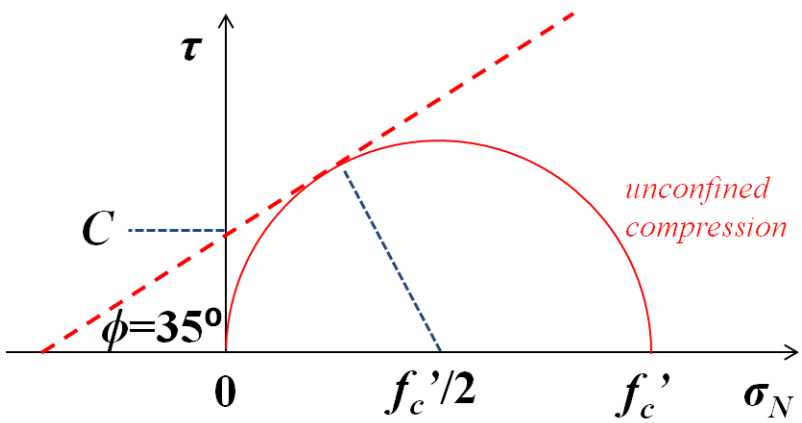

FIGURE C4

Mohr-Coulomb parameters from unconfined compression test

Experimental Plan

<u>Asphalt type (material)</u>

The hot mix asphalt (HMA) used in this research program was designed with a performance grade (PG) of PG 76-22 binder with ¾ inch maximum aggregate. This asphalt mix type is one of the most commonly used in road construction projects in Georgia.

<u>Test temperature : (3 levels): 32, 68, 104 ^{0}F</u>

Each level represents a typical temperature condition of winter, spring/fall, and summer IN Georgia, respectively.

Age of asphalt specimen (8 time durations): 26, 46, 67, 94, 105, 124, 159, 182 days

Due to time constraints in the project, aging durations were limited to approximately 6 months. For each time duration, three or more numbers of replicate specimens were tested.

Loading speed (controlled test condition): 5 mm/min (=0.2 in/min)

For asphalt sample testing, 5mm/min is the recommended loading speeds according to ASTM D1074 [60].

Moisture control (environmental factor)

To attempt to provide a uniform moisture level in all tested specimens, all samples were prepared simultaneously and then were moved to an oven (for high temperature conditions), a refrigerator (for low temperature conditions), or to a room whose temperature was kept constant at approximately 68 ^{0}F (Figure C5).

Oven – high temperature conditioning (104°F)

Refrigerator – low temperature conditioning (32°F)

FIGURE C5

Moisture control using an oven refrigerator

Compressive strength (response/result)

Specimens were loaded to failure in compression using a universal test machine as shown in Figure C6. The compressive strength was calculated from the maximum recorded load divided by the original cross sectional area of the specimen.

Loading alignment control (environmental factor)

Due to imperfections in the sample trimming process, the loading surface of a given sample may not have been completely horizontal. A high strength steel ball was placed on top of the sample to minimized effects due to misalignment of the specimen in the testing machine.

FIGURE C6

Compression test setup with alignment control

Test Results

TABLE C1
Unconfined compression test results showing effect of aging

Age of specimen (day)	Test temperature (^oF)	Number of specimens tested	Average compressive strength (psi)	Cohesion value (psi)
26	68	3	156.8	40.82
46	68	6	188.6	49.09
67	68	6	234.3	60.98
94	68	3	225.1	58.59
105	68	3	224.3	58.38
124	68	9	240.5	62.60
159	68	3	204.5	53.22
182	68	2	255.6	66.54

TABLE C2
Unconfined compression test results showing effect of temperature effect

Age of specimen (day)	Test temperature (^oF)	Number of specimens tested	Average compressive strength (psi)	Cohesion value (psi)
67	32	3	718.2	187.0
67	68	6	234.3	60.98
67	104	3	74.00	19.26
182	32	2	876.0	228.0
182	68	2	255.6	66.54
182	104	2	45.43	11.82

Empirical Models for the Effect of Temperature and Age on Asphalt Strength

Strength

Using the results from the compression tests, the effect of temperature and age can be roughly estimated by individual empirical equations. General curve fitting techniques were used to determine the two empirical equations: a cohesion-age relationship and a cohesion-temperature relationship.

For the cohesion-age test data, a rational function with zero intercept was selected for maximizing the goodness of fit. Since the cohesion increment over aging was not significant, using an exponential or log function would not represent the cohesion-age relationship. The general aging model was constructed as shown in Figures C7 and C8.

Cohesion-Age model

(x: age in day, y: cohesion in psi)

Equation	$f(x) = \frac{-ab}{x+a} + b$
Coefficients (with 95% confidence bounds)	
a	16.29 (2.432, 30.14)
b	69.29 (58.95, 79.63)
Goodness of fit	
R-square (adjusted R-square)	0.5808 (0.5389)
SSE	321.6
RMSE	5.671

FIGURE C7

Curve fit coefficients for empirical model of cohesion versus age

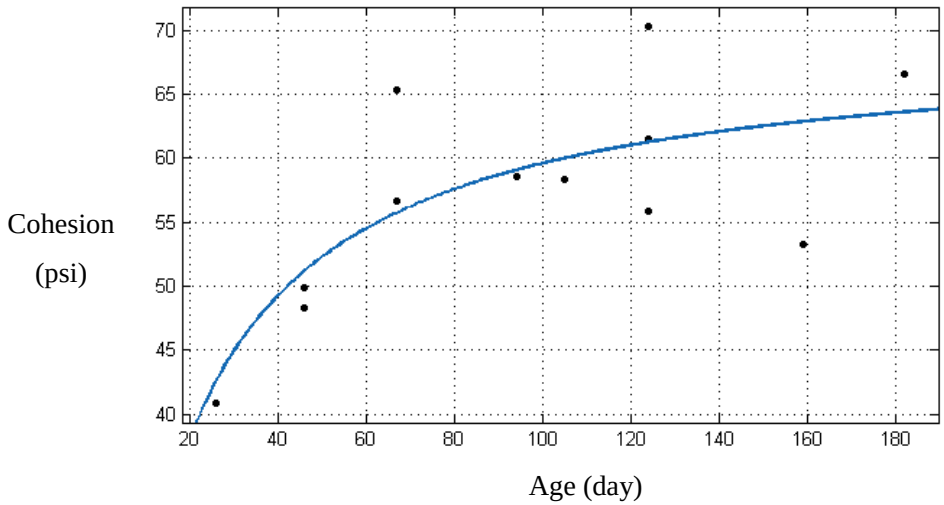

FIGURE C8

Empirical model of cohesion versus age

For the cohesion-temperature test data, a power function was selected for maximizing the goodness of fit. Unlike the aging model, the compressive strength had a strong correlation with the temperature. The general temperature model was constructed as shown in Figures C9 and C10.

Cohesion-Temperature model	
(x: temperature in F°, y: cohesion in psi)	
Equation	$f(x) = a \cdot x^b$
Coefficients (with 95% confidence bounds)	
a	72620 (7909, 137300)
b	-1.695 (-1.944, -1.446)
Goodness of fit	
R-square (adjusted R-square)	0.9612 (0.9588)
SSE	3897
RMSE	15.61

FIGURE C9

Curve fit coefficients for empirical model of cohesion versus temperature

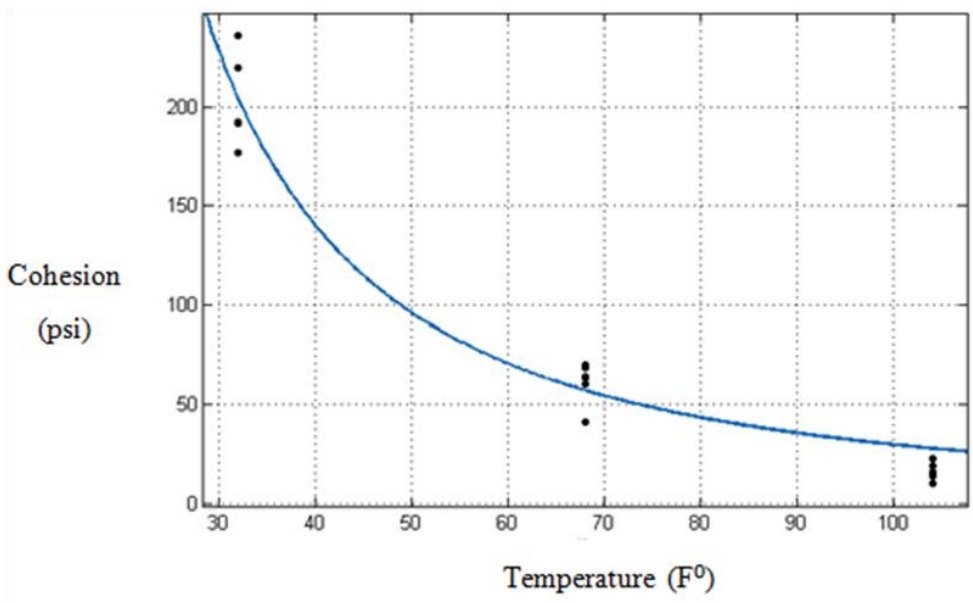

FIGURE C10

Empirical model of cohesion versus temperature